Norwegian
University of
Life Sciences

Transfer of radionuclides and stable analogues to edible plants in the semi-arid Tabernas desert, Spain
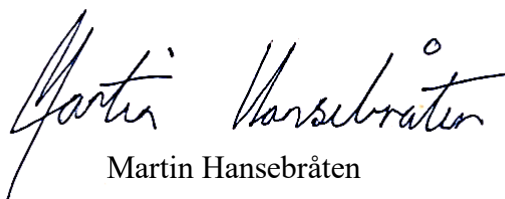
Martin Hansebråten

Preface

This thesis was written between June of 2024 and May of 2025 and are part of a master's degree in chemistry done over the past two of five years at NMBU. This work contributed to research activities undertaken in 1) the IAEA Coordinated Research Project K41022 "*Transfer of Radionuclides in Arid and Semi-Arid Environments for Radiological Environmental Impact Assessment*", implemented in 2021-2026 under the Research Agreement NOR-24798 between the IAEA and NMBU and 2) the European Atomic Energy Community's *RADONORM project (Towards effective radiation protection based on improved scientific evidence and social considerations – focus on radon and NORM project*).

First, I want to give a huge thanks to my supervisors Ole Christian Lind, Lindis Skipperud and Rafael Garcia-Tenorio for all guidance and support during my thesis. Thanks to Jose Antonio Suarez-Navarro and Víctor Manuel Expósito-Suárez at CIEMAT for guidance and all work prior to my thesis.

Thanks to Yetneberk Ayalew Kassaye, Karl Andreas Jensen, Marit Nandrup Pettersen, Hanae Hassani, Byron Spencer and Irina Dumitru at NMBU as well as Juan Mantero Cabrera at Universidad de Sevilla for all technical assistance. A huge thanks to Elina Turbina for all input in the writing process, and for helping to correcting the worst my weird and interesting writing mistakes.

Finally, thanks to all my friends and family that have supported me through my five years at NMBU and throughout my master work. A special thanks goes to all my friends at Tuntréet (TT) and Det Kongelige Norske Sangkoret Lærken (DKNSL) for all fun, support and learning during my studies. This would not have been possible without you!

Martin Hansebråten

14.05.2025

Abstract

Arid and semi-arid environments is an area of increasing interest, especially within the field of radioecology. More data are needed to get a better understanding of radionuclide behaviour and transfer to ensure good planning and operation of nuclear facilities. To predict the transfer of radionuclides from a media to an organism, concentration ratios (CRs) are commonly used.

The goal of this study is to assess CRs of radionuclides and stable analogues in the semi-arid Tabernas desert in Almeria, Spain and compare them to literature data for arid, semi-arid and temperate environments. In addition, a goal is to assess the impact of parameters such as soil composition, pre-treatment and deposition of radionuclides on the resulting CR. This study has been carried out in collaboration with USEV and CIEMAT, Spain and within the framework of the IAEA CRP *K41022* and the EU-project RADONORM.

All samples were collected during field work sept 2023 and subsequently subjected to a pre-treatment protocol that included two different methods of washing. Samples of fruit compartments (washed skin, non-washed skin, pulp, bone) were taken. Based on QQQ-ICPMS analyses of soil core samples and fruit compartment, CRs were determined for the radionuclides ^{238}U and ^{232}Th as well as the stable analogues ^{59}Co, ^{88}Sr and ^{133}Cs. In addition, supporting measurements of CEC, particle size, and mineralogical composition in soil were done.

The measured CRs in Tabernas varied between 4.23×10^{-5} measured in ^{232}Th and 1.49×10^{-1} in ^{88}Sr. CRs measured lower than for other reported values in the CRP *K41022*, both for date palms in Abu Dhabi, and apples in Turkey. While most measured CRs were within the range for IAEAs CR ranges in temperate environments, they were below the average values. Finding data for comparison, proved difficult since a lot of the reporting to the CRP are not yet published at the time of writing.

A significant difference in the concentration of radionuclides was found between the soil core positions, as well as between measuring sites. This is an indication that the soil is heterogenous, and analysis of multiple soil core samples are needed to ensure representative sampling. It also an indication that more sample sites should be chosen. However, the IAEAs CRP which measures many more CRs in different areas partially mitigates this problem. The horizontal layers of soil had indications of differences in particle size and minerology, but no significant difference in concentrations of the measured radionuclides and stable analogues were found. This indicates that soil sampling depth, have a negligible effect on the observed CR in Tabernas.

A significant difference was found between the bone and fruit pulp of dates and olives, and between the fruit and skin of figs. The difference is more apparent than the heterogeneity of the soil samples, suggesting it has a larger impact than the differences within the soil samples.

The two washing procedures had a significant difference for concentration of ^{88}Sr, ^{59}Co and ^{232}Th measured on the skin of figs Generally, SDs and RSDs tended to be smaller for the ultrasonic based pre-treatment method, than for the conventional method. However, the conventional method yielded lower concentrations of radionuclides and stable analogues in fruit. There is scope for improved washing procedures; the ultrasonic method appears to be more robust than the conventional method.

Micro-XRF elemental maps and point measurements demonstrated heterogeneous distributions of Si, Al and Fe on surfaces of olives and figs, strongly indicating the presence of mineral particles which was not found for dates. Differences in concentrations in fruits, differing CRs and deposition indicates that operating with a common CR for all fruits may give rise to relatively large uncertainties.

Samandrag

Aride og semiaride miljø er ei område med stadig meir interessante, særleg innanfor radioøkologi. Meir data er nødvendig for å få ei betre forståing av åtferd av radionuklidar, slik at planlegging og drift av nukleære fasilitetar kan sikrast. For å føreseie overføring av radionuklidar frå eit medium til ein organisme, vert konsentrasjonsforhold (CRs) ofte nytta. Denne metoden genererer ein generell verdi frå mange ulike faktorar. Likevel vert CRs ofte overdrive brukt.

Målet med denne studien er å vurdere CRs for radionuklidar og stabile analogar i den semi-aride Tabernas-ørkenen i Almeria, Spania, og samanlikne dei med relevant litteraturdata frå tørre, halvtørre og tempererte område. Eit anna mål å vurdere korleis parameterar som jordkomposisjon, førehandsbehandling og avsetting av radionuklidar på fruktskal påverkar dei endelege CR-verdiane. Denne studien er gjennomført i samarbeid med USEV og CIEMAT i Spania, innan ramma satt av IAEA CRP K41022 og EU-prosjektet RADONORM.

Alle prøvene vart samla inn under feltarbeid i september 2023 og deretter utsette for ein førehandsbehandlingsprotokoll som inkluderte to ulike metodar for vasking. I tillegg blei prøver av ulike fruktdelar (vaska skal, ikkje-vaska skal, fruktkjøt, kjerne) tatt. Basert på QQQ-ICPMS-analysar av jordkjerneprøver og fruktdelar, vart CRs bestemt for radionuklidane ^{238}U og ^{232}Th samt dei stabile analogane ^{59}Co, ^{88}Sr og ^{133}Cs. I tillegg vart støttemålingar av CEC, partikkelstorleik og mineralogisk samansetning gjennomført av jordprøvene.

Dei målte CR-verdiane i Tabernas varierte mellom 4.23×10^{-5} og 1.49×10^{-1}; lågare enn andre rapporterte verdiar i CRPen *K41022* , både for daddelpalmar i Abu Dhabi og eple i Tyrkia. Dei fleste målte CR-verdiane var innanfor området for rammverdiane til IAEA for tempererte miljø, men var under gjennomsnittsverdiane. Det viste seg vanskeleg å finne data som ein enkelt kunne samanlikne, ettersom mykje av rapporteringa til CRP-programmet enno ikkje var publisert på tidspunktet for studien.

Ein signifikant forskjell i konsentrasjon av radionuklidar blei funne mellom jordkjernene, samt mellom prøvetakingsstadane. Dette er ein indikasjon på at jorda er heterogen, og at ein treng å analysere fleire jordkjerneprøver for å sikre representativ prøvetaking. Det er også ein indikasjon på at ein bør velje fleire prøveområde. Likevel løyser IAEA sin CRP problemet delvis, ved å måle fleire CR i andre område. Jordsjikta hadde indikasjonar på forskjellar i partikkelstorleik og mineralogi, men ingen signifikante forskjellar i konsentrasjonane av dei målte radionuklidane og stabile analogane. Dette tyder på at jordsjiktet har ein neglisjerbar effekt på den observerte CR i Tabernas.

Ein signifikant forskjell vart også funne mellom steinen og frukta til daddel og oliven, samt mellom frukta og skalet på fiken. Denne forskjellen er tydelegare enn for heterogeniteten i jordprøvene, noko som tyder på at skilnader i konsentrasjonen mellom fruktdelar har høgre verknad på CR-verdien.

Dei to vaskeprosedyrane hadde ein signifikant forskjell i konsentrasjon av ^{88}Sr, ^{59}Co og ^{232}Th i fruktskalet. Generelt var standardavvika og relative standardavvika mindre for den ultralydsbaserte førehandsbehandlingsmetoden enn for den konvensjonelle metoden. Den konvensjonelle metoden gav likevel lågare konsentrasjonar av radionuklidar og stabile analogar i frukt. Resultata viser at det finst moglegheiter for forbetring av vaskeprosedyrane; ultralydmetoda virka meir robust enn den konvensjonelle metoden.

Micro-XRF målingar viste heterogene fordelingar av Si, Al og Fe på overflata av oliven og fiken, noko som sterkt indikerer at mineralpartiklar er til stade, medan dette ikkje vart funne for dadlar. Forskjellar i konsentrasjonar i frukt, ulike CR-ar og avsetning tyder på at det å operere med ein felles CR for all frukt kan gje opphav til relativt store usikkerheiter.

Contents

1. Introduction

1.1 Background

Arid and semi-arid areas encompass large parts of the globe and have become a subject of increasing importance in recent years. The International Atomic Energy Agency (IAEA) refers to these areas as "defined by excess evaporation compared to the amount of precipitation, enduring low and erratic rainfall, high temperature variations, and strong dry winds" (Harbottle and Yankovich, 2021). These areas are ever expanding, with large parts of the world becoming/already being subject to desertification. The consequences of desertification is estimated to directly affect 250 million people in the developing world alone (Reynolds et al., 2007).

An increasing amount of nuclear power plants are being considered to be built in arid and semi-arid areas, for example in North Africa (Jewell, 2011), and the Middle East (Hickey et al., 2021). Arid areas are also considered for nuclear waste sites, often in relation to mining of uranium, base-metals, as well as oil and gas production (Rea et al., 2021). Providing a better understanding of radionuclide behaviour and transfer in these areas helps to ensure the safe planning and operation of nuclear faculties and activities in arid and semi-arid climates (Harbottle and Yankovich, 2021).

The Tabernas region in the south of Spain is dominated by Badlands. The area is classified as a semi-arid area by the Köppen-Geiger climate classification (Beck et al., 2018). However, herbs and fruits like olives *(Olea europaea),* dates *(Phoenix dactylifera),* figs *(Ficus carica)* and prickly pears (*Opuntia stricta*) are commonly grown in the area. The monitoring of these plants is important to understand the fate of radionuclides in the arid and semi-arid environments. IAEA (2024) recommends that all plants used in monitoring are used for consumption, medicinal purposes or consumed by local wildlife.

In this study, the naturally occurring radionuclides ^{238}U and ^{232}Th as well as the stable analogous ^{133}Cs, ^{59}Co and ^{88}Sr, which serve as stable analogues for radioactive isotopes of the respective element. The radionuclides and stable analogues were chosen based on what was possible to measure by QQQ-ICP-MS in concentrations above the limit of detection.
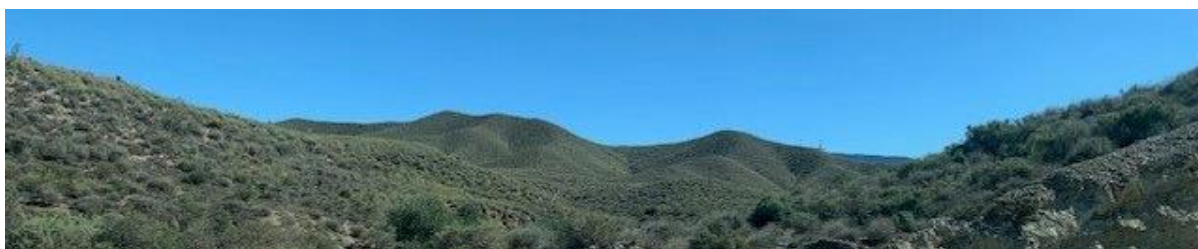
Figure 1.1: *Overview of the landscape in Tabernas (Photo: Marit N. Pettersen)*

Using CRs, concentrations in e.g. food stuff can easily be estimated from only the concentration in the medium. CRs are a very common way to quantify the transfer of radionuclides from one medium to another, such as from soil to plant, soil to cow milk or soil to mushroom (Urso, 2020). CRs are also used as a parameter in modelling. For example the ERICA tool used for risk quantification (Brown et al., 2016) and Food Chain and Dose Module for Terrestrial Pathways (FDMT) for transfer modelling (Hosseini et al., 2022), both uses CRs. However, there is often an overreliance put on CRs in assessment of transfer. CRs do not capture the dynamics of many environmental contamination situations, nor do they provide any insight to the mechanisms influencing transfer (Brown et al., 2024).

This study looks at the CRs of fruit samples and comparing them to literature values. IAEA recommends having a wide range of supporting measurement when considering soil-to-plant transfer. For example, soil characteristics such as soil type, soil pH, total organic matter, cation exchange capacity (CEC), mobile P, and others are recommended to provide in addition to the CR (IAEA, 2024).

As part of the sample treatment, fruits are often washed/cleaned. However, the methodology behind the pre-treatment is not standardized. Centro de Investigaciones Energéticas, Medioambientales y Tecnológicas[1] (CIEMAT) in Madrid, Spain has developed a method using the resuspension of particles on environmental samples by an ultrasonic method in the pre-treatment of samples (Rodríguez-Alonso et al., 2023). For this study, NMBU, CIEMAT and USEV designed a protocol for testing the impact of soil resuspension and subsequent deposition on fruit surfaces as well as the efficiency of different fruit washing procedures.

---

[1] The Centre for Energy, Environmental and Technological Research.

1.2 Aims, research questions and hypothesises.

This study aims to assess the CRs of the naturally occurring radionuclides ^{238}U and ^{232}Th and fallout radionuclides looking into their stable analogues and comparing them to values found in relevant literature. Another aim is to assess the pre-treatment methods established by CIEMAT. A last aim is to assess and categorize the deposition of resuspended soil particles on fruit surfaces contributing to the observed radionuclide at trace level concentrations. From these aims, one research question and two research hypothesises were put forward.

Research question
How does CRs measured in this study compare to ranges set by IAEA and limited literature values available and what factors influence the CR values?

Measurements of the concentrations of radionuclides and stable analogues can be affected by factors in the fruit, such as the fruit part, pre-treatment method, or heterogeneities in the soil.

Hypothesis 1
An ultrasonic bath pre-treatment removes more surface deposited contaminants from fruit skin surfaces than a conventional washing involving only soaking the sample in distilled water.

In the pre-treatment of fruit samples, two washing methods were used. One conventional, where fruit samples were soaked in distilled, deionized water, and one where an ultrasonic bath were used. Improved washing procedures may reduce uncertainties associated with CR values.

Hypothesis 2
Retention of radionuclides and stable analogues on fruit skin because of resuspension and deposition of soil mineral particles vary with fruit types.

IAEA and transfer models often use broad categories such as "fruit", for multiple species. Using X-ray fluorescence, the soil particle mineral contamination on fruit skin surfaces can be examined, and possible differences between the types of fruit can be discerned.

2. Theory

2.1 Study Area

The Tabernas is considered a semi-arid Badlands environment due to its dense drainage net. The desert is located 60 km west and 20 km north of the Mediterranean. The mountain ranges of Gador, Nevada, Filabres and Alhamilla surround the area. All except Alhamilla are 2000 meters above sea level (Kidron and Lazaro, 2020).
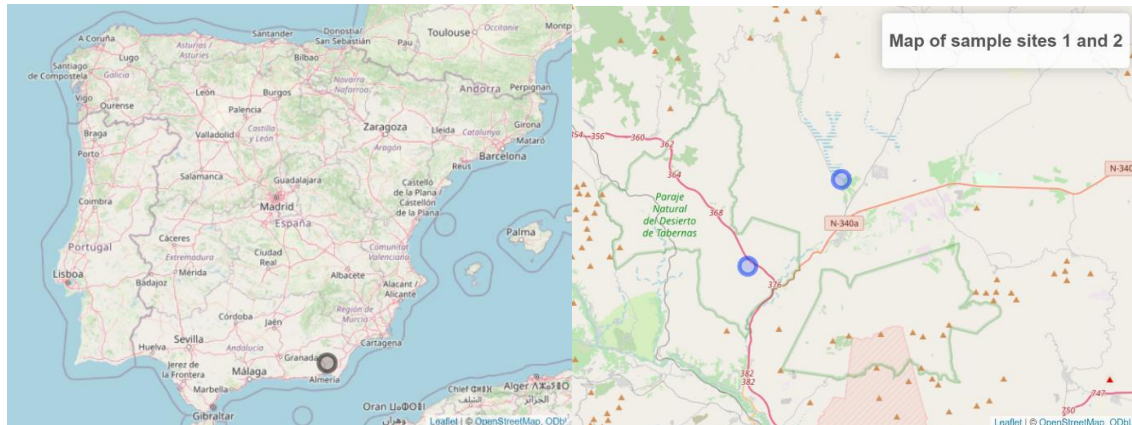
Figure 2.1.1: **Left:** *Map of Spain with the Tabernas desert marked in black.* **Right:** *The study area with site 1 and 2 marked in blue with the coordinates 37°2'7"N, 2°27'57"W and 37°05'23" N, 2°23'21" W respectively. Site 1 (on the left) is by the A 92 highway, and site 2 (on the right) is a farm. Both maps are made in R-studio using the leaflet package.*

It rarely rains in Tabernas, but when it rains, there is a tendency of a large amount of rainfall at once, occurring in short periods of the year. The annual rainfall is only between 200 and 250 mm per year with most rain-fronts coming from the Atlantic Ocean, but between 1967 and 1997 the maximum rainfall in one day was 98 mm (Lázaro et al., 2001). The Tabernas climate has multiple days of rainfall every year, which is typical of a Mediterranean climate. It also has a significant seasonal variation, with a dry period in the summer. However, the total amount of rainfall is also very low, and there are strong inter and intra annual variation which is more typical of deserts (Lázaro et al., 2001).

The region is dominated by Neogene marine sediments, which are mainly composed of gypseous mudstones and calcareous sandstones. The mineralogical composition of these shales consists of mainly muscovite, paragonite, chlorite/smectite, quartz, calcite, dolomite, and gypsum (Cantón et al., 2003). Both fruits (olives, figs, prickly pears, etc.) and herbs are grown and used in the area.

2.2 Radioactive elements in the environment

2.2.1 Sources of radionuclides in the environment

The sources of radionuclides in the environment are often divided into three categories a) cosmogenic, b) primordial and c) anthropogenic. a) is a result of cosmic radiation, b) are long lived radionuclides formed in the aftermath of the big bang and their daughters originating from Th and U. c) originates from human activities (Choppin et al., 2013b).

Although there are a vast number of materials that contains naturally occurring radionuclides, NORM (naturally occurring radioactive material) usually refers only to materials resulting from activities giving rise to significantly enhanced exposures, requiring regulatory control (IAEA, 2008). Examples of NORM in the environment can be found e.g.in the oil industry where ^{226}Ra and ^{228}Ra from produced water are released (Dal Molin et al., 2025). Another example are leaching of U from crushed rock waste, like black shales in Scandinavia (Pelkonen et al., 2025).

Anthropogenic radioactive elements, also referred to as artificial radioactive elements, are a result of human activity. Some common sources of these radionuclides are from nuclear weapons testing (Prăvălie, 2014), or from the nuclear fuel cycle. Examples of this are waste from nuclear reactors, reprocessing, and from nuclear accidents such as the Chernobyl and Fukushima Daiichi accidents (UNEP, 2016)

2.2.2 Speciation, distribution, and transport of radionuclides in soil

The transfer of radioactive elements is dependent upon speciation, i.e. the physio-chemical form of the element (Salbu, 2006). "The forms range from low molecular mass (LMM) species such as ions, molecules and complexes to high molecular mass (HMM) species such as colloids, pseudo-colloids, particles, fragments which can vary in size, shape structure morphology, density and charge properties" (Salbu et al., 2004).

Soils and sediments tend to act as sinks for HMM particles, while LMM species tend to be more mobile. LMM species are also more bioavailable, because of its ability to cross membranes. HMM are biologically inert but can be retained in for example filtering organisms. They can also be resuspended acting as point sources when inhaled or consumed. HMM particles can be remobilized by particle weathering. This weathering depends on the initial particle composition, structural changes during the transformation process, pH, redox conditions and microbial activity (Salbu et al., 2004). LMM species can, on the other hand, be permanently sorbed to solids (Salbu, 2006).

The distribution of radionuclides in soil is dependent upon the distribution coefficient K_d. The K_d is defined under equilibrium conditions. However, the apparent K_d will change over time due to interactions with for example clays and organic material (Salbu et al., 2004).

The soil characteristics have a substantial impact on the behaviour of radionuclides in the environment. Arid soils tend to be sandy in texture, low in humus and moisture, often categorized by highly eroded mineral structures, and therefore often containing a high concentration of soluble salts. Land use in arid environments tend to be driven by seasons, with fruits like olives and dates being grown in areas with surface water available (Semioshkina and Voigt, 2021). Soils from arid and semi-arid environments can also easily be blown over large distances by the wind. For example, dust from the north of Africa was blown to the south of Spain and Tenerife in two events in March 2022, when radionuclides such as ^{137}Cs, ^{40}K, ^{239}Pu were detected at measuring stations in Malaga and Tenerife (Liger et al., 2024).

2.2.3 Uptake and deposition of radionuclides in plants

The real uptake of radionuclides by plants can happen either directly or indirectly. Direct uptake in terrestrial environments can happen by adsorption to the surface of plants, or direct uptake via the stomata, where volatile radionuclides such as ^{14}C, ^{3}H (Gupta et al., 2014), and ^{131}I (Pröhl et al., 2012) can be taken up. In addition, indirect uptake through the plant root system can occur. The indirect uptake can vary significantly depending on the type of plant, especially in the case of long-lived radionuclides (Gupta et al., 2014). The uptake of an individual radionuclide depends on the physiochemical similarity between it and a plant nutrient. They are mostly taken up in the growth and development of the plant, where radionuclides are taken up along with essential plant nutrients (Phuong et al., 2023).

The deposition of radionuclides on plants can occur either through wet deposition or dry deposition. Dry deposition is the direct uptake of radionuclides by the natural surface of the plant (IAEA, 2009). Wet deposition, when radionuclides in air are washed out by rain, hail and/or snow can result in high concentrations of radionuclides in crops. The wet deposition is influenced by factors such as the developmental stage of the plant, water storage capacity of the canopy, and the properties of the radionuclide (Pröhl, 2009). Radionuclides can both be absorbed as gases and as small particles (IAEA, 2009). It is important to note that when measuring CRs as done in this study, not only the real uptake is looked at, which is just what is taken up by the plant, but also the deposition.

2.3 Investigated radioactive elements

Two of the elements measured in this study is ^{238}U and ^{232}Th, both actinides. U and Th were selected because of being relatively abundant as well as being possible to accurately measure by ICP-MS. In addition, ^{226}Ra was also considered as a potential element for analysis, but was not included because of the low concentrations, meeting the detection limits for the samples included in the present study.

2.3.1 Uranium (U)

Three isotopes of U are found naturally, ^{234}U, ^{235}U and ^{238}U. All are members of the natural decay series (Choppin et al., 2013a). ^{238}U heads the U series, with ^{234}U taking part in it. ^{235}U heads the actinium series. ^{238}U is the most abundant in nature; by weight ^{238}U is 99.27% of the total natural U. ^{235}U has a 0.72% abundance by weight, while ^{234}U has an abundance of 0.0057% (Kathren, 1998). The earth's crust contains in average about 3-4 ppm of U. It is most often found in the tetravalent state in minerals. Over 60 different minerals contain U. One important mineral is being uraninite (UO_{2+x}, x = 0.01 to 0.25) where the concentration of U are between 50 and 90% (Choppin et al., 2013a).

The main use of U is as nuclear fuel, but depleted U is also used, for instance, as metallic slugs in armour piercing ammunitions and as balance weights in airplanes (Choppin et al., 2013a). Previously, U was also used in the colouring of glass, glazes and enamels being used most extensively from the 1830s to the 1940s (Donna, 2001).

In the production of U, milling operations produce tailings, which contain most radioactive decay products of U. Having relatively low levels of radioactivity, the tailings are often dumped outside the production plant, where leach water can enter the local water systems. In dry areas it can also be spread by winds. Multiple radiation protection authorities now require e.g. recycling of waste water, removal of Ra, and adding lime to increase the pH to reduce harmful effects on the environment (Choppin et al., 2013a).

2.3.2 Thorium (Th)

Th has many different isotopes in nature of which $^{227, 228, 229, 230, 231, 232, 234}$Th exists naturally. However,^{232}Th, the parent nuclide of the Th decay series, is by far the most common. By weight, it is almost 100% of the existing Th. The specific radioactivity is also lower than U, and it is often treated as non-radioactive. It is somewhat more common in nature, with the average content in the earth crust being around 10 ppm. It has a much lower solubility than U. In addition U can exist in oxidation states like +VI which typically have higher solubility (Choppin et al., 2013a).

Th often occurs with other valuable elements such as Nb, U and Zr, and is often a byproduct in the extraction of these. Th is commonly used in high temperature furnace linings, and high temperature thermometers, but can also be used as fuel in nuclear reactors (Choppin et al., 2013a).

2.4 Stable analogues

In environmental studies, finding a good analogue of a process, element or an isotope is essential. Finding a correct analogue can lead to a better understanding of the behaviour of radionuclides in the environment (Varga et al., 2009). Some analogues may seem obvious at first glance, for example using pasture grass for forage. However, analogues must be chosen carefully. Using for example generic data of grain and fruit is not wise since growing conditions for grains and fruits tend to vary (IAEA, 2010).

For radionuclides in the environment, elemental analogues are common to use. They are elements with similar physiochemical properties. For example, it is common to use K as an analogue for Cs, or Ca for Sr. Lastly, there are isotopic analogues, the most common form of analogue used. Except for small elements like hydrogen, the behaviour tends to be the same between isotopes of the same element. An example is that short lived ^{134}Cs or the stable ^{133}Cs have been used to predict the long-term behaviour of ^{137}Cs (IAEA, 2010).

Stable analogues, a specific type of isotopic analogues, are commonly used as analogues for less studied/common radioactive isotopes found in the environment (Varga et al., 2009). An important consideration when using stable analogues is the timescale, since radioactive decay of short-lived radionuclides can affect the long-term behaviour of the nuclide which will not

be caught by the stable isotopes (IAEA, 2010). There are also other considerations, that must be considered. For example, ^{90}Sr in the Chernobyl exclusion zone is associated with fuel particles, while stable Sr is not (Kashparov et al., 2004). In this study, some radionuclides had a too low concentration to accurately measure by ICP-MS, or other problems such as short half-lives, or interferences making measurements difficult. To account for this, stable analogues were used.

2.4.1 Caesium (Cs)

Cs is a group one alkali metal and exists in at least 39 different isotopic forms. In the liquid state, Cs exists as Cs^+. Stable Cs, ^{133}Cs is naturally occurring and rarely occur in toxic amounts. As a result of nuclear weapons testing and nuclear accidents, long lived radioactive isotopes such as ^{134}Cs, ^{135}Cs and ^{137}Cs occur in the natural environment (Burger and Lichtscheidl, 2018). Cs have a particular ability to bind to clay minerals such as illite and vermiculite (Okumura et al., 2018). In this thesis, ^{133}Cs are used as a stable analogue for ^{137}Cs and ^{134}Cs.

2.4.2 Strontium (Sr)

Sr is a group two element and alkaline earth metal. It is associated with calcium and, in some cases, also magnesium. The ratio between Sr and Ca is relatively stable in the biosphere. It occurs mainly as Sr^{2+} (Greger, 2004). In plants, it is less fixed to the soil matrix and is therefore more available for root uptake by plants (UNSCEAR, 2000). The availability of Sr is dependent on pH and the OM content in soil. The radioactive ^{90}Sr is produced in many nuclear processes, often being a major dose contributor (Greger, 2004). In this thesis, ^{88}Sr are used as a stable analogue for ^{90}Sr.

2.4.3 Cobalt (Co)

Co is a transition metal and is not a plant nutrient. However, it is necessary for nitrogen fixation. In plants, it is bound to organic substances and can thus be translocated. In leaves, Co can easily be taken up by the cuticle (Greger, 2004). The mobility of Co in soil is low. It is assumed that 95% of induced Co stays in the top five cm of soil (Narendrula et al., 2011). The only naturally occurring isotope is ^{59}Co which is used as the stable analogue in the present work. However, ^{55}Co, ^{56}Co, ^{57}Co, ^{58}Co and ^{60}Co exist in the environment because of human activity; the main source coming from the nuclear industry (Kosiorek, 2019).

2.5 Concentration ratios and their applications

To assess the transfer of radionuclides in the environment, concentration ratios (CR) are commonly used. The CR is defined as the concentration of the sample divided by the concentration of the medium (eq. 1) (Brown et al., 2024). In this study, CRs will refer to the ratio when wet weight (ww) values of fruit are used in calculations (eq. 2), and transfer factors (TFs) will be used when the ratio is calculated with dry weights (dw) of fruit (eq. 3). The same value of soil concentration is used in both cases, where the dw of soil dried at 95°C were used.

$$eq.\ 1: CR_{general} = \frac{C_{org}}{C_{media}}$$

$$eq.\ 2: CR_{plant} = \frac{C_{plant(ww)}}{C_{soil}}$$

$$eq.\ 3: TF_{plant} = \frac{C_{plant(dw)}}{C_{soil}}$$

Concentration ratios are used in multiple models for risk assessment and transfer models. One such model is the ERICA 2.0 tool, which is a tool used to quantify environmental risk based on the Environmental Risk from Ionising Contaminants: Assessment and Management (ERICA) integrated approach (Brown et al., 2016). The ERICA tool was developed as a compatible model to the International Commission on Radiological Protection (ICRP) modelling approach (Ulanovsky et al., 2017), as the radiological protection framework changed from a focus on mainly radiation risk to humans to encompassing the environment as a whole (ICRP, 2007).

The model is based on the use of reference organisms, *"a series of entities that provide a basis for the estimation of radiation dose rate to a range of organisms which are typical, or representative, of a contaminated environment. These estimates, in turn, would provide a basis for assessing the likelihood and degree of radiation effects*" (Brown et al., 2016). The ERICA-tool is used in applications such as assessing the impact of releases from existing and potential nuclear powerplant (Nedveckaite et al., 2011), assessing potential impact and risk from deep geological facilities (Robinson et al., 2010), and deriving quality guidelines for mining sites (Doering and Bollhöfer, 2016).

Another model where CRs are used extensively is the Food Chain and Dose Module for Terrestrial pathways (FDMT) model, which is used in the ARGOS and JRODOS decision support systems. The model simulates transfer of radionuclides along terrestrial food chains and predicts the activity concentrations in human food (Hosseini et al., 2022).

However, there are multiple weaknesses with the use of concentration ratios. CRs do not capture the dynamics of many environmental contamination situations. They also do not provide insight to underlying mechanisms that influence radionuclide transfer. This makes other supporting information necessary (Brown et al., 2024), since properties such as leachability and bioavailability of soil-to-plant transfer may fluctuate based on the physiochemical properties of the soil. Although not essential for the CR calculation itself, other supporting measurements are important to understand the conditions that influence transfer and for accurate interpretation of CR results (IAEA, 2024).

Soils in arid and semi-arid regions tend to have low fertility, low water holding capacity, low pH and low soil organic content in addition to problems with low levels of phosphorous and nitrogen (Thomas et al., 2006). CRs are defined under equilibrium, (or "steady state") conditions with no rapid changes in the concentration of radionuclides and their stable analogues in biological or physical compartments. CRs presented are often not applicable to non-equilibrium conditions that occur after short term radionuclide releases to the environment (IAEA, 2021).

3. Experimental

3.1 Sampling, and sample selection

Samples of the edible fruits of olives, dates, figs, and prickly pears, were collected in the Tabernas desert on the 25th and 26th September 2023. Olives were collected on two sites. Site 1 was by the A 92 highway at 37°2'7'' N, 2°27'57'' W. Site 2 was at a local farm at 37°05'23'' N, 2°23'21'' W. Dates, figs and prickly pears were only collected on site 2. Fruits were collected by team from CIEMAT, Universidad de Sevilla[2] (USEV) and Noregs miljø og biovitskapelege universitet[3] (NMBU). The samples of fruit were calcinated by CIEMAT and sent to NMBU for the main analysis.

In addition, NMBU took soil core samples from the two sites in the Tabernas desert (figure 3.1.1). The soil samples from Tabernas were gathered on the two sites by senior engineer Marit N. Pettersen and other members of the field expedition in the autumn of 2023. For olives on site 1, three cores were taken, all being on the downhill side of the plant; the tree was on a hillside by the road. The samples were taken at different distances from the plant stem, with position E being closest, followed by A and B. On site 2, four soil core samples were taken around an olive tree, approximately 1 meter in the north, south, east, and west directions from the plant.

For dates, five different cores around the stem of the plant were collected. One closest to the stem, position E, and A, B, C and D were taken on all sides of the tree stem. A, B and C soil core samples for prickly pears were taken from the same distance of a hedgerow of the plant. For figs, only one singular soil core sample was taken, core A. This was mostly due to a lack of time when sampling. The core was taken in the middle of four fig trees to be as representative of the soil as possible.

---

[2] University of Seville
[3] Norwegian university of Life Science
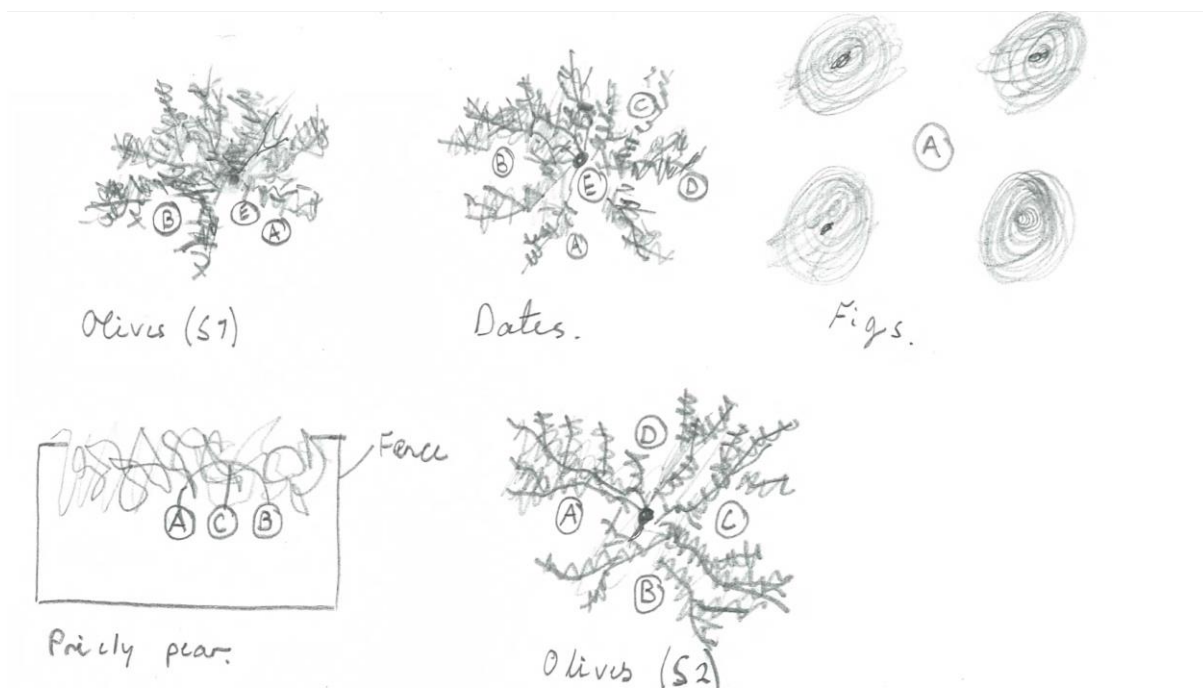
Figure 3.1.1: *Sketch of the positioning of soil core samples in Tabernas on sites 1 and 2. Three cores are taken by an olive tree on site 1 (S1), and four on site 2 (S2). Five cores are taken at a date tree, three for prickly pears. One core sample was taken associated with figs. The letter marked in the sketch is the same as the letter marked in later figures.*

All soil core samples were divided into individual horizontal layers, with each layer being 5 cm deep. Four layers (down to 20 cm) was used in this study. All soil cores had at least four layers that were analysed, except for soil core B, where only 3 layers (down to 15 cm) were recovered. The reason for using layers down to 20 cm instead of the usual 10, was to take into account the root systems that often grow deeper for plants in deserts than in temperate environments (IAEA, 2024).

More samples were taken than was possible to analyse. Therefore, a selection process for the samples for analysis in Norway was done. It was decided to focus on concentration ratios and washing water samples from the pre-treatment of the samples. Samples of figs and dates were prioritized in this work. This is because dates had the most comprehensive sampling of soil, while figs underwent both methods of washing established by CIEMAT.

3.2 Treatment of fruit samples

The fruit samples of figs, prickly pears and olives underwent two different washing procedures done by CIEMAT. The procedure involved using an ultrasonic technique to wash the fruits and comparing it to more conventional methods, where the samples were soaked in deionized water (Suarez and Navarro, 2023). The fruits were separated into the fruit, fruit-skin and bone parts before being calcinated and sent to NMBU.

3.2.1 Conventional method of pre-treatment

The conventional method was used on samples of figs and prickly pears. The procedure was done by adding distilled and de-ionized (MilliQ) water to fruits stored in 600 mL beakers and allowing them to soak for 30 minutes. This was done in three rounds. In the first round, 480 mL of water was used for figs, while 560 mL of water was used for prickly pears. In the second and third round, 300 mL was used in both cases. The water was then collected and evaporated to approximately 10-20 mL (Suarez and Navarro, 2023).

After the pre-treatment, the samples of fruit were peeled using a scalpel or razorblade, and the fractions of skin and fruit were first dried at 110°C until stable weight and calcinated at 450°C (Suarez and Navarro, 2023), before being sent to MINA's Isotope laboratory (Isotoplaboratoriet) for ICP-MS analysis, along with aliquot samples of the water used in the pre-treatment.

3.2.2 Pre-treatment by ultrasonic washing

The ultrasonic washing procedure was carried out on samples of dates, olives and figs. The samples were put in 600 mL beakers (90 mm in diameter), adding 300 mL of MilliQ per 100 grams of fruit. The samples were then run in an ultrasonic water bath (Ultrasons- H, JP selecta). The system was run with a temperature between 1°C and 4°C and a frequency of 50/60 kHz in wash cycles of 8 minutes. A control sample of the MilliQ water was taken in between each series as verification between each washing (Suarez and Navarro, 2023).

Three aliquots of about 10 mL of water were taken. They were stored on LSC vials and sent to Norway for measurements on ICP-MS. After the pre-treatment, the samples of fruit were peeled using a scalpel or razorblade into fractions of skin and fruit. For the olive samples, the olive fruit was separated from the bone (Suarez and Navarro, 2023).

Individual parts of each fruit were then dried at 110°C until stable weight and calcinated at 450°C (Suarez and Navarro, 2023). The calcinated samples were stored on LSC vials. Both water and calcinated samples were sent to NMBU for ICP-MS analysis.

3.2.3 Digestion of wash water samples for ICP-MS

First, ultrapure HNO_3 was added to all wash water samples analysed. Enough acid was added so that the final concentration ended up being ca. 2%. The samples were then left for about 24 hours before they could be evaporated.

After 24 hours had passed, 10-12 mL of the sample amount was added to 17 mL Teflon UltraCLAVE tubes. Three certified reference materials (CRMs) were used. One water, *NIST 1643f,* where about four grams of sample were added and diluted with MilliQ water to about 12 mL of the sample amount. Two soil CRMs were used, *NCS DC 73324a* and *NCS ZC73007.* Ca. 10 mg of sample was added to the Teflon tube and 12 mL of water was added. Five blanks containing 12 mL of MilliQ water were also taken. All samples, CRMs and blanks were then evaporated to dryness at 90 degrees in an oven for three days. When the sample liquid evaporated and the samples dried, 1.5 mL of ultrapure HNO_3 was added to all samples, blanks and CRMs and subsequently run on a UltraCLAVE at 260°C for 30 minutes.

Afterwards, the samples were placed in 15 mL ICP-MS tubes, diluted to 15 mL with MilliQ water and analysed on an Agilent 8900 ICP-MS in He-KED and oxygen reaction mode by senior engineer Karl Andreas Jensen at Isotoplaboratoriet (MINA, NMBU). The plasma was set to 4xHMI (4x gas dilution). Rh and Ir were used as Internal Standards.

3.2.4 Digestion and analysis of calcinated fruit samples by ICP-MS

To assess which acids to use for the digestion of the calcinated fruit samples, one replicate was measured using two different acid mixes. One contained 5 mL ultrapure HNO_3, and one contained a mixture of 3 mL ultrapure HNO_3 and 2mL of ultrapure HCl. From a visual assessment of the digestion, it was decided to use 5 mL of ultrapure HNO_3.Where possible, about 0.1 grams of the calcinated fruit samples were added to UltraWAVE Teflon tubes.

Three CRMs were used, *NIST 1633a*, a CRM of coal fly ash, *NCS ZC73036a,* a CRM of green tea*,* and *NIST 1570a* a CRM of spinach leaves. To all tubes, 5 mL ultrapure HNO_3 was added, and ran in an UltraWAVE at 260℃ for 30 minutes. In addition, five blanks with only 5 mL of acid were taken.

The samples had been diluted to 50 mL in ICP-MS tubes using MilliQ water, before being analysed on an Agilent 8900 ICP-MS in He-KED and oxygen reaction mode by senior engineer Karl Andreas Jensen at Isotoplaboratoriet, MINA, NMBU. The plasma was set to 4xHMI (4x gas dilution). Rh and Ir were used as Internal Standards in the same way as the wash water samples.

3.2.5 Analysis of fruit skin samples by micro-XRF

The preparation of samples for micro x-ray fluorescence (micro-XRF) analysis was done by CIEMAT. Samples cleaned by ultrasonic washing were peeled using a scalpel or razor blade, and dried on a petri dish. Four pieces of scotch tape were used in each corner to keep the sample flat. Pieces (2x2 cm) of peeled fig skin were prepared, whereas olives and dates were cut to 1x1 cm pieces (Suarez and Navarro, 2023). These pieces were sent to NMBU Isotoplaboratoriet for analysis by micro-XRF. At NMBU, the paper was cut to size and mounted onto a mylar foil stretched over an x-cell (31 mm Double Open-Ended X-CELL®) (Byrnes et al., 2020).

After mounting, the samples were analysed on a M4 Tornado (Bruker), with the resulting spectra analysed using the ESPIRIT software (Bruker). A rhodium target, running at 5 kV and 600 µA and polycapillary optics which resulted in a beam with a spot size of 25 µm. The fluorescent x-rays were counted by two XFlash® silicon drift detectors (50 keV, 600 µA, 25 µm spot size). The detectors were at an 45° angle to the beam and each fracture an active area of 30 mm^2 (Byrnes et al., 2020).

Under vacuum (20 mbar), an overview image (9.83 mm x 8.53 mm) was first taken at 30 ms, 30 µm for 3 cycles. From the original image, line and point spectra was chosen, comparing points with high concentration of a certain element, a so-called hotspot with the area just outside of it. One sample was measured of olives from site 1 and one image was taken for olives from site 2, as well as a skin sample of a fig and a date.

3.3 Treatment of soil samples

The soil samples from Tabernas underwent no pre-treatment in Spain but were sent directly to Norway. All soil samples were sieved with a 2mm sieve at the soil laboratory of the MINA faculty. The sieve was cleaned using a compressed air hose between every sample within a soil core. Between every core sample the sieve was rinsed with deionized water and dried with a paper towel.

Half of the sample amount (ca. 8 grams) were ground using an electric mortar. Each sample was ground between 1 and 3 minutes until the sample was a fine powder. The mortar and equipment were rinsed with deionized water and dried off with a paper towel between every sample. These samples were collected in paper envelopes and dried in a 105°C oven overnight.

3.3.1 Preparation and analysis of soil samples by ICP-MS

Between 0.19 and 0.25 grams of the finely ground soil from each depth was taken and added to 17 mL ultraWAVE Teflon tubes. To this, 8 mL of a mixture of 1:1:2 by volume of HNO_3, HBF_4 and H_3PO_4 was added to the samples. This mixture was chosen to get the most elements of interest in one decomposition. Four CRMs for soil and five blanks were taken along with the samples. The mixture of soil and acid was mixed thoroughly using a vortex. The CRMs used for soil samples was *NIST 2711a*, *NCS ZC 73007*, *NCS DC 73324a* and *IAEA 448*. The blanks were the acid mix alone. The samples of soils, blanks and CRM were subsequently digested using a UltraWAVE microwave digestion system at 260°C for 30 minutes.

The digested sample was diluted to 50 mL using MilliQ water. From this an aliquot of 1 mL was taken and diluted with 9 mL with 5% (V/V) HNO_3. The aliquot was then analysed on an Agilent 8900 ICP-MS in He-KED and oxygen reaction mode by senior engineer Karl Andreas Jensen at Isotoplaboratoriet. The plasma was set to 4xHMI (4x gas dilution). Rh and Ir were used as Internal Standards.

3.3.2 Preparation and analysis of soil by XRD

The x-ray diffraction (XRD) sample collection was done in cooperation with senior engineer Irina Dumitru at the MINA faculty. For XRD analysis, about 1 gram of the grounded soil sample was ground a second time and added to a sample container for XRD analysis. Five samples were taken in total. One from under the dates, figs and prickly pears each, and two samples of olives; one from site 1 and one from site 2. The 15-20 cm layer was used for every sample from the core closest to the stem of the plant.

For the five soil samples, X-ray powder diffraction data collection was done using Bruker D8 Advance diffractometer, with CuK α radiation ($\lambda = 1,54$ Å) generated at an acceleration voltage of 40kV and 40mA current. The diffractometer was equipped with a LynxEye XE-T detector in reflection geometry (Bragg-Brentano) with a step size of 0.01° and a step time of 2s. The X-ray diffraction patterns were collected in the 2θ range 5-70°.

Phase identification was performed using Bruker Diffraction Evaluation software (eva.) V5.1 and the open-source crystallographic database (COD). Semi-quantitative analyses were performed using Bruker Topas software V7.13 by employing whole-pattern Rietveld method but excluded the regions below 15°.

3.3.3 Soil for laser diffraction

For laser diffraction, five samples of about 10 grams were needed. There was no single sample that contained 10 g of sample, so composite samples for each layer at two positions was used. Here, samples from position E and C, about 6 grams of soil, were merged for the different layers. From position D, about 3 grams of each layer was merged into a sample for the measurement of LOI. Each sample was weighed before it was merged (Attachment A.1.)

The samples were then analysed by Byron Spencer at MINA. Each sample was dried at 40°C and sieved in a 2 mm sieve. The samples were homogenized before the analysis. They were then added to 1L glass beakers. To each sample, 20 mL of distilled water was added together with a ca. 2 mL of H_2O_2, adjusted for LOI and organic matter content. The samples were then heated to 70°C to increase the reaction rate and left to oxidize for a couple of days (Spencer, 2025).

After the volume had decreased after heating, 200 mL of distilled water was added, and the samples were heated to 90°C to get rid of any remaining H_2O_2. Subsequently, 10 mL of 2M HCl was added and the solution stirred for 1 minute to dissolve any inorganic sedimentary substances. Finally, the glass beakers were filled to about 1 cm from the brim with distilled water. Clear solutions were removed; the samples were wet sieved at 63μm, and washed with about 900mL of distilled water. To the prepared sample material, a few drops of 1M $MgCl_2$ was added, so that the material could sediment and the clear solutions could be removed. The sample material (<63μm) was dried at 40°C for multiple days (Spencer, 2025).

After the samples dried, between 0.12 g and 0.40 g was weighed for analysis, depending on the amount of fine-grained material. To the samples, about 50 mL of 0.05 M Na-pyrophosphate was added to prevent charged particles. The samples were then dispersed by using an ultrasonic rod at 37 J/mL. The sample material was added directly to the instrument until correct obscuration was reached (Spencer, 2025).

The samples were then analysed on a Beckman coulter LS 13320. The samples were run with the Fraunhofer optical model, with a pump speed of 45% without PIDS (Poralization Intensity Differential Scattering). Between every measurement, measure offsets, auto align, measured background and auto-rinse were performed. The grain size was measured between 0.4 μm and 2000 μm. The determination of the sand fraction was done by calculating the difference between the empty glass and the glasses with the sand fraction. To document accuracy in the lower particle size areas, the G15 certified reference material was used (Spencer, 2025).

3.3.4 CEC analysis of soil

About three grams of soil were weighed out from each individual horizontal layer and position. The top four horizontal layers and (with the exception of soil associated with the fig CR), three soil cores were used in the analysis. The cation exchange capacity was determined at USEV using atomic absorption/emission spectroscopy, by the method laid out by Sumner and Miller (Sumner and Miller, 1996).

3.4 Analytical methods

In addition to the analytical techniques of Micro-XRF and ICP-MS, analysis by laser diffraction, X-ray powder diffraction and CEC were used. Moreover, UltraCLAVE and UltraWAVE was used for digestion before ICP-MS. While not necessary for the calculation of CRs itself, methods other than ICP-MS are important for establishing an accurate interpretation of CRs (IAEA, 2024).

3.4.1 UltraCLAVE and UltraWAVE

Sample digestion is a necessary part of the sample preparation for analysis for ICP-MS analysis. This is done by heating the sample by using a UltraCLAVE or UltraWAVE microwave digestion systems (Milestone Inc.). Both were used in this study, depending on what machines were occupied or not. UltraCLAVE was used for the digestion of wash water samples, while a UltraWAVE was used for the digestion of soil and calcinated fruit samples.

UltraCLAVEs and UltraWAVEs are a type of closed vessel digestion microwave. The instruments utilize a single reaction chamber made of stainless steel. Samples are loaded into the vials and placed inside a reactor cavity and sealed. Nitrogen gas is then introduced to keep a constant pressure, and the sample is heated by microwaves to a desired temperature (Colnaghi et al., 2024).

3.4.2 ICP-MS

ICP-MS are commonly used to determine the concentration of radionuclides with medium and long half-lives. The method is used to analyse a plethora of different elements and can be employed quantitatively and semi-quantitatively. Over 80 elements can be analysed with the technique (PerkinElmer, 2011). ICP-MS consists of two main parts: an inductively coupled plasma (ICP) and a mass spectrometer (MS).

The ICP acts both as the source of atomization and ionization. Most commonly, a dissolved sample is introduced by a nebulizer, where it is made into an aerosol that is shot into an argon plasma, but solid samples can also be introduced by laser ablation (Skoog et al., 2017a). In this study, all samples are digested in acid and introduced as an aerosol to the machine.

Quadrupoles are the most common design type of MS part of the apparatus. The heart of the quadrupole is four parallel cylindrical rods that serve as electrodes, with opposite rods connected electrically. Ions are accelerated in the space between the rods. At any given moment, all ions, except the ones with a certain m/z ratio, strike the rods and are converted to neutral molecules. Only ions in a given range reach the another quadrupole/detector (Skoog et al., 2017a). The mass spectrometry (MS) part used in this study consists of a triple quadrupole (QQQ) design, also known as ICP-MS/MS. This design enables more filtering than for a single or double quad design, and reduces uncertainties and variances seen when using a reaction cell gas (Agilent, 2022).

The interface between the ICP and the MS part of the apparatus is essential. The ICP operates at atmospheric pressure, while the MS part has a pressure less than 10^{-2} Pa. The coupling is achieved by using a sampler and a skimmer. The plasma gas passes through a pressurized water-cooled sampler cone with a small orifice. An expansion of the gas occurs in this region, which results in it being cooled. Parts of the gas then pass through the skimmer and into the mass spectrometer chamber (Skoog et al., 2017a). More modern designs also have a third cone that eliminates the need for ion lenses, which is necessary when two cones are used. The cones are most often produced from nickel or platinum (PerkinElmer, 2011).

The simplicity of ICP-MS spectra led early users to believe that they had found an "interference-free" method. However, this proved not to be the case, as both spectroscopic and matrix interferences occur regularly (Skoog et al., 2022c). Spectroscopic interferences occur when the ionic species in the plasma have the same m/z (mass to charge ratio) values as an analyte ion. These interferences are divided into three categories. Isobaric interference, when two elements have isotopes with essentially the same mass. Polyatomic ion interference, when polyatomic structures form from interactions in the plasma. and lastly, Oxide and Hydroxide species interference, when oxides and hydroxides are formed from the oxide itself, matrix components, the solvent, and the plasma gasses. Hydroxide species interference is seen as the most serious interference, while isobaric can be corrected by software, and polyatomic ion can be resolved by using a blank (Skoog et al., 2017a).

The other category of interferences – matrix effects, usually become apparent in concentrations greater than 500 to 1000 mg/mL. Usually this comes as a reduction in the signal, but signal enhancements have also been observed. This effect can generally be dealt with by diluting the solution, altering the sample introduction procedure, or by separating out the offending species. The effect can also by and large be eliminated by using an internal standard (Skoog et al., 2017a).

Limit of detection and quantification for ICP-MS

The limit of detection (LOD) and limit of quantification (LOQ) was found by multiplying the standard deviation of the blank by 3 for LOD (eq. 4) and by 6 for LOQ (eq. 5). Five blanks were used to determine the standard deviations.

$$eq.\ 4\text{: } LOD = 3 * SD_{Blank}$$

$$eq.\ 5\text{: } LOQ = 6 * SD_{Blank}$$

The limit of detection and quantification for the main analytical elements ^{59}Co, ^{133}Cs, ^{88}Sr, ^{232}Th, ^{238}U as well as ^{90}Y, and ^{165}Ho in soil, calcinated fruit and wash water samples are shown in table 3.6.1.1.

Table 3.6.1.1: *Limit of detection (LOD) and quantification (LOQ) for ^{59}Co, ^{133}Cs, ^{88}Sr, ^{232}Th, ^{238}U, ^{90}Y, and ^{165}Ho measured in soil [mg/kg], calcinated fruit [mg/kg] and wash water [µg/kg].*

	Soil [mg/kg]		Calcinated fruit [mg/kg]		Wash water [µg/kg]	
	LOD	LOQ	LOD	LOQ	LOD	LOQ
^{133}Cs	0.01	0.042	0.003	0.0099	0.001	0.0036
^{59}Co	0.03	0.1	0.0005	0.0018	0.003	0.011
^{88}Sr	1	3.6	0.02	0.078	0.06	0.21
^{232}Th	0.005	0.017	0.001	0.0034	0.0008	0.0028
^{238}U	0.008	0.027	0.0006	0.0021	0.0006	0.0021
^{90}Y	0.004	0.014	0.0007	0.0023	0.004	0.013
^{165}Ho	0.0006	0.0021	0.0007	0.0022	0.0002	0.00066

For the concentration of ^{59}Co, ^{133}Cs, ^{88}Sr, ^{232}Th, ^{238}U in soil and calcinated fruit samples, all measured values were above the limit of quantification. ^{90}Y and ^{165}Ho were above the LOQ in soil, but not in calcinated fruit. For the main analytical elements in the wash water samples, only the measurement of ^{133}Cs and ^{88}Sr were above the LOQ for all measurements. ^{59}Co, ^{232}Th and ^{238}U all had multiple values below the LOD and LOQ, especially for the third round of washing (attachment E.1). Thus, the concentrations of ^{133}Cs and ^{88}Sr were prioritized in the assessment of the wash water itself.

3.4.3 Micro-XRF

To assess and evaluate the extent of deposition of radionuclides on a plant surface, the qualitative and semi-quantitative method Micro-X-ray fluorescence (Micro-XRF) was used. The absorption of X-rays in a sample produces electronically exited ions with a vacant K-shell. After a brief period, the ion returns to its ground state via a series of electronic transitions, characterized by the release of X-radiation (fluorescence) (Skoog et al., 2017b). This produces characteristic X-ray patterns of the excited atoms (Sarret et al., 2013).

XRF data is recorded as an energy spectrum, which counts per second (cps) as a function of energy (eV). Micro-XRF imaging proceeds by recording the emission of these characteristic X-rays on many points on a sample. High resolution optics focus the X-ray beam into a small spot, which is scanned for its full energy spectrum at each scan point (i.e. pixel) (Sarret et al., 2013). The excitation of small sample areas allows for the analysis of inhomogeneous samples, both of special sample areas and in distribution of elements, in one or two dimensions (Haschke, 2014).

The general design of a Micro-XRF detector consists of an excitation source, most often an X-ray tube. The X-rays emitted from the tube then run through a primary optic, which is used to change the energy distribution of the radiation or perform a beam sharpening. The energy distribution can be changed through filters, secondary targets or monochromators. The shape of the beam can be influenced by collimators or secondary X-ray optics. The samples are positioned using a sample tray. Lastly, two Si drift detectors that measures the photons emitted from the sample (Haschke, 2014).

Micro-XRF can be applied in many ways , such as examinations of minerals to determine the element distribution in mineralogical samples, pigment use in art or in forensic investigations (Haschke, 2014). In addition, very small biological samples can be analysed by the technique (Skoog et al., 2017b). To do this, only simple sample preparation is required (Haschke et al., 2012).

3.4.4 Particle size analysis by laser diffraction

For soil particle analysis, laser diffraction was utilized. The principle behind the method is that particles of a given size diffract light through a specific angle. The angle increases with decreasing particle size. When measuring the particle size, a narrow beam of monochromatic light is passed through a sample cell containing an upwards moving suspension. The size distribution is measured with the suspension continuously being pumped around, which ensures random orientation in relation to the laser beam (Beuselinck et al., 1998).

To determine the particle size, two different theories can be utilized: Mia and Fraunhofer. Mia is utilized for smooth, spherical and homogeneous particles that are smaller than 10 μm. Particles larger than 100 μm should be analysed by Fraunhofer. From 10 to 100 μm, the difference are considered inconsequential (Spencer, 2025). In this study, Fraunhofer was used.

3.4.5 X-Ray Diffraction

X-Ray Diffraction (XRD) is an analytical technique used for soil characterization. It provides information on structures, phases, texture and other structural parameters such as average grain size, crystallinity, strain and crystal defects. The most common use of XRD is for identification of unknown crystalline material, but it is used in for example measurements of sample purity, characterization of crystalline materials and identification of fine fine-grained minerals. (Bunaciu et al., 2015).

XRD is based on constructive interference of monochromatic x-rays and a crystalline sample. X-rays are generated in a cathode ray tube, which produces electrons that bombard the target. When the electrons have sufficient energy to dislodge inner shell electrons of the material, a characteristic x-ray spectra is produced, known as a diffractogram (Bunaciu et al., 2015).

3.4.6 CEC

The cation exchange capacity is the measurement of the most important cations in soil. This gives a quantitative assessment of the soil's ability to interact with cations. For many soils, only four cations are used. In order of importance, these are $Ca > Mg > K > Na$. However, in certain cases other cations are included. For example, when the soil is especially acidic, aluminium ions are often included (VanLoon and Duffy, 2017).

The base saturation in soil affects the CEC. In acidic soils, hydronium ions can occupy the cation exchange sites. The base saturation is the relation between metals and hydronium ions on the exchange sites in soils. A low base saturation can cause problems with acidification of the soil. The cation exchange capacity is necessarily a fixed value. In tropical climates in particular, hydrous oxides of iron and aluminium in the clay sized fraction gives the soil a pH-dependent CEC. However, in temperate regions which tend to contain clay minerals such as montmorillonite, the CEC is fixed (VanLoon and Duffy, 2017).

There are multiple different ways of determining the CEC, and the method of determination can impact the resulting value. This study follows a method by Summer and Miller (Sumner and Miller, 1996).

3.5 Calculation of CRs and TFs with SDs

The CRs and TFs were calculated by using the means of a type of fruit divided on the mean concentration with its associated soil (eq. 2 and 3). No weighing factor was used for fruit parts or for the horizontal soil layers. Using the geometric means was also considered, but the difference between the two were deemed too small to justify use, so the use of standard mean calculation was selected.

The standard deviation measurements (SD) were calculated for soil and fruits. For the fruit samples, it was done by calculating the standard deviation of each fruit part using the STDEV function in Excel and adding the squared SD divided by the sample number (eq. 6). The same was done for the soil sample, were the SDs were calculated for each layer using the core samples at different positions. For the singular soil core sample associated with figs, three technical replicates were measured by ICP-MS and used the same way as positions for the other samples.

$$\textit{eq. 6: } SD_{combined} = \sqrt{\left[\frac{SD_{Part\,A}^{2}}{n_{Part\,A}}\right] + \left[\frac{SD_{Part\,B}^{2}}{n_{Part\,B}}\right]}$$

For soil samples, calculating the SD from all the samples instead of individual horizontal layers were also considered. However, this resulted in a small difference, and it was thus decided to calculate SDs the same way as for the fruit samples. SDs for the CR and TF values were calculated the same way, using the relative standard deviation (eq. 7).

$$\textit{eq. 7: } SD_{CR} = CR * \sqrt{\left[\frac{SD_{Soil}}{Mean_{Soil}}\right]^{2} + \left[\frac{SD_{Fruit}}{Mean_{Fruit}}\right]^{2}}$$

The SD for the CR value itself was determined through multiplying the CR by the relative standard deviation, calculated as the root of the SD of soil divided by the mean concentration of soil plus the SD of fruit divided by the mean of the fruit concentration squared. Both the SD and CR values are measured as the concentration of the radionuclide of interest measured in mg/kg.

3.6 Quality assurance and statistical methods

3.6.1 Quality assurance of quantitative methods

To ensure quality of the results, a range of different methods was used. For samples of both soil and fruit, concentrations were measured quantitatively using ICP-MS. For soil samples, with one exception, one measurement was taken for each horizontal layer at each core position. For figs, where only one soil core sample was taken, three technical replicates of the same sample were used. The replicates of figs also help to assess the precision of ICP-MS measurement itself.

To guarantee that the decomposition of samples has been a success, many different methods was used. For example, when measuring soil, the Y/Ho ratio can be used. These elements have a stable ratio for all soils. The ratio of Y/Ho is around 26 (Leggett, 2017). If the ratio is normally distributed around 26, it is a sign that the digestion of the soil samples has been a success. Making a histogram resulted in a figure showing a normal distribution with an average concentration in all measured soil samples of 26.2 (attachment B.9). In addition to the Y/Ho ratio, certified reference materials, internal standards and precision evaluations were checked for ICP-MS analysis.

Certified reference materials

Certified reference materials (CRMs) were used to ensure quality of digestion in ICP-MS analysis. The concentration of a CRM can be determined through analysis with a previously validated measurement method, analysis of two or more independent and reliable measurement methods or analysis of a network of cooperating laboratories knowledgeable of the tested material (Skoog et al., 2022a).

For soil samples, four CRMs were measured, with only three used in the analysis. This is because the reference material *IAEA 448* is only certified for ^{226}Ra, which was not measured. The three CRMs analysed, *NCS DC 73324a, NIST 2711a* and *NCS ZC 73007* were all elements of interest in the range of the certification (attachment B.7).

For fruit samples, both *NCS ZC 73036a* and *NIST 1570a* had all refence values within the range. However, the reference material *NIST 1633a*, a fly ash sample, did give a single result within the range of the certified material (attachment B.8). The reasons for this might be a measurement mistake, or that the material did not sufficiently digest using only HNO_3. However, no single reason could be identified. But since both other CRMs were good, the digestion was deemed satisfactory.

For wash water samples, all CRMs for the elements of interest were either close to or within the certified range (attachment E.3). Values close to the reference value were from Sr measurements of *NCS DC 7332a* and *NCS ZC 73007,* which was measured to 21 000 μg/kg and 47 500 μg/kg respectively. This was just outside the range of 30 000 ± 4000 μg/kg and 68 000 ± 4000 for Sr. In addition, U measured just outside the range of NCS ZC 73007 measuring 4000 μg/kg, with the reference value being 5 900 ± 300 μg/kg. Overall, the reference materials indicate a successful digestion of samples.

Internal standards

To correct for instrument drift, instabilities and matrix effects in ICP-MS, an internal standard (IS) is used. The internal standard is an element that is absent from the samples and has an ionization potential near the measured analytes. Most often, ions such as ^{115}In, ^{113}In and ^{103}Rh are used. They are in the central mass range, while being rare to find in naturally occurring samples (Skoog et al., 2017a). This study uses Rh, and Ir as internal standards.

Precision

Precision is a measurement of the reproducibility of measurements, also described as the closeness of results that have been obtained in exactly the same way (Skoog et al., 2022a). The precision in this study is given as the standard deviation SD, or as the relative standard deviation (RSD). The RSD is found by taking the SD and dividing it on the mean of the measured samples. This often gives a clearer picture than using the absolute SD (Skoog et al., 2022b). In this study, the RSD is given as a percentage (%).

For the measured soil samples, excluding fig associated soil, the RSD varied between 3% and 38% on site 2 and 7% and 33% on site 1. Both highest measurements were for Sr; when excluding Sr, the highest level on any site was 19. In soil core samples associated with figs, where only technical replicates were taken, the RSD varied between 2% and 5% (attachment B.4). This indicates that there was no problem with the method itself, and the variation comes from differences in the samples.

In calcinated samples where the concentration is calculated by wet weight, the RSD varied between 47% and 94% for fruits prepared by the conventional method of pre-treatment, while it varied between 3% and 33% for samples prepared by an ultrasonic bath (attachment B.5). When the dry weights were used to calculate TFs, the conventional method varied between 3% and 85%, and the ultrasonic method retrieved an RSD between 23% and 129% (attachment B.6).

For the wash water results, the ultrasonic bath had an RSD between 4% and 108% for the ultrasonic bath (attachment E.2). SDs and RSDs were not calculated for the conventional method, since only one replicate was used.

3.6.2 Data treatment and statistical approach

The dataset warranted the comparison between categorical and response variables. This constitutes using ANOVA and two factor t-tests when analysing. However, using the ANOVA or a t-test requires meeting certain prerequisites. The samples need to be independently drawn from a population, can be described by a normal distribution, and the standard deviation of both groups must be equal (Montgomery, 2020).

Since normality often was not met, and the sample size was deemed too small for ANOVA, the Kruskal Wallice Test was performed. It is a non-parametric alternative to ANOVA, which instead of basing itself upon means, ranks the observations in ascending order and replaces each observation by its rank (Montgomery, 2020). For a pot hoc analysis, Dunn's test was used, adjusted by the Bonferroni method. In this study, a 5% significance level ($p < 0.05$) was set for all comparisons between groups.

The statistical software used in this study was R-studio version 4.4.2 (2024-10-31 ucrt). R-studio was not only used for the statistical analysis, but also for making figures. The packages used to make figures and for data treatment and statistics were "readxl" to import datasets, "tidyverse", "dplyr", "FSA" and "broom" for data treatment, "ggplot2" to make figures, "ggthemes" for figure aesthetics and, "gridExtra" for gathering multiple charts to one figure. In addition, 'leaflet' was used for making maps.

Tables were done in Microsoft Excel Version 2501. Calculations were also mostly done in Excel. The functions used in Excel were STDEV to determine the standard deviation, AVERAGE to determine means, SUM to add values together, MAX to determine the highest values, MIN to determine the lowest, and GEOMEAN to determine the geometric mean.

3.7 Use of AI and previous work

In this report, generative artificial intelligence (AI) has been used. All data and information have been processed according to the NMBU guidelines. I, Martin Hansebråten, as the author of this thesis take full responsibility for its content, claims and references. The use of AI was limited in this thesis for the coding process in R-studio, mainly for checking errors in the R-script code. The SIKT KI-chat tool, the recommended AI tool by NMBU, was used for this task (Dahl, 2024). In addition, Microsoft Copilot was used when SIKT KI-chat provided unsatisfactory results.

Some of the work in this thesis is based upon work done in the courses MINA310 (Methods in Natural Sciences), which laid the groundwork for the introduction, and STIN300 (Statistical Programming in R), where the programming for the soil analysis results by ICP-MS was done.

4. Results and discussion

4.1 Concentration ratios and transfer factors

4.1.1 Concentration ratios

The concentration ratios measured were calculated using the wet weight of the fruit. The CR was calculated for dates, figs, olives and prickly pears. The figs samples and olive samples were divided into the method of pre-treatment for figs and the site for olives to compare the two. A bar plot of the CR in ^{59}Co, ^{133}Cs, ^{88}Sr, ^{232}Th and ^{238}U is shown in figure 4.1.1.
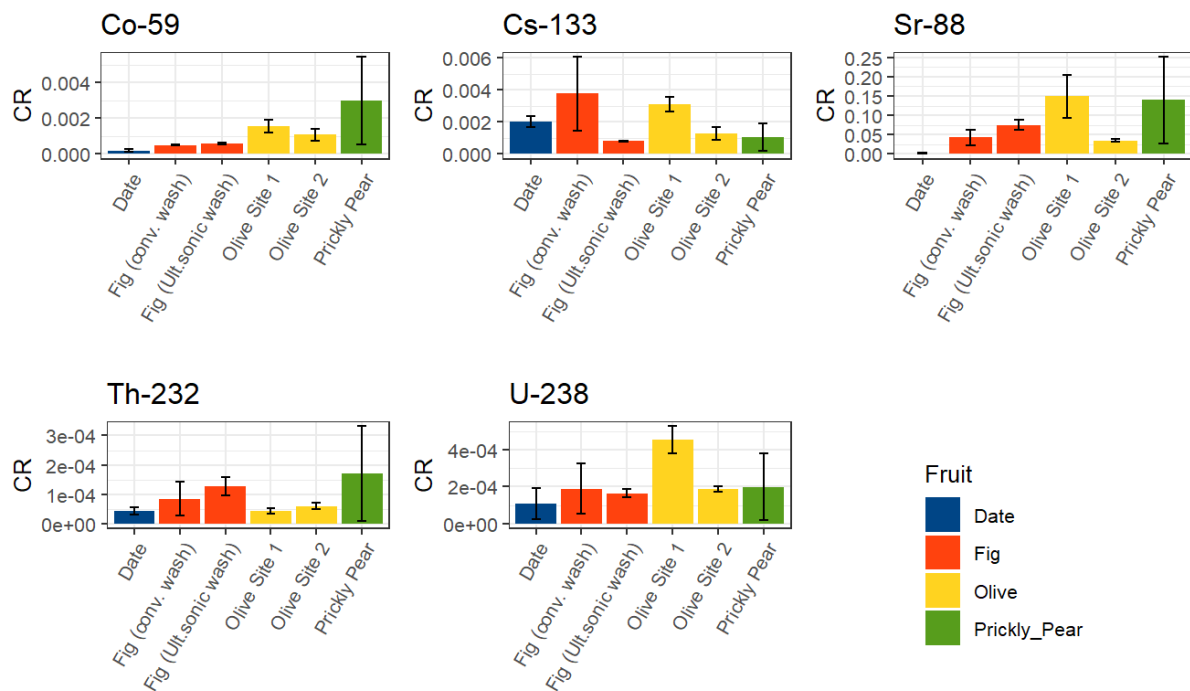
Figure 4.1.1: *Concentration ratios (CRs) of the five elements of interest, ^{59}Co, ^{133}Cs, ^{88}Sr, ^{232}Th and ^{238}U in the four measured fruits dates, figs, olives and prickly pears. The error bars are the SD for each group, with the fruit at different situations as the categorical variable and the CR as the response variable.*

In general, the highest measured CRs was found for ^{88}Sr (range 1.44×10^{-3} - 1.49×10^{-1}), whilst the lowest were found for ^{232}Th (range 4.23×10^{-5} - 1.70×10^{-4}) (attachment G.2). For olives at site 1 and site 2, except for ^{232}Th, all other elements had a higher CR at site1 than at site 2. Since site 1 is by a road, the source of this is most likely particles from the road settling on the plant material CR. For figs, the two washing procedures also is indicated to have differences in the resulting CR. Apart from ^{59}Co, the SD was smaller for all elements washed with the ultrasonic method of pre-treatment (attachment G.2).

4.1.2 Transfer factors

To follow the guidelines of the CRP K41022 which focuses on CR values, this study focuses on the measured wet weights of plants. However, the TF, using dry weight instead of wet weights is important information and a common way to report soil to plant transfer. Therefore, values of TF were measured and presented in attachments G1 and G3.

The measured TFs is an order of magnitude smaller than the CR. A corresponding figure as figure 4.1.1, is shown in attachment G.1. For all measured TFs, the highest ratio was found for ^{88}Sr with a TF of 8.69×10^{-1}. The lowest was found for ^{59}Co in dates measuring 5.63×10^{-6} (attachment G.3). All SDs were lower for the ultrasonic method except ^{59}Co, the same pattern as for the calculated CRs.

4.1.3 Comparison with IAEA and other reporting in the CRP

To compare the CR values found in this study to other findings, multiple sources was used. In IAEA's *Handbook of Parameter Values for the Prediction of Radionuclide Transfer in Terrestrial and Freshwater Environments,* data for the transfer of some of the radionuclides of interest can be found for temperate climates (IAEA, 2014). In addition, other reported CRs for arid and semi-arid areas has been published, as part of the CRP.

The reported CR value for Cs of fruits in woody trees for temperate regions is 5.8×10^{-3} with the range between 8.6×10^{-4} and 8.0×10^{-2} (IAEA, 2014) The Cs concentration found in dates, olives at both sites, and figs using a conventional pre-treatment all fell within IAEAs range for temperate areas. Figs treated by ultrasonic washing were below the range, measuring 7.6×10^{-4}. The CR for Co in loam soil for woody trees given by IAEA was 4.8×10^{-3} (IAEA, 2014), which is higher than any measured CR for ^{59}Co in this study.

For Sr, IAEA reports an average 1.7×10^{-2} with the minimum value being 1.2×10^{-3} and the maximum value being 7.0×10^{-2} for all soils in the terrestrial environment (IAEA, 2014). Apart from figs washed with ultrasonic washing, which measured to 7.48×10^{-2}, all measured values were within the range of IAEA values. Compared to the average, figs had a higher Sr ratio than the average, with dates and olives being measured as lower than the average reported by IAEA in temperate regions.

Dirican et. al, (2024) as part of the CRP reported a TF for ^{238}U of 0.08 and a TF of 0.030 for ^{232}Th in apples in Turkey. This reporting is higher than all measured CR and TF values in this study. This might be the result of different fruits, area, soil type etc. In addition, the washing procedure used might have played a difference. While this study used methods of ultrasonic baths, the study reported that the samples were washed with distilled water (Dirican et al., 2024).

CRs for Abu Dhabi date palms have been reported by Raj et. al (2022). For date fruits, the reported CR was 0.08 for ^{238}U and ^{226}Ra and 0.17 for ^{232}Th and ^{228}Ra (Raj et al., 2022). Both are higher than the measured ratios of ^{238}U and ^{232}Th in this study. However, Raj et. al reports large variances in the measurements, and problems with detection limits, which might give an overestimation. In addition, this study also includes the bone of the date fruit in the measurement, which possibly decreases the calculated CR.

In general, the calculated CRs found in this study tend to be lower than other reported in the CRP, but within IAEAs ranges for temperate environments, indicating that transfer pattern in Tabernas may act like temperate environments. However, finding comparable values to the ones measured in this study proved difficult at this stage, since few studies had comparable fruits in comparable areas. Because of this, drawing any definite conclusion is impossible.

4.1.4 Representativity of CRs

There are multiple limitations to CRs. In this thesis, one challenge is the representability of data. The CR come from only two sites in the Tabernas area and more data are needed to get a better understanding of the variation. In further research, samples from more sites in Tabernas and Andalucía should be taken to get a stronger statistical background for the CR calculated.

Use of calcination is a source of uncertainty for TFs and CRs. Calcination of biological samples before ICP-MS is not necessary when measuring the concentration of radionuclides and stable analogues. The technique is sensitive enough that the samples may be digested directly instead of calcinating them. The oven used in the calcination process can be a source of elemental loss and cross contamination, which might affect precision and accuracy of the results.

Large variance for prickly pears is most likely a result of the low sample number. Because of one sample having negative numbers, only two replicates of the fruit samples were used to calculate the CR for prickly pears. This suggest that using only three replicates of fruit samples it too small. In addition, only using three replicates makes statistical analysis more difficult, since statistical tools such as ANOVA requires larger datasets, and small datasets makes it difficult to prove requirements such as normality.

There are many parameters that can affect the final CR; factors such as the positions of the soil core, the depth of the measured soil, the sample site, the mineralogy and the pre-treatment all can change the final CR The next chapters assess the different parameters and how they affect the CRs in this study.

4.2 Parameters influencing CRs

4.2.1 Soil heterogeneities

To assess heterogeneities in soil, soil core samples of dates was selected because of its comprehensive sampling. The resulting sample number comes from the layers (n = 4). The boxplot of the concentrations of the radionuclides and stable analogues of interest, ^{59}Co, ^{133}Cs, ^{88}Sr; ^{232}Th and ^{238}U is shown in figure 4.2.1.
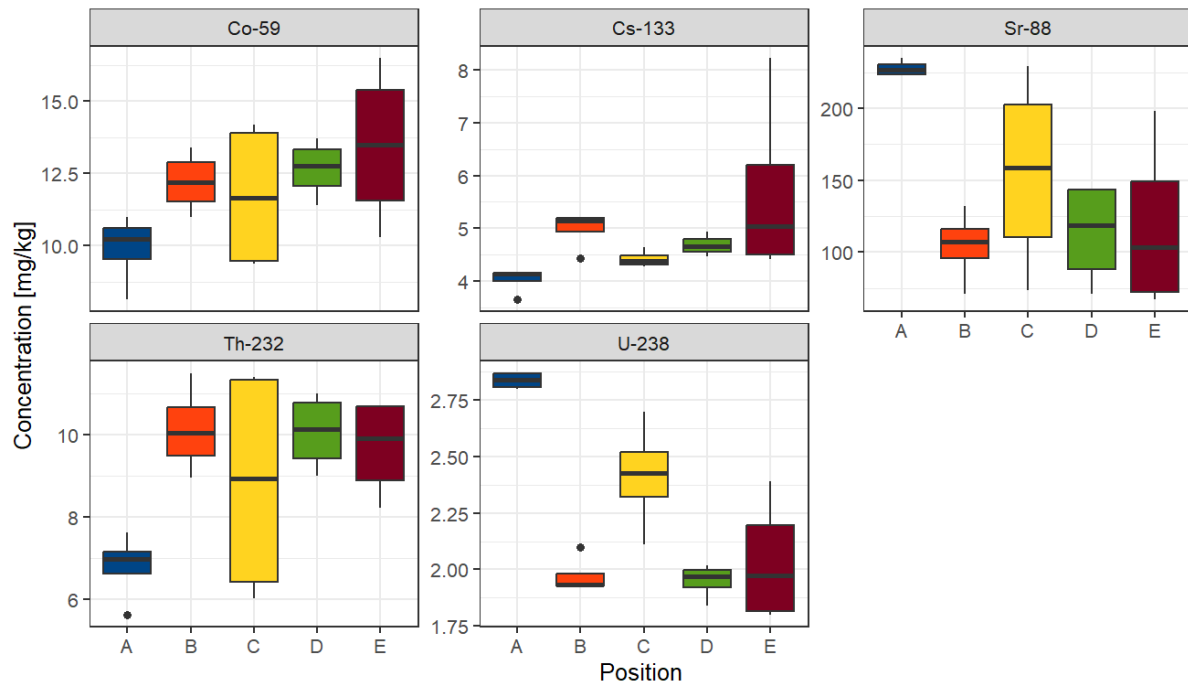
Figure 4.2.1: *Boxplot of the concentration [mg/kg] of ^{59}Co, ^{133}Cs, ^{88}Sr, ^{232}Th and ^{238}U on soil core position A, B, C, D and E in dates at site 2. Site E is closest to the plant followed by A, B, C and D furthest away from the stem. The position is the categorical variable, and the response variable is the concentration of the radionuclide.*

Position C and E had a wider variation than the other positions in the date soil core samples. No significant difference was found for ^{232}Th (p = 0.1583), ^{59}Co (p = 0.2106) and ^{88}Sr (p = 0.06102). However, significant differences were found for ^{238}U (p = 0.008651) and ^{133}Cs (p = 0.01377).

For ^{238}U a significant difference was found between position A and B (p = 0.0338) and between position A and D (p = 0.0494). A and E (p = 0.0651) showed no significant difference, but the p-value was close to 0.05. All other comparisons for U were above p = 0.1. For ^{133}Cs, a significant difference was found between position A and B (p = 0.0297) and between position A and E (p = 0.0496).

There is a significant difference between different soil core positions for ^{238}U and ^{133}Cs. This is an indication that the soil is heterogenous. Multiple soil core samples should be taken to account for this heterogeneity, supporting IAEAs (2024) recommendations for the sampling process.

4.2.3 Impact of soil depth on CRs

Concentrations differences between horizontal layers in soil

From the dataset, four horizontal layers were compared in date samples at site 2. Date samples were used since it had the most comprehensive soil core sample collection (n = 5) for each layer (fig. 4.2.2).
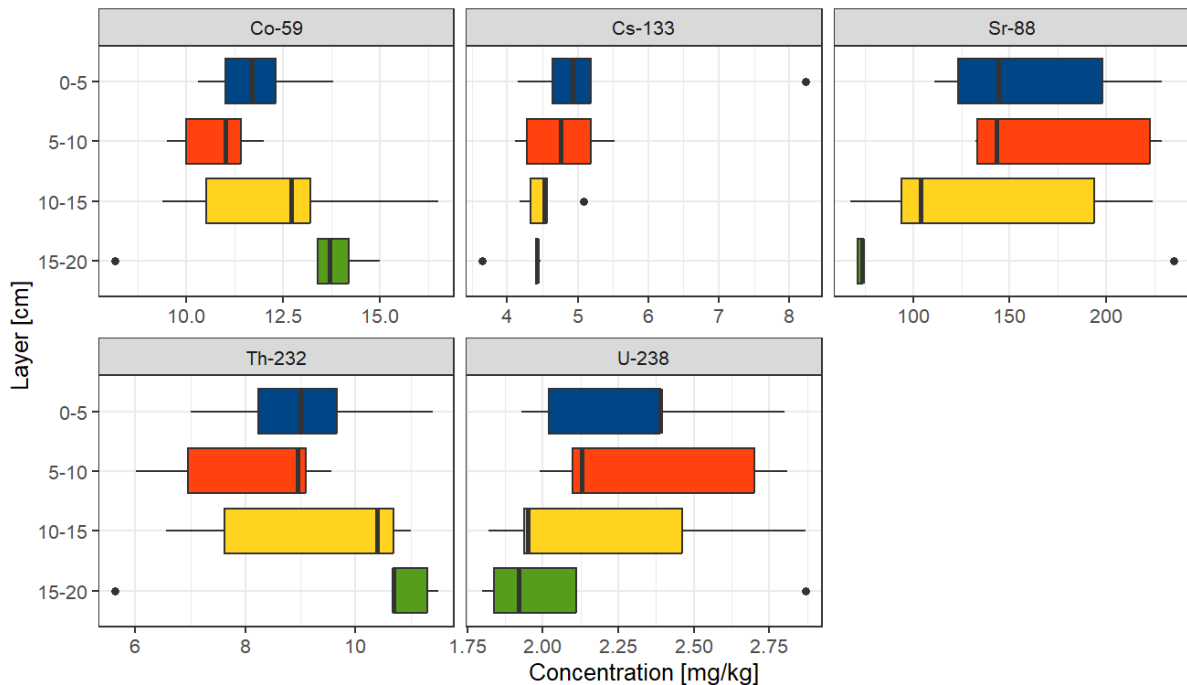
Figure 4.2.2*: Boxplot of the concentration [mg/kg] of radionuclides and stable analogues by soil depth. ^{59}Co, ^{133}Cs, ^{88}Sr, ^{232}Th and ^{238}U at in soil associated with dates with the horizontal layer [cm] as the categorical variable, and the measured concentration as the response variable.*

No significant difference was found between the horizontal layers in soils associated with dates for ^{238}U (p = 0.5513), ^{232}Th (p = 0.3435), ^{88}Sr (p = 0.235), ^{59}Co (p = 0.3272) or ^{133}Cs (p = 0.3302). This indicates that in Tabernas, the soil depth has a limited impact on the concentration, and no weighing factor needs to be used when calculating the CR for a specific type of fruit. In future studies, the need for measuring different layers in the analysed area might be unnecessary, and composite samples may be sufficient based on this data.

Loss on ignition and dry weight in date samples

The LOI and the dry weight was measured at the same time as the particle size analysis was done. This gives qualitative data for the different depth levels. The dry weights and LOI for the four depth levels and the merged sample for all four, are given in table 4.2.3.

Table 4.2.3: *Dry weight (DW) [%] and loss on ignition (LOI) [%] for the four horizontal levels as well as a merged sample from all horizontal levels in soil associated to dates. The weights used are shown in attachment A1:*

Sample	DW (%)	LOI (%)
Merged	99.5	5.9
0-5	99.3	8.9
5-10	99.6	5.7
10-15	99.8	3.4
15-20	99.8	3.0

The general tendency seems to be that the LOI are the highest at the higher depth levels, with the LOI percentage decreasing for each layer, with the highest LOI being the 0-5 layer with 8.91% and the lowest being 15-20 with 3.03%. This indicates that there is a decrease of organic matter with depth, which is expected from the study area. The dry weight is relatively consistent but increasing slightly for lower depth levels.

Particle size for horizontal layers

A particle size analysis was done for merged samples of date associated soil cores. Merged samples were because of lack of sample material. Identifying the clay fraction as <4 nm, the particle size was largest in the silt fraction of the soil. For the 0-5 cm layer it represented 81.8%, for the 5-10 cm layer it represented 83.2%, for the 10-15 cm layer it was 83.6% and for the 15-20 cm layer it represented 85.1%.

The clay fraction, which is most mobile represented between 7.69 % and 10.99 % when the clay diffraction is defined as <4 nm. The 0-5 cm layer had the highest percentage of 10.99 %, with the percentage decreasing for each horizontal layer (attachment A.3) This indicates that LMM species are more apparent in the 0-5 layer than deeper in the ground. However, because of the low number of samples, this cannot be statistically verified in this study.

Even though the samples were wet sieved at 63µm, there was still residues of larger fractions of soil. This is mainly caused by the shape of the soil particles, which can still be part of the sieved fraction, because of irregular shapes of the particles.

CEC for horizontal layers

A significant difference was found for CEC in all soil at site 2 (p = 0.01694), with a significant difference between the 5-10 and 15-20 cm layers (p = 0.0498). This is an indication that there is a difference between the CEC of horizontal layers within a site. However, since the p-value is close to 0.05, and the sample size is very low (n = 3), a consistent difference between other layers than between 5-10 and 15-20 at site 2 cannot be proven.

4.2.4 Impact of measurement sites

Concentration difference in soil

To compare site 1 and 2, the samples of soil associated with sampling of olives were selected. A boxplot of the difference in concentration between the two areas are shown in figure 4.2.4.
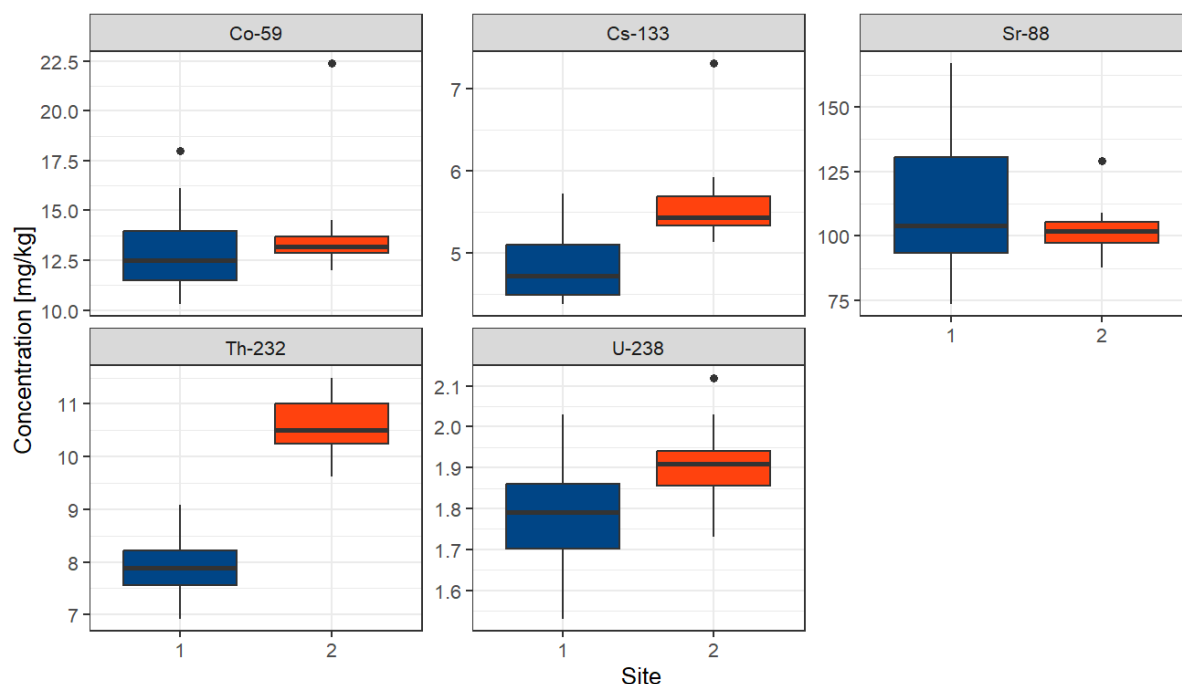
Figure 4.2.4: *Concentration of radionuclides and stable analogues at the two measured sites: Boxplots of stable Co, Cs, Sr; ^{232}Th and ^{238}U, with site 1 (Blue) or 2 (Red) as the categorical variable, and concentration in [mg/kg] as the response variable.*

A significant difference ($p < 0.05$) was shown between site 1 and site 2 for ^{232}Th ($p = 0.03877$) and ^{133}Cs ($p = 0.0135$). A little counterintuitive to the appearance of the plot (fig. 4.2.4), ^{88}Sr also showed a significant difference ($p = 0.01634$), This might have to do with the low sample size, increasing the risk of false positives. The concentration at site 2 was larger for all significant elements. ^{238}U ($p = 0.3504$) and ^{59}Co ($p = 0.0875$) did not show a significant difference. When selecting soil associated with olives, no significant difference was found for the CEC ($p = 0.119$) between the two sites. However, some cations associated with CEC had significant differences such as Na ($p = 0.1107$), K ($p = 0.009375$) and Mg ($p = 0.02434$). This suggest that even though differences in the concentrations of individual cations are found, the CEC itself are relatively stable from site to site in Tabernas .

The significant difference in concentration between elements measured point to there being the need of using multiple samples sites in future studies. In addition, there is a difference between the resulting CRs measured at the two sites, which also suggest more sample areas are in order. However, it is important to note that this part of a larger project, and data going into a database with similar measured values from many sites across the world, which partially resolves this weakness.

4.2.5 Impact of mineralogy on CR.

Using ICP-MS and micro-XRF results as well as literature data, likely candidates for minerals were first selected. The chemical formulas of the minerals are given as ideal formulas and are taken from mindat.org (retrieved 2025-03-17 at 1:13pm). The diffractograms for the five samples is shown in Attachment C.1.

The 14 Å and 7 Å peaks first and second order diffraction for Chlorite/Vermiculite are well defined. In the higher regions, the most noticeable peaks are found for Quartz *(SiO$_2$) and* Illite/Muscovite *(KAl$_2$(AlSi$_3$O$_{10}$)(OH)$_2$)*. For the rest of the major elements, only few peaks are found, and is not found in all samples. This is the case for. Paragonite *(NaAl$_2$(AlSi$_3$O$_{10}$)(OH)$_2$)*, Calcite *(CaCO$_3$)*, and Orthoclase *(K(AlSi$_3$O$_8$))* are also found. All these peaks are marked in the diffractogram (Attachment C.1.)

In addition, there are minor elements, that is not shown on the diffractogram. These are mineral phases that exist within other peaks, and/or exist in only trace amounts and can only be found in a few of the diffractograms. These are Dolomite *(CaMg(CO$_3$)$_2$)*, Rhodochrosite *(MnCO$_3$)*, and Titanite *(CaTi(SiO$_4$))*. Gibbsite *(Al(OH)$_3$)*, which is found is found at the 4.8 Å peak in the diffractogram is overshadowed by Chlorite at the same peak. However, because of the high levels of aluminium in the soil samples, it is certain that there is Gibbsite in the samples. There is also a possible presence of smectite minerals indicated by the peaks at 15.8 Å and 8 Å.

The results of qualitative and quantitative analysis are given in Table 4.2.5. Paragonite is assumed to only be in trace amount due to indications of low levels of sodium from the XRF data.

Table 4.2.5: Results from XRD analysis comprising the phases identified and Rietveld quantification [wt%]. The X mark means that the mineral phase was not found or is under the detection limit. The first letters mean the fruit; olive (O), fig (F), date (D) and prickly pear (CH). The middle number is of the site, and the last letter is the position of the soil core. No letter is given to F, since there was only one soil core taken.

Sample ID	O1E (%)	O2A (%)	F2 (%)	D2E (%)	CH2C (%)
Quartz SiO_2	64.58	66.97	58.67	51.62	67.5
Illite/Muscovite $KAl_2(AlSi_3O_{10})(OH)_2$	22.14	25.32	22.92	34.18	26.03
Calcite $CaCO_3$	x	4.33	0.71	5.2	1.03
Dolomite $CaMg(CO_3)_2$	0.13	0.21	0.58	x	x
Rhodochrosite $MnCO_3$	x	0.49	x	x	3.81
Chlorite/Vermiculite	3.99	1.58	10.99	9	1.3
Titanite $CaTi(SiO_4)$	4.09	x	x	x	1.64
Orthoclase $K(AlSi_3O_8)$	5.07	1.1	x	x	x
Gibbsite $Al(OH)_3$	x	x	2.95	x	2.47

The wt% was higher than the LOD for Quartz, Illite/Muscovite and Chlorite/Vermiculite The largest fraction for all samples were Quartz, which ranged from 51.62% for soil associated with dates, to 67.5% for prickly pears. For Illite/Muscovite the wt% ranged from 22.14% in olives at site 1 to 34.18% in date samples. For the mineral fractions Calcite, Dolomite, Rhodochrosite, Titanite, Orthoclase and Gibbsite in all samples represent less than 5.2% and are not found in all of them. No gypsum was found in the soil samples, counter to the theoretical composition of the soil in the area.

For the analysis of XRD data, other supporting data from XRF and ICP-MS proved valuable, making the XRD analysis simpler. For example, Paragonite which is related to Muscovite could be found in the diffractogram. However, since the concentration of Na is small, as shown in the XRF and ICP-MS data there cannot be more than trace amounts of Paragonite in the mineral fraction.

4.2.6 Impact of fruit part on the CR

The part of the fruit used in the calculation of CR can potentially have a large impact on the resulting CRs Figs and prickly pears were split into the skin and fruit pulp (fig 4.2.6), while olives and dates were split into bone and fruit pulp.
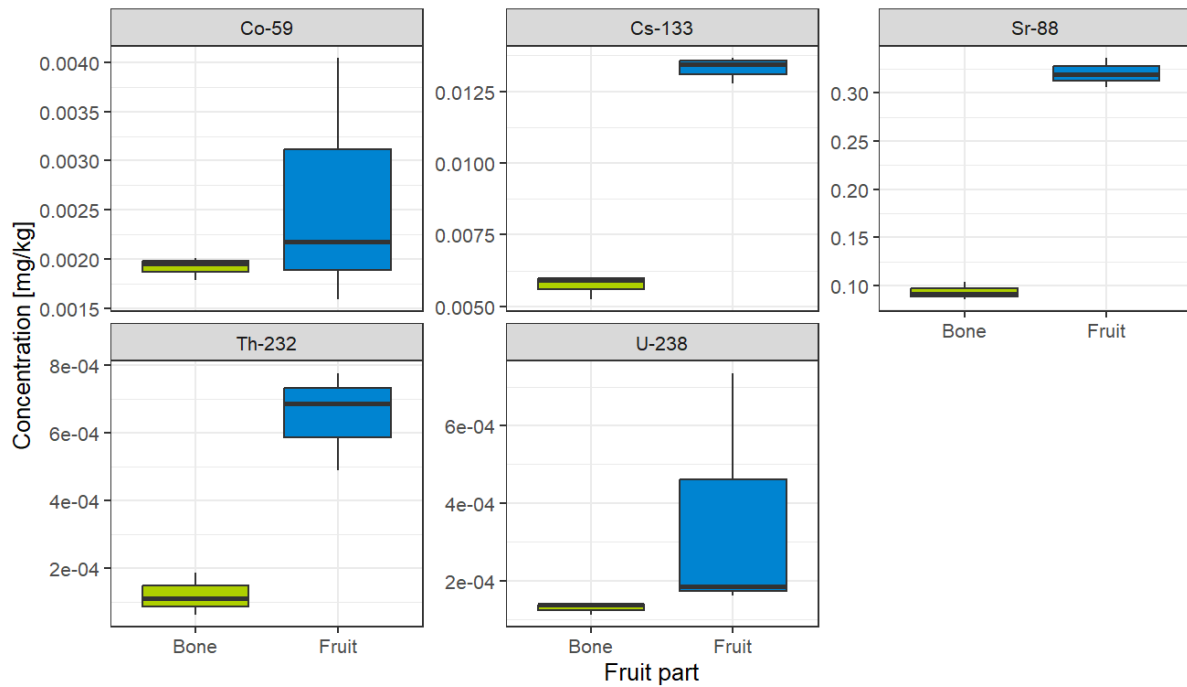
Figure 4.2.6: *Difference in concentration [mg/kg] of ^{59}Co, ^{133}Cs, ^{88}Sr, ^{232}Th and ^{238}U in bone and fruit pulp (fruit) samples for dates washed by ultrasonic pre-treatment. The concentration is the response variable, and the part of the date is the categorical variable.*

Concentrations of ^{133}Cs, ^{88}Sr, ^{232}Th and ^{238}U in pulp of fruits were significantly ($p = 0.4953$) higher than in bones (fig 4.2.6.). The only element not to be significant was ^{59}Co ($p = 0.5127$). Admittedly, the number of samples in each group is limited ($n=3$). However, it is a clear indication that there is significantly higher concentration of the measured radionuclides in the fruit pulp of figs.

For olives ($n = 6$), a significant difference was found between fruit and bone for ^{238}U ($p = 0.00617$), ^{232}Th ($p = 0.003948$) and ^{133}Cs ($p = 0.003948$). Concentrations of these radionuclides were significantly higher in fruit than in bone. No significant difference was found for ^{59}Co ($p = 0.631$) and ^{88}Sr ($p = 0.1093$).

The difference between fruit and fruit skin was measured in figs and prickly pears. For the assessment of skin and fruit, figs were selected because it was washed by both methods of pre-treatment, giving a larger sample size.
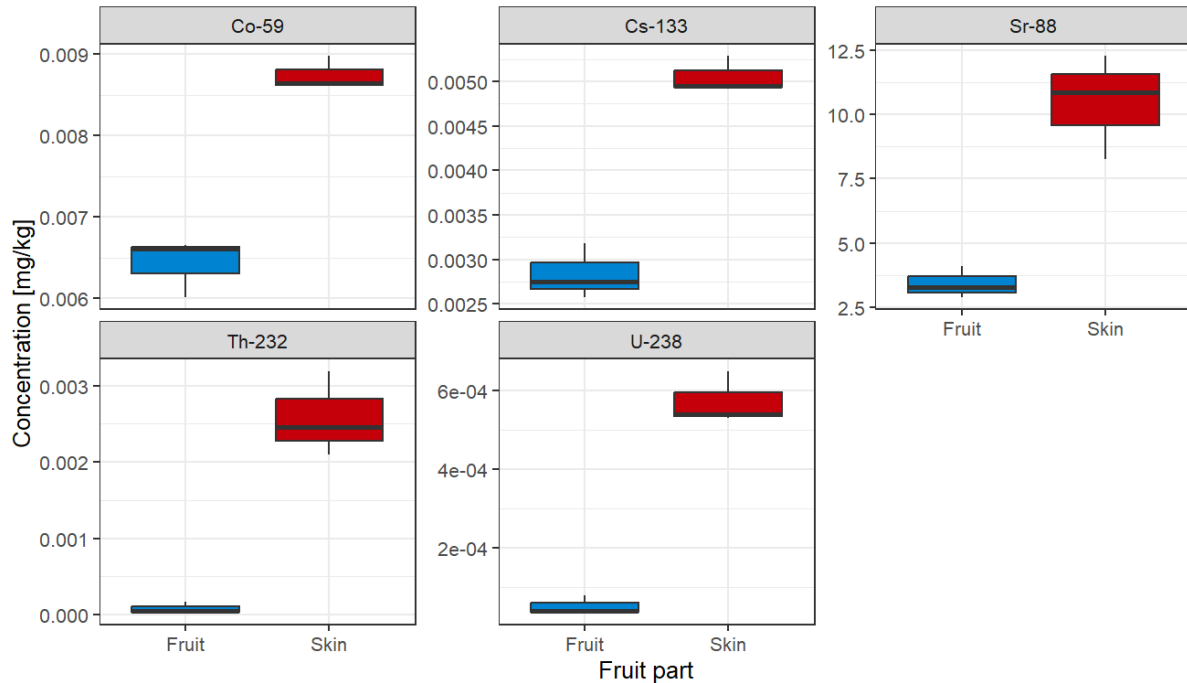
Figure 4.2.7: *Difference in concentration [mg/kg] of ^{59}Co, ^{133}Cs, ^{88}Sr, ^{232}Th and ^{238}U in fruit pulp (fruit) and fruit skin samples for figs washed by ultrasonic pre-treatment. The concentration is the response variable, and the part of the date is the categorical variable.*

When assessing figs washed only with ultrasonic washing (n = 3) all elements of interest showed a significant difference (p = 0.04953 for all elements) with the highest average concentration being in the fruit skin (fig 4.2.7). Including the samples of figs washed conventionally (n = 6) ^{88}Sr (p = 0.02497) and ^{232}Th (p = 0.01631) both showed a significant difference with the highest concentration being in the skin part. No significant differences were observed for^{59}Co (p = 0.7488) and ^{133}Cs (p = 0.4233). No significant difference was showed for ^{238}U (p = 0.05466), but the p value was on the edge of 5% significance value set.

There is a tendency that the highest concentration of radionuclides is found in the fruit skin, second highest in fruit pulp and lowest in bone in dates, olives and figs. Using the bone of the fruit as part of the calculated CR value, might be excluded from the CR in the future; the bone is it not consumed directly by humans, and using it might result in an underestimate of final TFs or CRs.

The impact of the fruit part seems to be larger than the one of the soil heterogeneities. While some soil core samples differed, there was a clear difference in every case when assessing the fruit part. While in this study, no weighing factor was used, the difference between the concentrations may warrant using a weighing factor in future studies, either by calculating inventory or by using merged samples of fruit pulp and skin (the edible part of the fruit).

4.3 Impact of pre-treatment procedures.

To assess the difference between the two methods of pre-treatment of fruit samples, both wash water and fruit skin samples were assessed. Figs underwent both methods of pre-treatment with skin and wash water samples being collected for both methods, making it the focus of the comparison.

4.3.1 Impact of number of washings and wash water differences

The results indicate a higher concentration of the selected elements in the measured wash water for the conventional washing. While the wash procedures for example retrieved 5.83 µg of ^{59}Co in the first wash, for the ultrasonic wash the mean total value was just 0.006 µg.

For figs washed by ultrasonic washing, the RSD varied between 4% and 50%. There was also a small difference between the means for each wash for the ultrasonic bath. This made it impossible to assess any difference between the number of washes, and no clear indication was established that there was any difference between the first, second and third wash of the fruit sample. However, there was an indication of a difference in the conventional washing with the wash water from the first wash containing 13.3 µg of total ^{133}Cs, and the second and third wash containing 0.538 and 2.29 µg respectively.

The wide SD and RSDs most likely comes from problems during the digestion of the samples. During the evaporation of the wash water samples, one of the highly concentrated samples from the conventional washing of figs bubbled over causing cross contamination. All evaporated sample tubes were cleaned with a Q-Tip that had been washed in a 15% acid. This should normally not be done, however there was so much cross contamination that it was deemed necessary. This gives doubt to the results from the wash water analysis.

Due to problems with the digestion, large SDs and RSD, many values below LOQ, and relatively similar means, making any strong conclusion based on the wash water alone is impossible. The evaluation of the washing procedure will therefore lean on differences between the calcinated fruit skin samples measured by the two methods.

The measured samples that were washed conventionally also had a high level of lead in them (attachment E.1). This is probably due to some mistake in the treatment of samples and is not from the method itself. It indicates a source of contamination from somewhere, for example, from the handling of lead before in another project before starting the work on the conventional pre-treatment. However, the source of the contamination could not be verified.

4.3.2 Impact of pre-treatment method

While the RSD of calcinated samples of skin and fruit varied between 7% for Co, and 24% for Th when using the ultrasonic methos, the RSD varies between 23% for Sr and 115% for Co when washing fruits by the conventional method (Attachment B.4). For certain elements, such as Cs and U, this is also apparent when looking at the resulting CRs.
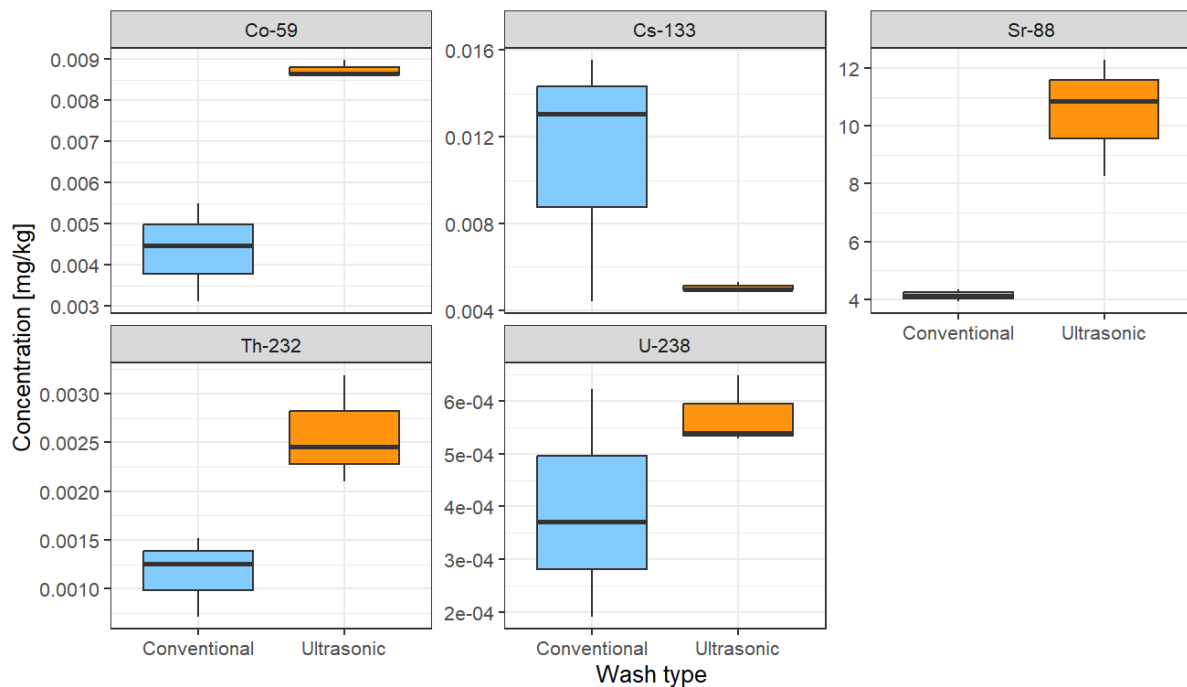
Figure 4.3.1: *Difference in concentration [µg/kg] of ^{59}Co, ^{133}Cs, ^{88}Sr, ^{232}Th and ^{238}U in fig skin samples at site 2 measured by conventional and ultrasonic washing. The concentrations are the response variable, with the washing procedures being the categorical.*

A larger variation shows is apparent in the fruit skin samples of ^{59}Co, ^{133}Cs and ^{238}U, with the variation being similar for ^{232}Th. The opposite was the case for ^{88}Sr with a much smaller variation for the conventional method. Looking at the resulting CRs, the variation seems larger for ^{133}Cs, ^{238}U and ^{232}Th for the conventional mean of pre-treatment (fig. 4.1.1).

A significant difference was shown for ^{88}Sr, ^{59}Co and ^{232}Th, comparing the washing procedures for figs. All had a p-value of p = 0.04953. However, it is important to note that the sample size is only three, which is a source of uncertainty. In ^{238}U (p = 0.2752), and ^{133}Cs (p = 0.5127) the difference in concentration were not statistically significant, but the variation is wider for the conventional method.

For all these samples, the concentration of the elements in the ultrasonic method tends to be higher, while the variation is wider for the conventional method. This indicates that the ultrasonic method removes less of the surface layer contamination but providing higher precision of measurements. There is scope for improved washing procedures in the pre-treatment of fruit samples when measuring samples for CRs. Because of its higher precision, and the already low CRs compared to other reported values, the ultrasonic method seems more robust.

How the calculated CR relates the "real-life" uptake in humans, are difficult to assess. How different fruits are treated before they are consumed varies from place to place and from fruit to fruit. This poses problems when using a standardized method for measuring CRs to measure the final uptake of a radionuclide to humans. However, having a degree of standardization, e.g using similar washing procedures and sampling methods, makes comparison between laboratories and areas easier.

4.4 Elemental deposition

Four samples of fruit skin washed by ultrasonic washing were analysed by micro-XRF. One sample of dates, one of figs, and two of olives at the two sample sites. In the mapping, a middle hight was chosen for every sample in relation to the crevasses on the fruit when adjusting the measuring lens. Using high and low points was also tested, but no visible difference was found in the resulting images.

4.4.1 Olive samples

Skin of an olive at site 1 was analysed by Micro-XRF. The most abundant elements in the sample are K, Ca, and Cl which represent 79.2, 12.8 and 3.9 normalised % mass, respectively. However, it is important to note that these are semi-quantitative data, that for example don't include H, C and O, meaning that these values are much lower in reality. Elements such as Fe, Al, and Si, which are commonly found in the minerals in the account for a much smaller part of the total concentration of elements in the sample, with none of these elements being above 1%. A map of the surface of the olive sample at site 1 is shown in figure 4.4.1.
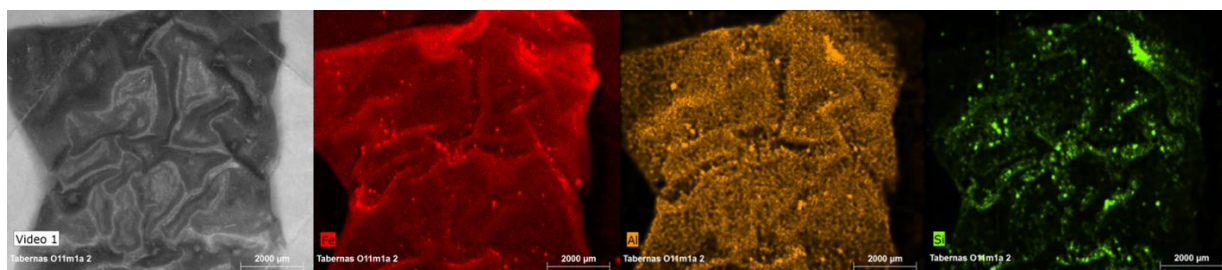
Figure 4.4.1: *Map of the distribution of iron (red), aluminium (orange) and silicon (green) on the surface of an olive at site 1. The stronger the colour, the higher the concentration in a singular spot. The maps were recorded with 30 ms dwell time, 30 μm step size and over 3 cycles. The sum spectra for the element map is presented in attachment F.2.*

Figure 4.4.1 shows clear hotspots for elements such as Si, Al, and Fe The hotspots have a visibly larger concentration of these elements than the rest of the sample. The hotspots seem to be assosiated with the crevices of the fruit skin. The amount of hotspots are higher in the bottom of the crevices, than at the top.

Point measusurements were taken from hotspots and just outside the hotspot area . One point measurement returned a weight percentage of 0.77% for Si, 0.84% for Al and 0.31% for Fe. Taking a point measurement outside the hotspot gave a lower weight percentage of 0.05% for Si, 0.41% for Al, and 0.22% for Fe (attachment F.6 and F7).

The hotspot was also larger than the average for the whole map for Si, and Al with 0.28% and 0.52% respectivly. At site 2, the composition of the sample itself remained like the one at site 1. The distribution of iron, Al and Siin the olive sample at site 2 is shown in attachment F.1. Fe accounted for 0.32%, Al for 0.52% and Si for 0.28%. As found in site 1, the highest percentages were found for K, Ca and Cl with 83.92%, 8.14% and 2.86%. A map of the distribution of Fe, Al and Si is shown in figure 4.4.2.
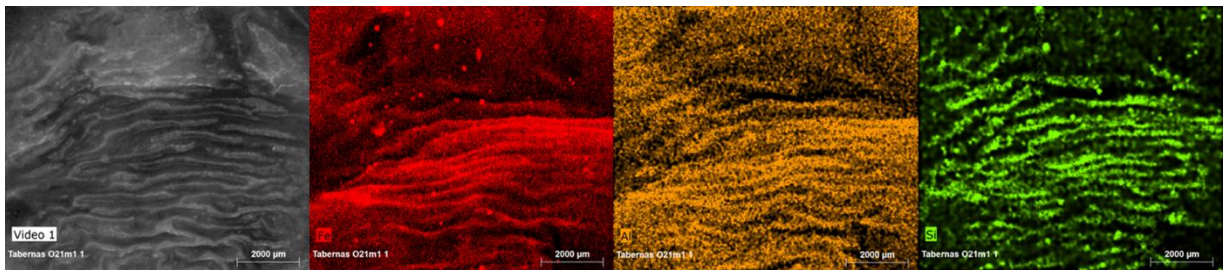
Figure 4.4.2: *Map of the distribution of Fe (red), AL (orange) and Si(green) on the surface of an olive at site 2. The stronger the colour, the higher the concentration in a singular spot. The maps were recorded with 30 ms dwell time, 30 μm step size and over 3 cycles. The spectra for the element map is presented in attachment F.3.*

The olive samples from site 2, there was fewer clear hotspots for Al and Fe than in the olive sample at site 1. There reason for site 2 having fewer hotspots, is probably because of the location of the sampling. Site, 1 will have more dust from passing traffic, will have more and larger particles settle on the plant.

4.4.2 Dates

A skin sample of dates was taken from site 2 and analysed in the same manner as the olive samples. From the semi-quantitative analysis, the most abundant elements were K, Ca and Cl representing 66%, 10% and 12% of the measured sample. Fe, and Al had a weight percentage of 0.30% and 0.34% of the sample. Si for dates was than measured in olives, being 3% (attachment F.1). The sample had less K, and more Si which implicates that there is a difference of the deposition pattern in different fruits. A map of the distribution of Fe, Al and Si in dates is shown in figure 4.4.3.
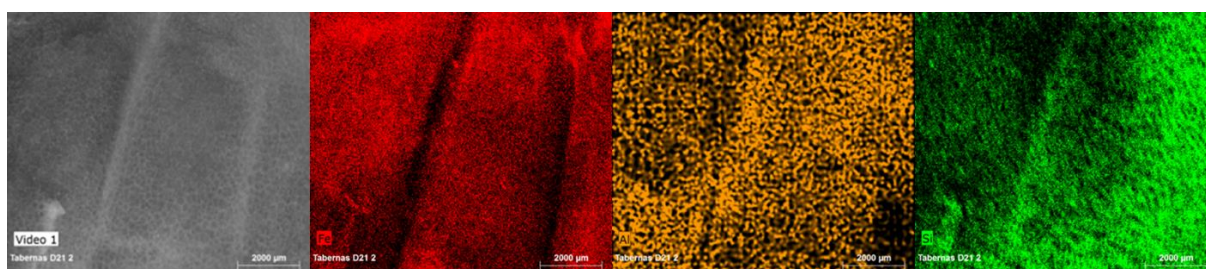
Figure 4.4.3: Map of the distribution of Fe (red), Al (orange) and Si (green) on the surface of a date at site 2. The stronger the colour, the higher the concentration in a singular spot. The maps were recorded with 30 ms dwell time, 30 µm step size and over 3 cycles. The spectra for the element map is presented in attachment F.4.

No clear visual hotspots were measured for the date samples for any of the soil associated elements in dates. However, the measured Si, which are associated with the minerology and the area, is high compared to the olive sample. This indicates that, even though elements still deposit on the plant surface, the type of fruit and their skin impact the pattern of deposition.

4.4.3 Figs

Lastly, a fig skin sample was taken. The fig sample were the only sample to have more Ca than K with Ca having a weight percentage of 52.40% with Ca representing 28.34%. Cl represented 1.66%. Fe represented 0.61%, Al had 2.74% and Si represented 5.62%. The high percentage of Al and Si indicates that minerals such as Muscovite, Orthoclase and Gibbsite is deposited on the plant surface. The map of the deposition pattern in Fe, Al and Si is shown in figure 4.4.4.
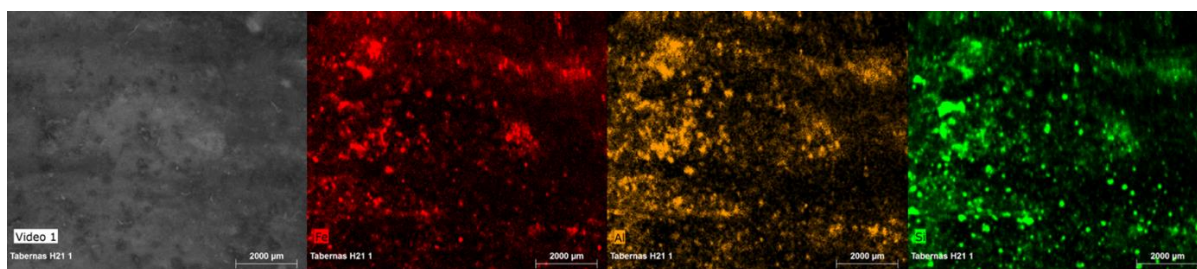
Figure 4.4.4: *Map of the distribution of Fe (red), Al (orange) and Si (green) on the surface of a fig at site 2. The stronger the colour, the higher the concentration in a singular spot. The maps were recorded with 30 ms dwell time, 30 μm step size and over 3 cycles. The spectra for the element map is presented in attachment F.5.*

The surface of the date sample had visible hotspots with high concentrations of Fe, Al and Si, which are found in the minerals such as Muscovite, Gibbsite and Orthoclase. Noticeable hotspots were also found for Fe, Al and Si on the surface of dates; the hotspots appear somewhat larger than for the corresponding olive samples.

4.4.4 Impact of deposition and resuspension of radionuclides on fruit

The composition and deposition of elements commonly found in soils seem to vary between different fruit shells. While the samples of dates had no noticeable hotspots, both figs and olives showed clear hotspots, where elements appeared to reflect the mineralogy in the area such as Gibbsite, Muscovite and Orthoclase exist.

The resulting CR will be affected by the deposition of elements and radionuclides. Both where the sample are taken, as well as which fruit are used will impact the resulting measured CR This indicates using a common CR value for a group of crops, e.g. "fruit", may give rise to relatively large uncertainties. It may also be an indication that dates are less impacted by surface contamination. However, since only one sample was taken more research is needed to come with any definite conclusion.

5. Conclusions

This study measured CRs in common fruits in the Tabernas region (Olives, figs, dates and prickly pears) with the goal of assessing the CRs in semi-arid environments and comparing them to CRs given by IAEAs CRP, K41022 and other literature data. In addition, this study aims to develop a better understanding of the deposition and uptake of radionuclides in edible plants in arid and semi-arid environments as well as assessing the influence of pre-treatment methods on the resulting CRs for fruits.

The CRs found in this study tend to be lower than for the average values for the terrestrial environment and other measured values in IAEAs CRP, K41022. However, most CRs for the measured fruits fell within the range of measurements found in IAEAs values for temperate climates, while being much lower than the ones found in arid environments.

The position of soil core samples, and the site has a significant impact on the resulting CR. Since only two sites were selected, and e.g. figs had only one soil core sample taken, expanding the number of sites, and core samples in future studies would be preferable. However, through the CRP, many more sites and CRs are calculated, which partially mitigates this weakness. The horizontal layer of the soil samples seems to have a negligible impact on the final CR, no significant different in concentration of any radionuclide could be found in dates which had the most extensive soil core measurements. However, there were indications that there were differences in OM content and in particle size.

The CR was impacted by the fruit part, and how the difference is addressed. The highest measured concentrations in fruit were generally measured in the skin samples, followed by the fruit pulp and the bone. These differences were more pronounced than for the soil heterogeneities, suggesting it has a larger impact on the final CR-value. In future studies using a weighing factor or changing the sampling, so skin and fruit (the edible part of the fruit) are sampled as one is warranted.

The two different pre-treatment procedures done by CIEMAT showed significant differences. Because of problems in the sample digestion, no clear difference between the number of washings could be established, but differences could be found in the calcinated samples and the final CRs. The conventional washing process removed more of the elemental deposition

on the fruit surface. However, the ultrasonic method of pre-treatment gave more precision in the resulting CR values than the conventional method. RSDs and SDs both in the calcinated samples as well as the final variation within the CRs tended to be lower for the ultrasonic pre-treatment suggesting, suggesting it is a more robust method. These results indicate there is scope for further improvements of washing procedures in the pre-treatment of fruit samples.

How the calculated CR relates to the real-life dose rate is challenging. For example, the washing of samples if the fruit is eaten without any cleaning will lead to an underestimation of the real transfer. The opposite might be the case if it is common to peel a fruit, the skin concentration of radionuclides is irrelevant for the resulting CR. However, using standardized protocols make comparisons between e.g. sampling sites and fruits easier.

The deposition of radionuclides can also affect the resulting CR. This study only found hotspots with higher concentrations of e.g. Fe, Al and Si on skin of olives and figs. Dates showed no distinguishable hotspots. The retention of radionuclides and stable analogues because of resuspension and deposition seem to vary between fruits. Differences in concentrations in fruits, differing CRs and deposition indicates that operating with a common CR for all fruits may give rise to relatively large uncertainties.

6. References

Agilent 2022. Principles of ICP Tandem Mass Spectrometry (ICP-MS/MS) - Agilent ICP-MS technology brief. *In:* Inc., A. T. (ed.). Aglient Technologies Inc.

Beck, H. E., Zimmermann, N. E., McVicar, T. R., Vergopolan, N., Berg, A. & Wood, E. F. 2018. Present and future Köppen-Geiger climate classification maps at 1-km resolution. *Scientific Data,* 5**,** 180214.

Beuselinck, L., Govers, G., Poesen, J., Degraer, G. & Froyen, L. 1998. Grain-size analysis by laser diffractometry: comparison with the sieve-pipette method. *CATENA,* 32**,** 193-208.

Brown, J., Teien, H. C., Thørring, H., Skipperud, L., Hosseini, A., Lind, O. C., Oughton, D. & Salbu, B. 2024. Transfer of radionuclides through ecological systems: Lessons learned from 10 years of research within CERAD CoE. *Science of The Total Environment,* 940**,** 173503.

Brown, J. E., Alfonso, B., Avila, R., Beresford, N. A., Copplestone, D. & Hosseini, A. 2016. A new version of the ERICA tool to facilitate impact assessments of radioactivity on wild plants and animals. *Journal of Environmental Radioactivity,* 153**,** 141-148.

Bunaciu, A. A., Udriştioiu, E. g. & Aboul-Enein, H. Y. 2015. X-Ray Diffraction: Instrumentation and Applications. *Critical Reviews in Analytical Chemistry,* 45**,** 289-299.

Burger, A. & Lichtscheidl, I. 2018. Stable and radioactive cesium: A review about distribution in the environment, uptake and translocation in plants, plant reactions and plants' potential for bioremediation. *Science of The Total Environment,* 618**,** 1459-1485.

Byrnes, I., Lind, O. C., Hansen, E. L., Janssens, K. & Salbu, B. 2020. Characterization of radioactive particles from the Dounreay nuclear reprocessing facility. *Science of The Total Environment,* 727**,** 138488.

Cantón, Y., Solé-Benet, A. & Lázaro, R. 2003. Soil–geomorphology relations in gypsiferous materials of the Tabernas Desert (Almería, SE Spain). *Geoderma,* 115**,** 193-222.

Choppin, G., Liljenzin, J.-O., Rydberg, J. & Ekberg, C. 2013a. The Actinide and Transactinide Elements. *Radiochemistry and nuclear chemistry.* 4th ed. Amsterdam: Elsevier.

Choppin, G., Liljenzin, J.-O., Rydberg, J. & Ekberg, C. 2013b. Cosmic Radiation and Radioelements in Nature. *Radiochemistry and Nuclear Chemistry.* United States: United States: Elsevier.

Colnaghi, G., Carnaroglio, D., Volpi, M., Rota, G., Rossetti, M., Fenili, A. & Lorenzi, S. 2024. *Revolutionizing elemental analysis: A comprehensive guide to Microwave Digestion Technology*, Milestone Srl.

Dahl, B. H. 2024. *Using AI as a student - do's and don'ts* [Online]. NMBU. Available: https://www.nmbu.no/en/library/using-ai-student-dos-and-donts [Accessed 29.09 2024].

Dal Molin, F., Hunt, D., Dewar, A., Lozach, S., Phillips, C., Thomas, B., Warford, L., Parker, J. E., Walker, J., Chocholek, M., Paterson, D. M., Woodward-Rowe, H. & Hicks, N. 2025. A new approach for assessing the radioecological risk associated with the legacy discharge of oil derived natural radioactivity in the UK North Sea. *Marine Pollution Bulletin,* 212**,** 117585.

Dirican, A., Dikmen, H., Şahin, M., Gülay, Y., Özkök, Y. Ö., Kaya, N. & Vural, M. 2024. Transfer factors of 238U, 232Th, 40K, 210Pb to crops and radiation impact assessment in semi-arid environment. *Journal of Radioanalytical and Nuclear Chemistry,* 333**,** 5597-5606.

Doering, C. & Bollhöfer, A. 2016. A soil radiological quality guideline value for wildlife-based protection in uranium mine rehabilitation. *Journal of Environmental Radioactivity,* 151**,** 522-529.

Donna, S. 2001. Uranium in glass, glazes and enamels: history, identification and handling. *Studies in Conservation,* 46**,** 181--195.

Greger, M. 2004. Uptake of nuclides by plants. Sweden: ; Swedish Nuclear Fuel and Waste Management Co., Stockholm (Sweden).

Gupta, D. K., Walther, C., Walther, C. & Gupta, D. K. 2014. *Radionuclide Contamination and Remediation Through Plants,* Cham, Cham: Springer International Publishing AG.

Harbottle, A.-R. & Yankovich, T. 2021. *New CRP: Transfer of Radionuclides in Arid and Semi-Arid Environments for Radiological Environmental Impact Assessment (K41022)* [Online]. IAEA. Available: https://www.iaea.org/newscenter/news/new-crp-transfer-of-radionuclides-in-arid-and-semi-arid-environments-for-radiological-environmental-impact-assessment-k41022 [Accessed 25.04 2024].

Haschke, M. 2014. *Laboratory Micro-X-Ray Fluorescence Spectroscopy Instrumentation and Applications*, Springer Cham.

Haschke, M., Rossek, U., Tagle, R. & Waldschläger, U. Fast Elemental Mapping with Micro-xrf. 2012.

Hickey, S. M., Malkawi, S. & Khalil, A. 2021. Nuclear power in the Middle East: Financing and geopolitics in the state nuclear power programs of Turkey, Egypt, Jordan and the United Arab Emirates. *Energy Research & Social Science,* 74**,** 101961.

Hosseini, A., Brown, J. E., Avila, R., Beresford, N. A. & Oughton, D. 2022. Redesigning the FDMT Food Chain Transfer Model: Now Probabilistically Enabled and Fully Flexible. *Environmental Modeling & Assessment,* 27**,** 311-326.

IAEA 2008. *Naturally Occurring Radioactive Material (NORM V),* Vienna, INTERNATIONAL ATOMIC ENERGY AGENCY.

IAEA 2009. *Quantification of Radionuclide Transfer in Terrestrial and Freshwater Environments for Radiological Assessments,* Vienna, INTERNATIONAL ATOMIC ENERGY AGENCY.

IAEA 2010. Ch. 12 Use of Analogues. *Handbook of Parameter Values for the Prediction of Radionuclide Transfer in Terrestrial and Freshwater Environments.* Vienna: INTERNATIONAL ATOMIC ENERGY AGENCY.

IAEA 2014. *Handbook of Parameter Values for the Prediction of Radionuclide Transfer to Wildlife,* Vienna, INTERNATIONAL ATOMIC ENERGY AGENCY.

IAEA 2021. *Soil–Plant Transfer of Radionuclides in Non-temperate Environments,* Vienna, INTERNATIONAL ATOMIC ENERGY AGENCY.

IAEA 2024. A protocol for CRP K41022: Field Studies and Experiments for Determination of Radionuclide Concentration Ratios in Arid Areas *International Atomic Energy Agency Coordinated Research Project K41022,.*

ICRP 2007. The 2007 Recommendations of the International Commission on Radiological Protection. ICRP publication 103. *Ann ICRP,* 37**,** 1-332.

Jewell, J. 2011. A nuclear-powered North Africa: Just a desert mirage or is there something on the horizon? *Energy Policy,* 39**,** 4445-4457.

Kashparov, V. A., Ahamdach, N., Zvarich, S. I., Yoschenko, V. I., Maloshtan, I. M. & Dewiere, L. 2004. Kinetics of dissolution of Chernobyl fuel particles in soil in natural conditions. *Journal of Environmental Radioactivity,* 72**,** 335-353.

Kathren, R. L. 1998. NORM sources and their origins. *Applied Radiation and Isotopes,* 49**,** 149-168.

Kidron, G. & Lazaro, R. 2020. Are coastal deserts necessarily dew deserts? An example from the Tabernas Desert. *Journal of Hydrology and Hydromechanics,* 68**,** 19-27.

Kosiorek, M. 2019. EFFECT OF COBALT ON THE ENVIRONMENT AND LIVING ORGANISMS - A REVIEW. *Applied Ecology and Environmental Research,* 17.

Lázaro, R., Rodrigo, F. S., Gutiérrez, L., Domingo, F. & Puigdefábregas, J. 2001. Analysis of a 30-year rainfall record (1967–1997) in semi–arid SE Spain for implications on vegetation. *Journal of Arid Environments,* 48**,** 373-395.

Leggett, R. 2017. Biokinetics of yttrium and comparison with its geochemical twin holmium. *J Radiol Prot,* 37**,** 434-449.

Liger, E., Hernández, F., Expósito, F. J., Díaz, J. P., Salazar-Carballo, P. A., Gordo, E., González, C. & López-Pérez, M. 2024. Transport and deposition of radionuclides from northern Africa to the southern Iberian Peninsula and the Canary Islands during the intense dust intrusions of March 2022. *Chemosphere,* 352**,** 141303-141303.

Montgomery, D. C. 2020. Ch. 3 Experiments with a Single Factor: The Analysis of Variance. *In:* Rosatone, L. (ed.) *Design and analysis of experiments 10th ed. .* Wiley.

Narendrula, R., Nkongolo, K. & Beckett, P. 2011. Comparative Soil Metal Analyses in Sudbury (Ontario, Canada) and Lubumbashi (Katanga, DR-Congo). *Bulletin of environmental contamination and toxicology,* 88**,** 187-92.

Nedveckaite, T., Filistovic, V., Marciulioniene, D., Prokoptchuk, N., Plukiene, R., Gudelis, A., Remeikis, V., Yankovich, T. & Beresford, N. A. 2011. Background and anthropogenic radionuclide derived dose rates to freshwater ecosystem – Nuclear power plant cooling pond – Reference organisms. *Journal of Environmental Radioactivity,* 102**,** 788-795.

Okumura, M., Kerisit, S., Bourg, I. C., Lammers, L. N., Ikeda, T., Sassi, M., Rosso, K. M. & Machida, M. 2018. Radiocesium interaction with clay minerals: Theory and simulation advances Post–Fukushima. *Journal of Environmental Radioactivity,* 189**,** 135-145.

Pelkonen, M. K., Reinoso-Maset, E., Law, G. T. W., Lind, O. C. & Skipperud, L. 2025. Environmental impact of an acid-forming alum shale waste rock legacy site in Norway. *Environ Sci Process Impacts,* 27**,** 225-243.

PerkinElmer. 2011. *The 30-Minute Guide to ICP-MS* [Online]. PerkinElmer Available: https://resources.perkinelmer.com/corporate/pdfs/downloads/tch_icpmsthirtyminuteguide.pdf [Accessed 06.09 2024].

Phuong, H. T., Ba, V. N., Thien, B. N. & Truong Thi Hong, L. 2023. Accumulation and distribution of nutrients, radionuclides and metals by roots, stems and leaves of plants. *Nuclear Engineering and Technology,* 55**,** 2650-2655.

Prăvălie, R. 2014. Nuclear Weapons Tests and Environmental Consequences: A Global Perspective. *AMBIO,* 43**,** 729-744.

Pröhl, G. 2009. Interception of dry and wet deposited radionuclides by vegetation. *Journal of Environmental Radioactivity,* 100**,** 675-682.

Pröhl, G., Twining, J. R. & Crawford, J. 2012. Chapter 7 - Radiological Consequences Modelling. *In:* Twining, J. R. (ed.) *Radioactivity in the Environment.* Elsevier.

Raj, P., Padiyath, N., Semioshkina, N., Foulon, F., Alkaabi, A. K., Voigt, G. & Addad, Y. 2022. Transfer of Natural Radionuclides from Soil to Abu Dhabi Date Palms. *Sustainability,* 14**,** 11327.

Rea, M. A. D., Johansen, M. P., Payne, T. E., Hirth, G., Hondros, J., Pandelus, S., Tucker, W., Duff, T., Stopic, A., Green, L., Pring, A., Lenehan, C. E. & Popelka-Filcoff, R. S. 2021. Radionuclides and stable elements in vegetation in Australian arid environments: Concentration ratios and seasonal variation. *J Environ Radioact,* 234**,** 106627-106627.

Reynolds, J. F., Smith, D. M. S., Lambin, E. F., Turner, B. L., Mortimore, M., Batterbury, S. P. J., Downing, T. E., Dowlatabadi, H., Fernández, R. J., Herrick, J. E., Huber-Sannwald, E., Jiang, H., Leemans, R., Lynam, T., Maestre, F. T., Ayarza, M. & Walker, B. 2007. Global Desertification: Building a Science for Dryland Development. *Science,* 316**,** 847-851.

Robinson, C. A., Smith, K. L. & Norris, S. 2010. Impacts on non-human biota from a generic geological disposal facility for radioactive waste: some key assessment issues. *Journal of Radiological Protection,* 30**,** 161.

Rodríguez-Alonso, J., Cabrales-García, C. & Millán, R. 2023. Factors influencing the cleaning of plant samples with ultrasonic technology. *International Journal of Phytoremediation,* 25**,** 359-367.

Salbu, B. 2006. Speciation of radionuclides in the environment. *Encyclopedia of analytical chemistry: applications, theory and instrumentation*.

Salbu, B., Lind, O. C. & Skipperud, L. 2004. Radionuclide speciation and its relevance in environmental impact assessments. *Journal of Environmental Radioactivity,* 74**,** 233-242.

Sarret, G., Smits, E. A. H., Castillo-Michel, H., Isaure, M. P., Zhao, F.-J. & Tappero, R. 2013. Use of Synchrotron-Based Techniques to Elucidate Metal Uptake and Metabolism in Plants.

Semioshkina, N. & Voigt, G. 2021. Soil - Plant transfer of radionuclides in arid environments. *Journal of Environmental Radioactivity,* 237**,** 106692.

Skoog, D. A., Holler, F. J. & Crouch, S. R. 2017a. Ch. 11 Atomic Mass Spectrometry. *Principles of instrumental analysis 7th ed.*: Cengage.

Skoog, D. A., Holler, F. J. & Crouch, S. R. 2017b. Ch. 12 Atomic X-ray spectrometry. *Principles of instrumental analysis 7th ed.*: Cengage.

Skoog, D. A., West, D. M., Holler, F. J. & Crouch, S. R. 2022a. Ch. 3 Precision and Accuracy in Chemichal analysis. *Fundamentals of analytical chemistry.* Tenth edition, student edition. ed. Pacific Grove: Brooks/Cole.

Skoog, D. A., West, D. M., Holler, F. J. & Crouch, S. R. 2022b. Ch. 4 Random errors in Chemical Analysis. *Fundamentals of analytical chemistry.* Tenth edition, student edition. ed. Pacific Grove: Brooks/Cole.

Skoog, D. A., West, D. M., Holler, F. J. & Crouch, S. R. 2022c. Ch. 27 Mass Spectrometry. *Fundamentals of analytical chemistry.* Tenth edition, student edition. ed. Pacific Grove: Brooks/Cole.

Spencer, B. 10.03.2025 2025. *RE: Kornfordelingsbestemmelse ved bruk av Laser Metoden* Personal communication to Hansebråten, M. & Holthusen, O.

Suarez, V. M. E. & Navarro, J. A. S. 27.09 2023. *RE: Tabernas – alternative protocols for figs, Olives, chumbo (chumbera).* Personal communication to Hansebråten, M.

Sumner, M. E. & Miller, W. P. 1996. Cation Exchange Capacity and Exchange Coefficients. *Methods of Soil Analysis*.

Thomas, R., El Dessougi, H. & Tubeileh, A. 2006. Soil System Management Under Arid and Semi-Arid Conditions.

Ulanovsky, A., Copplestone, D. & Batlle, J. V. I. 2017. ICRP Publication 136: Dose Coefficients for Non-human Biota Environmentally Exposed to Radiation. *Ann ICRP,* 46**,** 1-136.

UNEP 2016. *Radiation Effects and Sources*, United Nations Environment Programme.

UNSCEAR 2000. Sources and effects of ionizing radiation. New York :: UN Scientific Committee on the Effects of Atomic Radiation.

Urso, L. 2020. D9.62 – Methodology to quantify improvement - Guidance on uncertainty analysis for radioecological models. European Joint Programme for the Integration of Radiation Protection Research

VanLoon, G. W. & Duffy, S. J. 2017. Ch. 18: Soil properties. *Environmental chemistry : a global perspective.* Fourth edition. ed. Oxford: Oxford University Press.

Varga, B., Leclerc, E. & Zagyvai, P. 2009. The role of analogues in radioecology. *Journal of Environmental Radioactivity,* 100**,** 802-805.

7. Attachments

A: LOI and particle size analysis

Attachment A 1: *Weights [g] of the merged samples of soil associated with dates. For the four horizontal layers a mixture of soil from position E and C was used. For the sample of soil as a whole, all layers of position D was used.*

Depth	Position	Part or total	Weight [g]	Comment
0-5	*E*	*Part*	*3.8438*	
0-5	*C*	*Part*	*7.8614*	
LD 0-5	***EC***	***Total***	***11.705***	*Merged sample for particle size analysis*
5-10	*E*	*Part*	*7.3338*	
5-10	*C*	*Part*	*6.3613*	
LD 5-10	***EC***	***Total***	***13.6951***	*Merged sample for particle size analysis*
10-15	*E*	*Part*	*6.4963*	
10-15	*C*	*Part*	*6.3080*	
LD 10-15	***EC***	***Total***	***12.8043***	*Merged sample for particle size analysis*
15-20	*E*	*Part*	*6.7862*	
15-20	*C*	*Part*	*7.8340*	
LD 15-20	***EC***	***Total***	***14.6202***	*Merged sample for particle size analysis s*
0-5	*D*	*LOI*	*3.0068*	
5-10	*D*	*LOI*	*3.4454*	
10-15	*D*	*LOI*	*3.4337*	
15-20	*D*	*LOI*	*4.0594*	
LD LOI	***D***	***LOI_TOT***	***13.9453***	*Merged sample for LOI measurement*

Table A.2: *The percentage [%] of particle size in clay (<2 nm), medium silt, coarse silt, fine sand, medium sand and coarse sand in the 0-5 cm, 5-10 cm, 10-15 cm and 15-20 cm layer from a merged soil core sample associated with dates at position E and C. In addition, a merged sample was measured, from position D.*

	Clay [%]	Fine silt [%]	Medium silt [%]	Coarse silt [%]	Fine sand [%]	Medium sand [%]	Coase sand [%]
0-5	2.17	18.00	35.62	37.06	7.15	0.00	0.00
5-10	1.87	17.42	36.52	37.61	6.58	0.00	0.00
10-15	1.06	15.58	35.20	40.00	8.16	0.01	0.00
15-20	0.80	15.50	36.99	39.54	7.19	0.00	0.00
Merged	1.15	15.77	34.36	39.79	8.93	0.00	0.00

Table A.3: The percentage [%] of particle size in clay (<4 nm), medium silt, coarse silt, fine sand, medium sand and coarse sand in the 0-5 cm, 5-10 cm, 10-15 cm and 15-20 cm layer from a merged soil core sample associated with dates at position E and C. In addition, a merged sample was measured, from position D.

	Clay [%]	Fine silt [%]	Medium silt [%]	Coarse silt [%]	Fine sand [%]	Medium sand [%]	Coase sand [%]
0-5	10.99	9.18	35.62	37.06	7.15	0.00	0.00
5-10	10.22	9.07	36.52	37.61	6.58	0.00	0.00
10-15	8.23	8.42	35.20	40.00	8.16	0.01	0.00
15-20	7.69	8.60	36.99	39.54	7.19	0.00	0.00
Merged	8.54	8.39	34.36	39.79	8.93	0.00	0.00
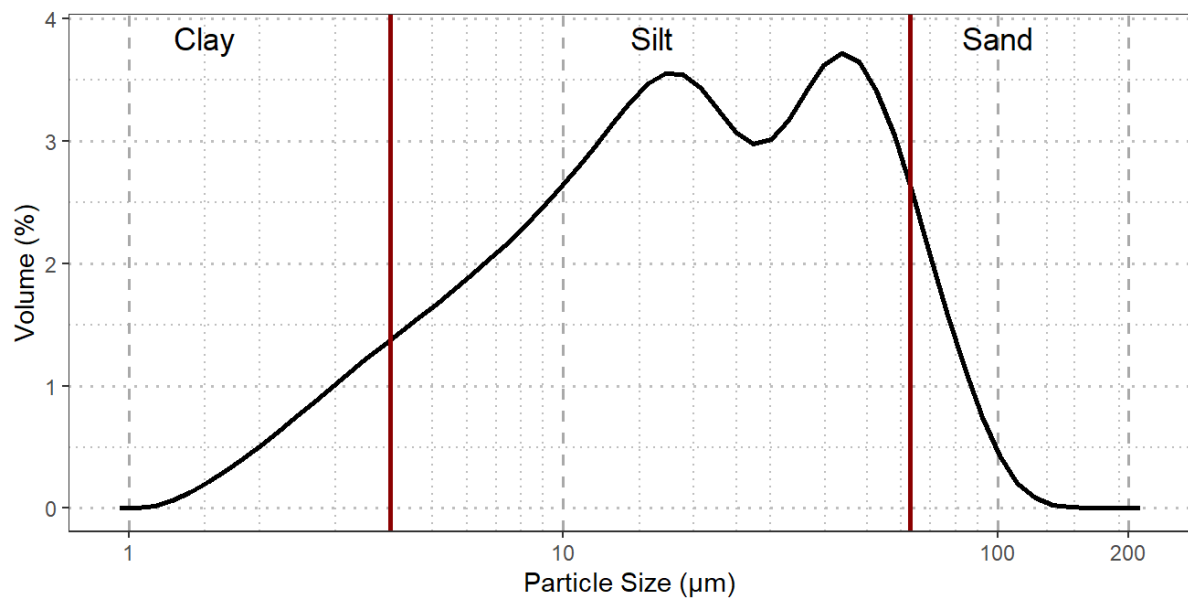
Figure A.4: Particle size [μm] as a function of volume [%] in the merged soil sample LD-LOI. The clay fraction, here defined as <4μm, the silt fraction is between 4 and 63μm and the sand fraction is >63μm. The sample is from date samples at site 2, and consist off all layers in position D. The composition of the sample is shown in Attachment A1.

B: ICP-MS data for soil and calcinated fruit

Table B. 1*: Raw data of the concentration [µg/kg] of the radionuclides* ^{232}Th *and* ^{238}U *and stable analogues* ^{59}Co, ^{88}Sr *and* ^{133}Cs *as well as the concentration of Yttrium and Holmium in each measured sample of soil measured at the two sites in Tabernas. The position, site and horizontal layer of the soil sample is given for each sample.*

Sample number	Site	Position	Fruit type	Layer [cm]	^{59}Co [mg/kg]	^{88}Sr [mg/kg]	Y [mg/kg]	^{133}Cs [mg/kg]	Ho [mg/kg]	^{232}Th [mg/kg]	^{238}U [mg/kg]
57	2	A	Fig	0-5	12.4	100	26.8	5.3	1.01	9.68	1.8
58	2	A	Fig	0-5	13.3	105	26.4	5.41	1.01	10.3	1.82
59	2	A	Fig	0-5	12.7	105	27.1	5.4	1.03	10.7	1.91
60	2	A	Fig	5-10	12.3	102	27.8	5.38	1.07	10.4	1.92
61	2	A	Fig	5-10	12.2	98	29.6	5.09	1.11	9.91	1.83
62	2	A	Fig	5-10	12.4	100	24.5	5.21	0.942	9.78	1.86
63	2	A	Fig	10-15	14.4	101	27.4	4.63	1.05	9.85	1.81
64	2	A	Fig	10-15	12.7	89.4	28.1	4.64	1.09	10.1	1.94
65	2	A	Fig	10-15	13.8	98.5	26.5	4.53	1.02	9.71	1.9
66	2	A	Fig	15-20	14.3	71.9	29.6	4.83	1.15	11	1.93
67	2	A	Fig	15-20	14.5	72	32.7	4.92	1.25	12	2.11
68	2	A	Fig	15-20	14.3	72.2	30.5	4.86	1.17	11.6	1.99
69	2	E	Date	0-5	10.3	198	19.2	8.23	0.731	8.23	2.39
70	2	E	Date	5-10	12	133	23.9	5.53	0.912	9.1	2.13
71	2	E	Date	10-15	16.5	67.1	33.5	4.53	1.25	10.7	1.82
72	2	E	Date	15-20	15	74.1	26.6	4.41	1.02	10.7	1.8
73	2	A	Date	0-5	11	229	17.9	4.15	0.665	7.01	2.8
74	2	A	Date	5-10	9.98	223	18.4	4.11	0.697	6.96	2.81
75	2	A	Date	10-15	10.5	224	20	4.18	0.768	7.62	2.87
76	2	A	Date	15-20	8.14	235	14.4	3.65	0.537	5.62	2.87
77	2	B	Date	0-5	11.7	111	25.6	5.19	0.98	9.67	1.93
78	2	B	Date	5-10	11	132	22.6	5.19	0.86	8.95	2.1

79	2	B	Date	10-15	12.7	104	24.6	5.09	0.968	10.4	1.94
80	2	B	Date	15-20	13.4	71.1	26.9	4.44	1.04	11.5	1.92
81	2	C	Date	0-5	13.8	123	26.9	4.64	1.05	11.4	2.39
82	2	C	Date	5-10	9.5	229	15.8	4.28	0.588	6.01	2.7
83	2	C	Date	10-15	9.37	194	19.2	4.33	0.709	6.56	2.46
84	2	C	Date	15-20	14.2	73.4	28.8	4.43	1.15	11.3	2.11
85	2	D	Date	0-5	12.3	144	20.5	4.93	0.807	8.99	2.02
86	2	D	Date	5-10	11.4	143	22	4.76	0.857	9.57	1.99
87	2	D	Date	10-15	13.2	94	24.6	4.57	0.984	11	1.95
88	2	D	Date	15-20	13.7	70.9	27.1	4.47	1.08	10.7	1.84
89	2	A	P_pear	0-5	12.6	92.6	26.2	4.56	1.02	10.9	1.85
90	2	A	P_pear	5-10	13.5	96	28.8	4.6	1.11	11.1	1.98
91	2	A	P_pear	10-15	13.2	95.3	30	4.7	1.16	11	1.99
92	2	A	P_pear	15-20	13.1	89.2	28.9	4.65	1.11	11.7	2.02
93	2	B	P_pear	0-5	13.6	84.6	31.6	4.77	1.21	11.9	2
94	2	B	P_pear	5-10	13.4	82.1	26.6	4.53	1.05	10.6	1.81
95	2	B	P_pear	10-15	14.2	86	28.4	4.73	1.09	11.5	2.09
96	2	B	P_pear	15-20	14	95.5	28.6	4.96	1.11	11.5	2.06
97	2	C	P_pear	0-5	14.1	78.2	28.8	4.48	1.12	10.1	1.8
98	2	C	P_pear	5-10	15.5	84.1	27.9	4.58	1.1	10.7	1.9
99	2	C	P_pear	10-15	15.1	81.4	30.1	4.51	1.17	10.7	1.97
100	2	C	P_pear	15-20	13.9	84.8	28.6	4.88	1.09	10.5	1.81
101	1	E	Olive	0-5	12.4	97.8	30	5.1	1.1	7.46	1.61
102	1	E	Olive	5-10	18	95.4	81.5	4.71	2.9	8.15	1.71
103	1	E	Olive	10-15	15.6	152	57.5	4.38	2.11	8.06	2.03
104	1	E	Olive	15-20	10.3	135	50.3	4.46	1.8	6.92	1.68
105	1	A	Olive	0-5	11.6	89.5	67.6	5.72	2.37	7.6	1.86
106	1	A	Olive	5-10	13.4	73.6	77.2	4.45	2.8	7.82	1.8
107	1	A	Olive	10-15	16.1	94.9	50.9	4.75	1.87	9.08	1.94
108	1	A	Olive	15-20	11.5	80.8	56.6	4.5	2.08	7.75	1.77

109	1	B	Olive	0-5	10.3	167	41.6	5.07	1.53	7.34	1.53
110	1	B	Olive	5-10	11.4	129	34.9	5.11	1.32	8.66	1.86
111	1	B	Olive	10-15	13	113	46.8	4.57	1.73	7.95	1.85
112	1	B	Olive	15-20	12.6	110	31.9	5.24	1.2	8.42	1.78
113	2	A	Olive	0-5	13.5	98.1	28.2	5.33	1.1	11	1.97
114	2	A	Olive	5-10	13.2	105	25.2	5.33	0.983	10.3	1.82
115	2	A	Olive	10-15	14	109	24.9	5.42	0.983	11.5	1.87
116	2	A	Olive	15-20	13.8	103	25.9	5.24	1.04	11	1.93
117	2	B	Olive	0-5	12.1	102	27	5.13	1.05	10.5	1.91
118	2	B	Olive	5-10	12	109	34.8	5.36	1.36	9.62	1.8
119	2	B	Olive	10-15	12.6	129	36.6	7.31	1.38	10.2	1.95
120	2	C	Olive	0-5	13.6	97.2	33.7	5.61	1.3	11.3	2.12
121	2	C	Olive	5-10	13	91.4	25.8	5.19	0.969	9.68	1.73
122	2	C	Olive	10-15	12.8	97.2	26.6	5.8	1.02	10.1	1.92
123	2	C	Olive	15-20	13.2	94.7	31.1	5.55	1.2	11	2.03
124	2	D	Olive	0-5	14.5	105	24.2	5.92	0.94	10.9	1.91
125	2	D	Olive	5-10	13.4	106	24.5	5.77	0.952	10.3	1.85
126	2	D	Olive	10-15	22.4	87.8	28.4	5.44	1.11	10.9	1.89
127	2	D	Olive	15-20	12.9	102	23	5.56	0.9	10.4	1.86

Table B. 2: *Concentration [mg/kg] of the radionuclides ^{238}U, ^{232}Th and the stable analogues ^{133}Cs, ^{59}Co and ^{88}Sr in calcinated fruit samples adjusted for the measured wet weight [g] of the original material. As well as the sample number, the fruit species, wash process, fruit part, Loss on ignition (LOI) [%] and dry matter content (DM) [%] is given for each measured sample.*

Sample number	Fruit type	Wash process	Fruit part	Site	LOI [%]	DM [%]	^{238}U [mg/kg]	^{232}Th [mg/kg]	^{133}Cs [mg/kg]	^{59}Co [mg/kg]	^{88}Sr [mg/kg]
137	Fig	Ultrasonic	Skin	2	95%	29%	5.4E-04	2.1E-03	4.9E-03	8.6E-03	1.2E+01
138	Fig	Ultrasonic	Fruit	2	96%	19%	4.0E-05	2.9E-05	2.8E-03	6.6E-03	4.1E+00
139	Fig	Ultrasonic	Skin	2	95%	23%	6.5E-04	3.2E-03	5.3E-03	9.0E-03	8.3E+00
140	Fig	Ultrasonic	Fruit	2	96%	18%	7.9E-05	1.6E-04	2.6E-03	6.7E-03	2.9E+00
141	Fig	Ultrasonic	Skin	2	95%	23%	5.3E-04	2.5E-03	5.0E-03	8.6E-03	1.1E+01
142	Fig	Ultrasonic	Fruit	2	96%	18%	3.4E-05	5.5E-05	3.2E-03	6.0E-03	3.3E+00
143	Olive	Ultrasonic	Bone	1	96%	75%	4.3E-04	1.0E-04	3.8E-03	1.1E-02	9.6E+00
144	Olive	Ultrasonic	Fruit	1	73%	39%	9.9E-04	7.9E-04	3.1E-02	2.7E-02	1.8E+01
145	Olive	Ultrasonic	Bone	1	93%	74%	8.6E-04	2.3E-04	7.8E-03	2.6E-02	2.3E+01
146	Olive	Ultrasonic	Fruit	1	76%	39%	7.7E-04	6.2E-04	2.5E-02	2.4E-02	1.5E+01
147	Olive	Ultrasonic	Bone	1	96%	73%	3.4E-04	1.4E-04	3.4E-03	1.2E-02	9.0E+00
148	Olive	Ultrasonic	Fruit	1	75%	38%	1.2E-03	3.6E-04	2.4E-02	2.6E-02	1.4E+01
149	Olive	Ultrasonic	Bone	1	99%	75%	8.9E-04	1.9E-04	5.7E-03	2.1E-02	2.3E+01
150	Olive	Ultrasonic	Fruit	1	76%	38%	9.2E-04	5.2E-04	2.1E-02	2.1E-02	1.6E+01
151	Olive	Ultrasonic	Bone	1	97%	74%	6.2E-04	1.4E-04	5.3E-03	1.5E-02	1.7E+01
152	Olive	Ultrasonic	Fruit	1	76%	39%	1.1E-03	4.0E-04	2.6E-02	2.0E-02	1.8E+01
153	Olive	Ultrasonic	Bone	1	94%	73%	8.8E-04	1.4E-04	6.9E-03	2.2E-02	2.3E+01
154	Olive	Ultrasonic	Fruit	1	78%	39%	8.3E-04	4.4E-04	1.9E-02	1.8E-02	1.5E+01
155	Olive	Ultrasonic	Bone	2	99%	69%	3.3E-04	3.0E-04	4.6E-03	9.0E-03	4.2E+00
156	Olive	Ultrasonic	Fruit	2	72%	34%	4.8E-04	9.7E-04	1.5E-02	8.0E-03	3.1E+00
157	Olive	Ultrasonic	Bone	2	97%	70%	3.0E-04	3.0E-04	4.5E-03	9.2E-03	4.3E+00
158	Olive	Ultrasonic	Fruit	2	71%	34%	4.1E-04	9.0E-04	1.4E-02	8.9E-03	3.1E+00
159	Olive	Ultrasonic	Bone	2	98%	70%	2.7E-04	1.9E-04	5.1E-03	7.5E-03	3.8E+00
160	Olive	Ultrasonic	Fruit	2	72%	35%	3.6E-04	9.9E-04	1.7E-02	8.6E-03	3.4E+00

161	Olive	Ultrasonic	Bone	2	97%	70%	2.3E-04	2.1E-04	1.7E-03	2.1E-02	3.4E+00
162	Olive	Ultrasonic	Fruit	2	81%	41%	3.9E-04	8.7E-04	5.2E-03	2.1E-02	2.9E+00
163	Olive	Ultrasonic	Bone	2	97%	71%	3.5E-04	2.2E-04	2.1E-03	1.7E-02	3.1E+00
164	Olive	Ultrasonic	Fruit	2	80%	43%	7.2E-02*	1.1E-03	6.1E-03	2.2E-02	3.4E+00
165	Olive	Ultrasonic	Bone	2	88%	70%	3.2E-04	2.6E-04	2.7E-03	2.0E-02	3.5E+00
166	Olive	Ultrasonic	Fruit	2	80%	44%	4.1E-04	1.3E-03	8.0E-03	2.3E-02	3.9E+00
167	Date	Ultrasonic	Bone	2	99%	60%	1.4E-04	1.1E-04	6.0E-03	2.0E-03	8.6E-02
168	Date	Ultrasonic	Fruit	2	96%	27%	1.8E-04	7.8E-04	1.4E-02	2.2E-03	3.1E-01
169	Date	Ultrasonic	Bone	2	99%	58%	1.4E-04	1.8E-04	5.2E-03	2.0E-03	1.0E-01
170	Date	Ultrasonic	Fruit	2	96%	25%	1.6E-04	6.8E-04	1.3E-02	4.0E-03	3.4E-01
171	Date	Ultrasonic	Bone	2	99%	57%	1.1E-04	6.2E-05	5.9E-03	1.8E-03	9.1E-02
172	Date	Ultrasonic	Fruit	2	95%	28%	7.4E-04	4.9E-04	1.3E-02	1.6E-03	3.2E-01
173	Fig	Conventional	Skin	2	97%	17%	6.2E-04	1.5E-03	1.3E-02	5.5E-03	4.1E+00
174	Fig	Conventional	Fruit	2	91%	30%	7.8E-04	1.7E-03	4.2E-02	1.5E-02	7.6E+00
175	Fig	Conventional	Skin	2	97%	18%	3.7E-04	1.3E-03	4.4E-03	4.5E-03	4.4E+00
176	Fig	Conventional	Fruit	2	97%	18%	4.4E-05	6.1E-05	4.9E-03	5.2E-03	2.0E+00
177	Fig	Conventional	Skin	2	97%	15%	1.9E-04	7.1E-04	1.6E-02	3.1E-03	3.9E+00
178	Fig	Conventional	Fruit	2	97%	18%	1.5E-04	4.6E-05	3.4E-02	5.6E-03	2.0E+00
179	P_pear	Conventional	Skin	2	97%	17%	1.5E-04	9.7E-04	1.3E-03	7.9E-03	3.5E+00
180	P_pear	Conventional	Fruit	2	95%	10%	9.7E-05	1.5E-04	1.5E-03	1.7E-02	3.9E+00
181	P_pear	Conventional	Skin	2	66%	17%	1.4E-03	7.0E-03	1.3E-02	8.8E-02	3.6E+01
182	P_pear	Conventional	Fruit	2	91%	17%	5.0E-05	1.2E-04	4.8E-03	6.5E-02	9.2E+00
183	P_pear	Conventional	Skin	2	86%	16%	5.9E-04	2.9E-03	5.1E-03	2.9E-02	1.5E+01

*Sample excluded in further calculation because high value compared to other similar samples.

Table B. 3: *Concentration [mg/kg] of the radionuclides ^{238}U, ^{232}Th and the stable analogues ^{133}Cs, ^{59}Co and ^{88}Sr in calcinated fruit samples adjusted for the measured dry weight [g] of the original material. As well as the sample number, the fruit species, wash process, fruit part, Loss on ignition (LOI) [%] and dry matter content (DM) [%] is given for each measured sample.*

Sample number	Fruit type	Wash process	Fruit part	Site	LOI [%]	DM [%]	^{238}U [mg/kg]	^{232}Th [mg/kg]	^{133}Cs [mg/kg]	^{59}Co [mg/kg]	^{88}Sr [mg/kg]
137	Fig	Ultrasonic	Skin	2	95%	29%	1.9E-03	7.2E-03	1.7E-02	3.9E-04	4.2E+01
138	Fig	Ultrasonic	Fruit	2	96%	19%	2.0E-04	1.5E-04	1.4E-02	2.6E-04	2.1E+01
139	Fig	Ultrasonic	Skin	2	95%	23%	2.8E-03	1.4E-02	2.3E-02	4.4E-04	3.5E+01
140	Fig	Ultrasonic	Fruit	2	96%	18%	4.4E-04	9.2E-04	1.4E-02	3.0E-04	1.6E+01
141	Fig	Ultrasonic	Skin	2	95%	23%	2.3E-03	1.1E-02	2.2E-02	3.9E-04	4.7E+01
142	Fig	Ultrasonic	Fruit	2	96%	18%	1.9E-04	3.0E-04	1.7E-02	2.4E-04	1.8E+01
143	Olive	Ultrasonic	Bone	1	96%	75%	5.7E-04	1.4E-04	5.0E-03	4.2E-04	1.3E+01
144	Olive	Ultrasonic	Fruit	1	73%	39%	2.5E-03	2.0E-03	7.9E-02	7.3E-03	4.7E+01
145	Olive	Ultrasonic	Bone	1	93%	74%	1.2E-03	3.0E-04	1.1E-02	1.8E-03	3.0E+01
146	Olive	Ultrasonic	Fruit	1	76%	39%	2.0E-03	1.6E-03	6.6E-02	5.8E-03	3.9E+01
147	Olive	Ultrasonic	Bone	1	96%	73%	4.7E-04	1.9E-04	4.6E-03	4.3E-04	1.2E+01
148	Olive	Ultrasonic	Fruit	1	75%	38%	3.0E-03	9.3E-04	6.4E-02	6.3E-03	3.6E+01
149	Olive	Ultrasonic	Bone	1	99%	75%	1.2E-03	2.5E-04	7.6E-03	2.2E-04	3.1E+01
150	Olive	Ultrasonic	Fruit	1	76%	38%	2.4E-03	1.4E-03	5.5E-02	4.9E-03	4.2E+01
151	Olive	Ultrasonic	Bone	1	97%	74%	8.3E-04	2.0E-04	7.2E-03	4.6E-04	2.3E+01
152	Olive	Ultrasonic	Fruit	1	76%	39%	2.8E-03	1.0E-03	6.6E-02	4.8E-03	4.5E+01
153	Olive	Ultrasonic	Bone	1	94%	73%	1.2E-03	2.0E-04	9.5E-03	1.3E-03	3.1E+01
154	Olive	Ultrasonic	Fruit	1	78%	39%	2.1E-03	1.1E-03	5.0E-02	4.0E-03	3.9E+01
155	Olive	Ultrasonic	Bone	2	99%	69%	4.7E-04	4.3E-04	6.7E-03	9.2E-05	6.0E+00
156	Olive	Ultrasonic	Fruit	2	72%	34%	1.4E-03	2.9E-03	4.4E-02	2.2E-03	9.3E+00
157	Olive	Ultrasonic	Bone	2	97%	70%	4.3E-04	4.3E-04	6.5E-03	2.7E-04	6.1E+00
158	Olive	Ultrasonic	Fruit	2	71%	34%	1.2E-03	2.6E-03	4.1E-02	2.5E-03	9.1E+00
159	Olive	Ultrasonic	Bone	2	98%	70%	3.9E-04	2.7E-04	7.3E-03	1.5E-04	5.4E+00
160	Olive	Ultrasonic	Fruit	2	72%	35%	1.0E-03	2.9E-03	4.9E-02	2.4E-03	9.7E+00

161	Olive	Ultrasonic	Bone	2	97%	70%	3.3E-04	2.9E-04	2.4E-03	6.0E-04	4.9E+00
162	Olive	Ultrasonic	Fruit	2	81%	41%	9.4E-04	2.1E-03	1.3E-02	4.1E-03	7.1E+00
163	Olive	Ultrasonic	Bone	2	97%	71%	5.0E-04	3.1E-04	3.0E-03	5.1E-04	4.3E+00
164	Olive	Ultrasonic	Fruit	2	80%	43%	1.7E-01	2.6E-03	1.4E-02	4.4E-03	8.0E+00
165	Olive	Ultrasonic	Bone	2	88%	70%	4.5E-04	3.7E-04	3.9E-03	2.3E-03	5.1E+00
166	Olive	Ultrasonic	Fruit	2	80%	44%	9.5E-04	3.0E-03	1.8E-02	4.6E-03	9.0E+00
167	Date	Ultrasonic	Bone	2	99%	60%	2.3E-04	1.9E-04	1.0E-02	2.5E-05	1.4E-01
168	Date	Ultrasonic	Fruit	2	96%	27%	1.7E-01*	2.9E-03	5.0E-02	8.7E-05	1.1E+00
169	Date	Ultrasonic	Bone	2	99%	58%	2.4E-04	3.2E-04	9.0E-03	2.4E-05	1.8E-01
170	Date	Ultrasonic	Fruit	2	96%	25%	6.4E-04	2.7E-03	5.1E-02	1.7E-04	1.3E+00
171	Date	Ultrasonic	Bone	2	99%	57%	2.0E-04	1.1E-04	1.0E-02	2.4E-05	1.6E-01
172	Date	Ultrasonic	Fruit	2	95%	28%	2.6E-03	1.7E-03	4.8E-02	7.9E-05	1.1E+00
173	Fig	Conventional	Skin	2	97%	17%	3.7E-03	9.0E-03	7.7E-02	1.8E-04	2.4E+01
174	Fig	Conventional	Fruit	2	91%	30%	2.6E-03	5.5E-03	1.4E-01	1.4E-03	2.5E+01
175	Fig	Conventional	Skin	2	97%	18%	2.0E-03	6.9E-03	2.4E-02	1.4E-04	2.4E+01
176	Fig	Conventional	Fruit	2	97%	18%	2.4E-04	3.4E-04	2.7E-02	1.7E-04	1.1E+01
177	Fig	Conventional	Skin	2	97%	15%	1.3E-03	4.8E-03	1.1E-01	8.0E-05	2.7E+01
178	Fig	Conventional	Fruit	2	97%	18%	8.2E-04	2.6E-04	1.8E-01	1.6E-04	1.1E+01
179	P_pear	Conventional	Skin	2	97%	17%	8.5E-04	5.6E-03	7.3E-03	2.2E-04	2.0E+01
180	P_pear	Conventional	Fruit	2	95%	10%	9.5E-04	1.5E-03	1.5E-02	9.3E-04	3.8E+01
181	P_pear	Conventional	Skin	2	66%	17%	7.7E-03	4.0E-02	7.6E-02	2.9E-02	2.0E+02
182	P_pear	Conventional	Fruit	2	91%	17%	3.0E-04	7.2E-04	2.8E-02	6.0E-03	5.5E+01
183	P_pear	Conventional	Skin	2	86%	16%	3.8E-03	1.9E-02	3.2E-02	4.1E-03	9.3E+01

Sample excluded in further calculation because high value compared to other similar samples.

Table B. 4: *Average (Mean) concentrations, geometric mean (GM), standard deviation (SD), minimum (Min) and maximum (Max) measured in mg/kg as well as relative standard deviation (RSD) [%] and sample number (n) of the radionuclides [328]U and [232]Th and stable analogues [133]Cs, [88]Sr and [59]Co in soil in Tabernas. The type of fruit which the samples are associated, are also given.*

Fruit	Site		Uranium	Thorium	Caesium	Strontium	Cobalt
Fig	2	Mean	1.9	10	5.0	92.9	13.3
		GM	1.9	10	5.0	92.0	13.2
		SD	0.1	0.5	0.1	4.07	0.6
		Min	1.8	9.68	9.68	71.9	12.2
		Max	2.1	12	5.41	105	14.5
		RSD	4%	5%	2%	4%	4%
		n	3	3	3	3	3
Date	2	Mean	2.2	9.1	4.76	144	12
		GM	2.2	8.9	5.01	131	12
		SD	0.4	1.7	0.8	55	2
		Min	1.8	5.62	3.65	67.1	8.14
		Max	2.87	11.5	8.23	235	16.5
		RSD	16%	19%	17%	38%	16%
		n	5	5	5	5	5
Prickly pear	2	Mean	2	11	4.7	87	14
		GM	2	11	4.7	87	14
		SD	0.1	0.7	0.1	8	1.0
		Min	1.8	10.1	4.48	78.2	12.6
		Max	2.09	11.9	4.96	96	15.5
		RSD	6%	6%	3%	9%	7%
		n	3	3	3	3	3
Olive	1	Mean	1.8	7.9	4.8	112	13
		GM	1.8	11	4.8	108	13
		SD	0.1	0.6	0.4	37	2
		Min	1.53	6.92	4.38	73.6	10.3
		Max	2.03	9.08	5.72	167	18
		RSD	7%	8%	8%	33%	18%
		n	3	3	3	3	3
Olive	2	Mean	1.9	11	5.6	102	14
		GM	1.9	11	5.6	102	14
		SD	0.1	0.5	0.5	10	2.4
		Min	1.73	9.62	5.13	87.8	12
		Max	2.12	11.5	7.31	129	22.4
		RSD	4%	4%	9%	10%	18%
		n*	4 (3)	4(3)	4 (3)	4 (3)	4 (3)

* n=4 for =-5, 5-10, and 10-15 layers. For layers 15-20, n=3

Table B. 5: *Average (Mean) concentrations, geometric mean (GM), standard deviation (SD), minimum (Min) and maximum (Max) measured in mg/kg as well as relative standard deviation (RSD) [%] and sample number (n) of the radionuclides ^{328}U and ^{232}Th and stable analogues ^{133}Cs, ^{88}Sr and ^{59}Co in calcinated fruit samples adjusted for wet weight in the fruits. The site and washing procedure are also given.*

Fruit	Site	Washing procedure		^{238}U	^{232}Th	^{133}Cs	^{88}Sr	^{59}Co
Fig	2	Ultrasonic	Mean	3.11E-04	1.33E-03	3.95E-03	6.95E+00	7.58E-03
			GM	1.64E-04	4.03E-04	3.78E-03	5.91E+00	7.49E-03
			SD	4.09E-05	3.24E-04	2.13E-04	1.23E+00	2.39E-04
			Min	3.42E-05	2.87E-05	2.57E-03	2.88E+00	6.01E-03
			Max	6.49E-04	3.19E-03	5.29E-03	1.23E+01	8.98E-03
			RSD	13%	24%	5%	18%	3%
			n	3	3	3	3	3
Olive	1	Ultrasonic	Mean	8.14E-04	3.38E-04	1.49E-02	1.66E+01	2.02E-02
			GM	7.71E-04	2.76E-04	1.12E-02	1.60E+01	1.95E-02
			SD	1.2E-04	6.8E-05	1.8E-03	2.8E+00	2.9E-03
			Min	3.42E-04	1.03E-04	3.37E-03	8.98E+00	1.07E-02
			Max	1.15E-03	7.86E-04	3.10E-02	2.31E+01	2.67E-02
			RSD	14%	20%	12%	17%	14%
			n	6	6	6	6	6
Olive	2	Ultrasonic	Mean	3.55E-04	6.33E-04	7.17E-03	3.51E+00	1.47E-02
			GM	3.44E-04	4.95E-04	5.60E-03	3.49E+00	1.33E-02
			SD	2.6E-05	1.1E-04	2.1E-03	2.3E-01	4.0E-03
			Min	2.29E-04	1.89E-04	1.69E-03	2.93E+00	7.46E-03
			Max	4.76E-04	1.30E-03	1.71E-02	4.26E+00	2.28E-02
			RSD	7%	17%	30%	7%	27%
			n	6(5)*	6	6	6	6
Date	2	Ultrasonic	Mean	2.45E-04	3.84E-04	9.51E-03	2.07E-01	2.26E-03
			GM	1.89E-04	2.63E-04	8.72E-03	1.73E-01	2.15E-03
			SD	1.9E-04	9.2E-05	3.7E-04	1.0E-02	7.4E-04
			Min	1.12E-04	6.19E-05	5.24E-03	8.57E-02	1.59E-03
			Max	7.35E-04	7.76E-04	1.37E-02	3.37E-01	4.05E-03
			RSD	77%	24%	4%	5%	33%
			n	3	3	3	3	3
Fig	2	Conventional	Mean	3.60E-04	8.79E-04	1.88E-02	4.00E+00	6.54E-03
			GM	2.47E-04	4.32E-04	1.35E-02	3.59E+00	5.71E-03
			SD	2.6E-04	5.9E-04	1.2E-02	1.9E+00	1.1E-05
			Min	4.37E-05	4.64E-05	4.41E-03	2.00E+00	3.12E-03
			Max	7.83E-04	1.68E-03	4.15E-02	7.59E+00	1.53E-02
			RSD	73%	67%	62%	47%	51%
			n	3	3	3	3	3
Prickly pears	2	Conventional	Mean	3.86E-04	1.88E-03	4.85E-03	1.22E+01	4.15E-02
			GM	2.24E-04	8.13E-04	3.62E-03	9.16E+00	2.97E-02
			SD	3.5E-04	1.8E-03	3.9E-03	9.8E+00	3.4E-02

			Min	4.97E-05	1.21E-04	1.27E-03	3.48E+00	7.95E-03
			Max	1.35E-03	6.98E-03	1.33E-02	3.48E+00	8.80E-02
			RSD	92%	94%	81%	80%	82%
			n	3(2)**	3(2)**	3(2)**	3(2)**	3(2)**

*n=5 for uranium in the fruit part

** n = 3 for skin samples, and n = 2 for fruit sample

Table B 6: *Average (Mean) concentrations, geometric mean (GM), standard deviation (SD), minimum (Min) and maximum (Max) measured in mg/kg as well as relative standard deviation (RSD) [%] and sample number (n) of the radionuclides ^{328}U and ^{232}Th and stable analogues ^{133}Cs, ^{88}Sr and ^{59}Co in calcinated fruit samples adjusted for dry weight of fruits. The site and washing procedure are also given.*

Fruit	Site	Wash procedure		^{238}U	^{232}Th	^{133}Cs	^{88}Sr	^{59}Co
Fig	2	Ultrasonic	Mean	1.29E-03	5.50E-03	1.78E-02	3.00E+01	3.37E-04
			GM	7.63E-04	1.87E-03	1.75E-02	2.75E+01	3.28E-04
			SD	2.8E-04	1.9E-03	2.0E-03	3.7E+00	2.3E-05
			Min	1.87E-04	1.47E-04	1.41E-02	1.60E+01	2.36E-04
			Max	2.79E-03	1.37E-02	2.27E-02	4.73E+01	4.40E-04
			RSD	22%	34%	11%	12%	7%
			n	3	3	3	3	3
Olive	1	Ultrasonic	Mean	1.69E-03	7.78E-04	3.53E-02	3.23E+01	3.15E-03
			GM	1.44E-03	5.16E-04	2.10E-02	2.99E+01	1.80E-03
			SD	2.1E-04	1.7E-04	4.2E-03	4.1E+00	5.4E-04
			Min	4.67E-04	1.37E-04	4.60E-03	1.23E+01	2.16E-04
			Max	3.02E-03	2.01E-03	7.90E-02	4.71E+01	7.27E-03
			RSD	12%	22%	12%	13%	17%
			n	6	6	6	6	6
Olive	2	Ultrasonic	Mean	7.71E-04	1.51E-03	1.75E-02	7.00E+00	2.02E-03
			GM	6.53E-04	9.57E-04	1.08E-02	6.74E+00	1.09E-03
			SD	9.4E-05	1.5E-04	6.8E-03	4.9E-01	5.7E-04
			Min	3.25E-04	2.69E-04	2.40E-03	4.30E+00	9.23E-05
			Max	1.42E-03	2.98E-03	4.93E-02	9.69E+00	4.60E-03
			RSD	12%	10%	39%	7%	28%
			n	6(5)*	6	6	6	6
Date	2	Ultrasonic	Mean	7.66E-04	1.32E-03	2.97E-02	6.81E-01	6.75E-05
			GM	4.79E-04	6.65E-04	2.21E-02	4.37E-01	5.03E-05
			SD	6.5E-04	3.6E-04	1.0E-03	7.2E-02	2.8E-05
			Min	1.96E-04	1.09E-04	8.98E-03	1.43E-01	2.39E-05
			Max	2.62E-03	2.85E-03	5.09E-02	1.34E+00	1.66E-04
			RSD	85%	27%	3%	11%	41%
			n	3	3	3	3	3
Fig	2	Conventional	Mean	1.77E-03	4.47E-03	9.26E-02	2.03E+01	3.53E-04
			GM	1.31E-03	2.29E-03	7.16E-02	1.90E+01	2.07E-04
			SD	9.9E-04	2.1E-03	5.2E-02	4.7E+00	1.7E-07

			Min	2.43E-04	2.55E-04	2.41E-02	1.11E+01	8.04E-05
			Max	3.67E-03	8.97E-03	1.85E-01	2.66E+01	1.38E-03
			RSD	56%	47%	56%	23%	115%
			n	3	3	3	3	3
Prickly pears	2	Conventional	Mean	2.38E-03	1.12E-02	3.01E-02	7.60E+01	7.36E-03
			GM	1.48E-03	5.35E-03	2.38E-02	6.02E+01	2.72E-03
			SD	2.0E-03	1.0E-02	2.1E-02	5.4E+01	9.5E-03
			Min	2.97E-04	7.23E-04	7.31E-03	2.01E+01	2.21E-04
			Max	7.74E-03	3.99E-02	7.61E-02	2.01E+01	2.95E-02
			RSD	85%	89%	70%	71%	129%
			n	3(2)**	3(2)**	3(2)**	3(2)**	3(2)**

*n=5 for uranium in the fruit part

** n = 3 for skin samples, and n = 2 for fruit sample

Table B 7: Results of certified reference materials (CRM) NCS DC 73324a, NIST 2711a and NCS ZC 73007 analysed by ICP-MS for soil. All samples were diluted 500 times taking a 1 mL aliquot from a 50 mL and diluting to 10 mL. The samples were digested using a 1:1:2 ratio mix of HNO_3, HBF_4, and H_3PO_4. Green = within certified range, red = outside certified range, orange = close to certified range.

Element	NCS DC 73324a	NIST 2711a	NCS ZC 73007
Caesium	🟩	🟩	🟩
Cobalt	🟩	🟩	🟩
Strontium	🟩	🟩	🟩
Thorium	🟩		🟩
Uranium	🟩	🟩	🟩
Yttrium	🟩		🟩
Holmium	🟩		🟩

Table B. 8: Results of certified reference material (CRM) NIST 1633a, NCS ZC 73036a and NIST 1570a analysed by ICP-MS for calcinated fruit samples. All samples were diluted to 50 mL and digested using HNO_3. Green = within certified range, red = outside certified range, orange = close to certified range.

Element	NIST 1633a	NCS ZC 73036a	NIST 1570a
Caesium		🟩	
Cobalt	🟥	🟩	🟩
Strontium	🟥	🟩	🟩
Thorium	🟥	🟩	🟩
Uranium	🟥	🟩	🟩
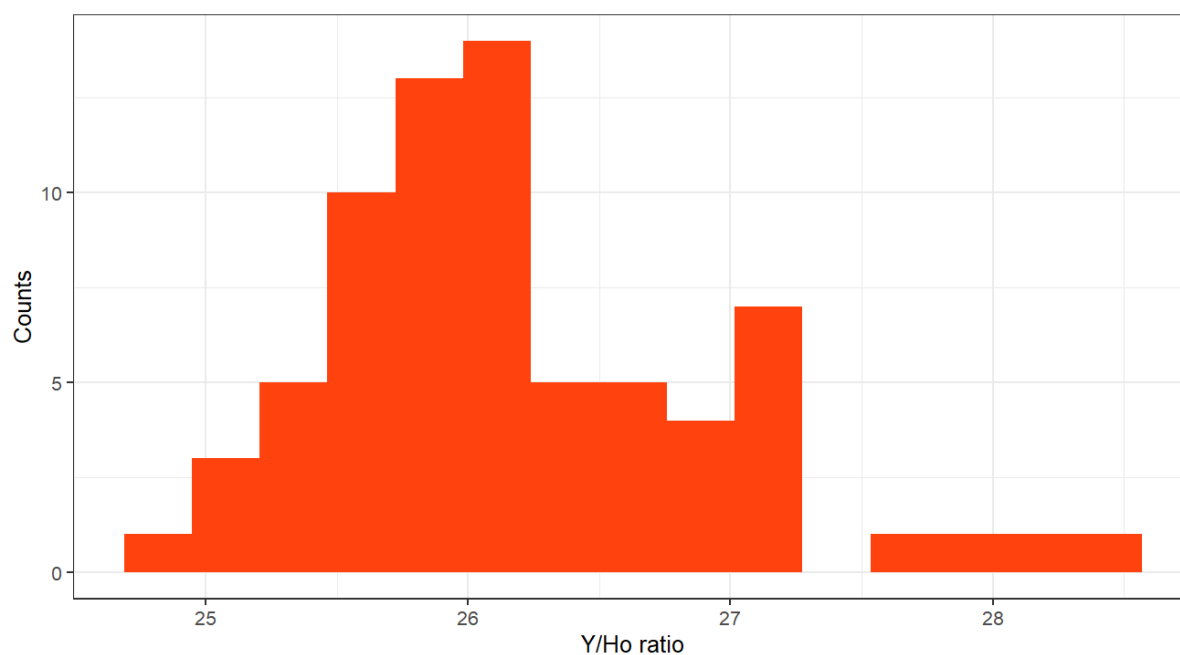
Figure B. 9: *Histogram of the ratio of the concentration [mg/kg] of Yttrium (Y) divided by the concentration of Holmium (Ho) in all measured soil samples. On the x-axis the Y/Ho ratio is shown, (bins = 15) and the count is shown on the y-axis. The average ratio between Y and H for all soil was 26.2.*

C: XRD data
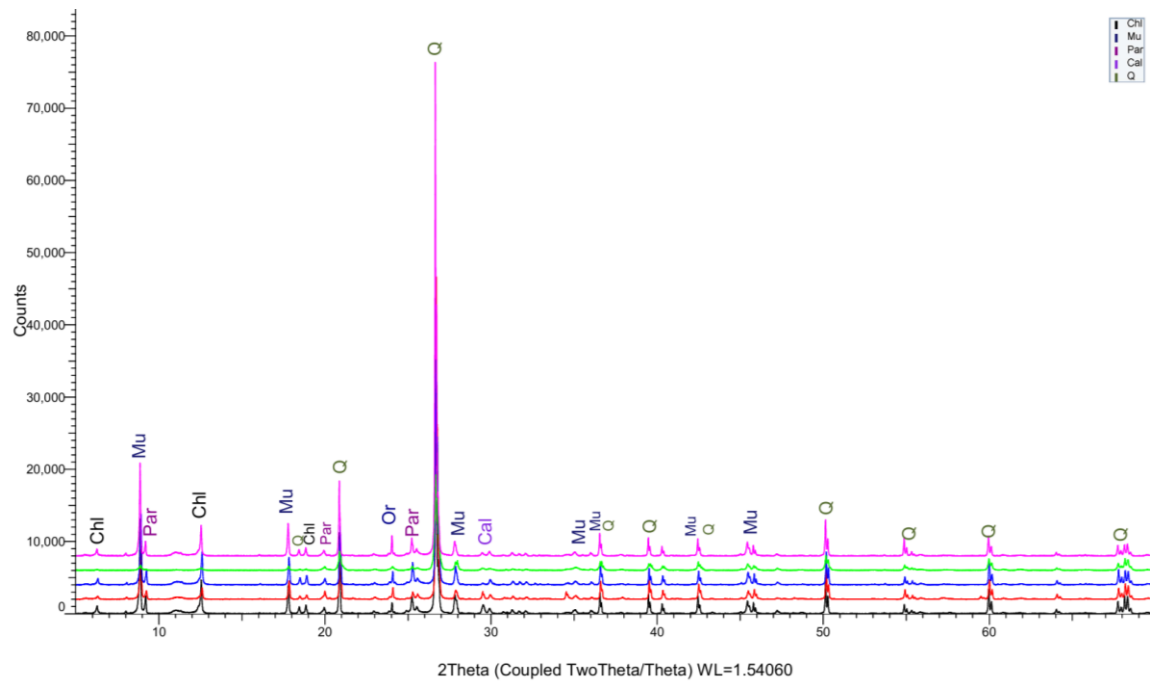
Figure C.1: _The diffractogram of all five soil samples by XRD. The black diffractogram in the bottom is sample O2A (Olive site 2), the red is O1E (Olive site 1), the blue is F2 (Fig site 2), the green is D2E (Date site 2), and the pink is sample CH2C (Prickly pear site 2). All samples are from the 15-20 cm depth from the core closest to the plant. For the mineral, the IMA symbol is used for instead of the full name of the mineral._

D: CEC data

Table D1: *Raw data from CEC measurements [cmolc/Kg]. Ca, Mg, K, Na, Ca estimated (the difference between CEC and the sum of Mg, Na and K), and CEC are measured for the different soil core samples at the two different sites in Tabernas. The sample is marked with the site, core position, associated fruit and the soil layer. Figs only have one soil core position (A), while all other samples have multiple core positions measured.*

Sample number	Site	Position	Fruit	Layer [cm]	Ca [cmolc/Kg]	Mg [cmolc/Kg]	K [cmolc/Kg]	Na [cmolc/Kg]	Ca estimated* [cmolc/Kg]	CEC [cmolc/Kg]
Z-1	2	A	Fig	0-5	65.633	2.460	0.537	0.080	1.324	4.401
Z-2	2	A	Fig	5-10	70.716	2.390	0.372	0.099	1.288	4.149
Z-3	2	A	Fig	10-15	56.471	1.614	0.325	0.182	0.353	2.474
Z-4	2	A	Fig	15-20	39.439	1.191	0.098	0.151	0.055	1.495
Z-5	2	E	Date	0-5	86.152	5.452	0.212	0.616	3.265	9.546
Z-6	2	E	Date	5-10	71.290	3.176	0.115	0.333	1.693	5.317
Z-7	2	E	Date	10-15	39.226	1.041	0.058	0.130	0.375	1.605
Z-8	2	E	Date	15-20	73.762	1.289	0.078	0.173	n.d.	1.435
Z-9	2	A	Date	0-5	99.374	3.441	0.545	0.781	1.042	5.808
Z-10	2	A	Date	5-10	85.880	3.824	0.542	0.899	2.348	7.613
Z-11	2	A	Date	10-15	93.683	4.638	0.545	1.265	n.d.	1.921
Z-12	2	A	Date	15-20	82.876	4.032	0.173	2.005	0.202	6.411
Z-13	2	B	Date	0-5	66.191	3.055	0.915	0.111	4.754	8.835
Z-14	2	B	Date	5-10	73.986	3.874	1.279	0.151	7.398	12.702
Z-15	2	B	Date	10-15	63.020	2.664	0.766	0.214	3.120	6.764
Z-16	2	B	Date	15-20	43.535	1.138	0.412	0.081	0.973	2.604
Z-17	2	A	P_pear	0-5	63.281	1.917	0.294	0.635	0.609	3.454
Z-18	2	A	P_pear	5-10	62.986	1.782	0.230	0.779	1.608	4.400
Z-19	2	A	P_pear	10-15	65.198	2.097	0.406	0.656	n.d.	2.646
Z-20	2	A	P_pear	15-20	61.870	1.715	0.202	0.775	0.763	3.456
Z-21	2	B	P_pear	0-5	60.562	1.847	0.157	0.698	1.493	4.195
Z-22	2	B	P_pear	5-10	60.421	1.737	0.187	0.589	1.464	3.977

Z-23	2	B	P_pear	10-15	64.190	2.324	0.119	1.287	0.239	3.969
Z-24	2	B	P_pear	15-20	69.757	3.575	0.105	2.406	n.d.	4.682
Z-25	2	C	P_pear	0-5	58.920	1.815	0.142	0.885	0.960	3.803
Z-26	2	C	P_pear	5-10	57.196	1.763	0.144	0.831	0.362	3.101
Z-27	2	C	P_pear	10-15	56.372	1.934	0.227	0.922	0.786	3.867
Z-28	2	C	P_pear	15-20	63.946	1.893	0.086	0.905	0.477	3.361
Z-29	1	E	Olive	0-5	59.580	0.547	0.301	0.047	0.197	1.093
Z-30	1	E	Olive	5-10	42.802	0.501	0.336	0.034	0.078	0.949
Z-31	1	E	Olive	10-15	64.446	2.043	1.093	0.081	2.899	6.115
Z-32	1	E	Olive	15-20	76.044	2.073	0.992	0.093	1.728	4.886
Z-33	1	A	Olive	0-5	64.580	0.552	0.134	0.037	0.231	0.955
Z-34	1	A	Olive	5-10	45.526	0.391	0.179	0.037	0.224	0.831
Z-35	1	A	Olive	10-15	44.129	0.513	0.358	0.027	0.675	1.574
Z-36	1	A	Olive	15-20	43.258	0.496	0.317	0.025	0.542	1.379
Z-37	1	B	Olive	0-5	67.613	4.192	2.218	0.299	n.d.	6.589
Z-38	1	B	Olive	5-10	64.699	2.327	1.063	0.149	0.893	4.431
Z-39	1	B	Olive	10-15	58.347	1.722	0.867	0.065	0.067	2.721
Z-40	1	B	Olive	15-20	59.812	0.928	0.730	0.070	n.d.	1.363
Z-41	2	A	Olive	0-5	59.790	2.035	0.635	0.088	1.215	3.972
Z-42	2	A	Olive	5-10	61.180	2.076	0.623	0.088	0.894	3.681
Z-43	2	A	Olive	10-15	59.182	1.927	0.588	0.092	1.045	3.654
Z-44	2	A	Olive	15-20	61.950	1.948	0.410	0.095	0.482	2.935
Z-45	2	C	Olive	0-5	56.370	1.929	0.111	0.084	0.976	3.099
Z-46	2	C	Olive	5-10	60.357	2.566	0.173	0.121	2.503	5.364
Z-47	2	C	Olive	10-15	61.460	2.425	0.157	0.119	2.794	5.496
Z-48	2	C	Olive	15-20	62.522	1.940	0.107	0.134	0.782	2.963
Z-49	2	D	Olive	0-5	60.556	2.098	0.121	0.093	0.690	3.001
Z-50	2	D	Olive	5-10	65.376	2.411	0.139	0.106	1.213	3.869
Z-51	2	D	Olive	10-15	63.425	1.883	0.092	0.105	0.576	2.656
Z-52	2	D	Olive	15-20	65.446	2.090	0.109	0.114	0.547	2.860
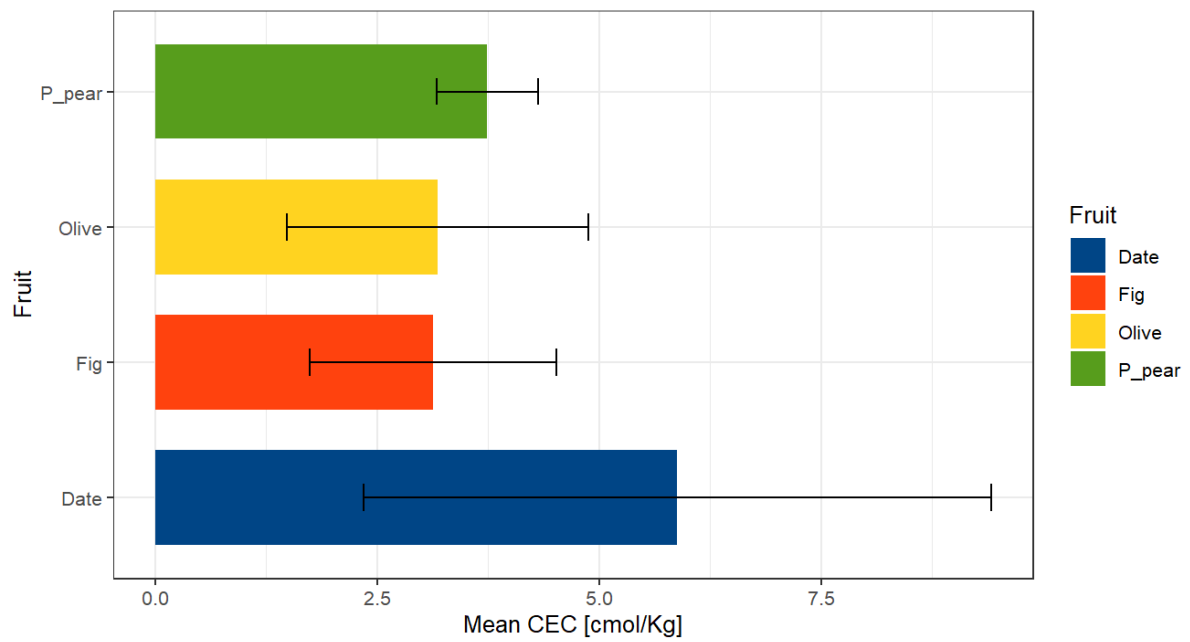
Figure D2: *Barplot of the average cation exchange capacity[cmolc/kg] measured for soil cores at site 2. The type of associated fruit is used as the categorical variable and the average CEC is the response variable.*
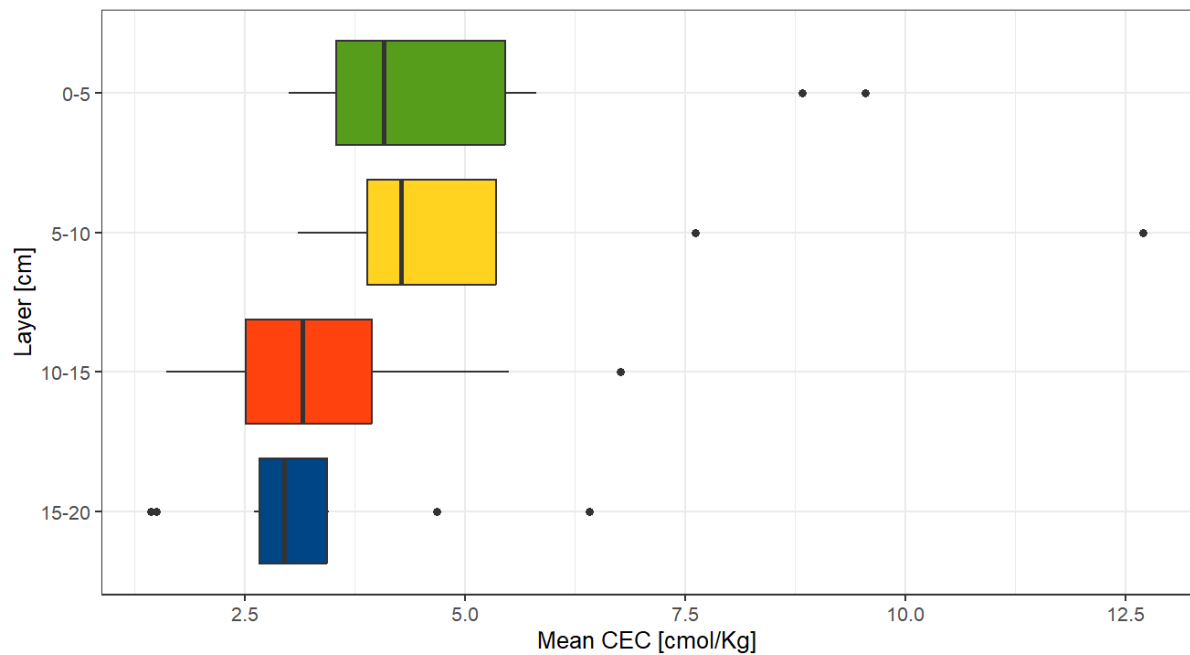
Figure D.3: *Boxplot of the mean CEC [cmol/kg] in each soil horizontal layer [cm] at site 2. The mean serve as the response variable and the layer serves as the response variable.*

E: Wash water results measured by ICP-MS

Table E1: *Total amount [μg] of* ^{59}*Co,* ^{133}*Cs,* ^{88}*Sr,* ^{232}*Th and* ^{238}*U in all samples of figs, olives, dates and prickly pears washed by ultrasonic or conventional methods of pre-treatment. In addition, Pb was measured. The measured samples are adjusted to calculate the total amount in each procedure. Blanks and internal controls are not part of the table.*

Sample number	Fruit	Wash procedure	Wash number	Site	Co [μg]	Cu [μg]	Sr [μg]	Cs [μg]	Pb [μg]	Th [μg]	U [μg]
2	Fig	Ultrasonic	1	2	0.04	1.30	2.58	0.02	6.66	0.01	0.03
3	Fig	Ultrasonic	1	2	0.05	1.85	2.52	0.02	7.02	0.01	0.01
4	Fig	Ultrasonic	1	2	0.10	1.48	2.70	0.02	8.13	0.01	0.02
7	Fig	Ultrasonic	2	2	0.05	1.36	3.28	0.04	7.33	0.02	0.01
8	Fig	Ultrasonic	2	2	0.04	2.47	3.12	0.03	5.20	0.02	0.01
9	Fig	Ultrasonic	2	2	0.06	1.53	3.06	0.03	4.57	0.01	0.01
11	Fig	Ultrasonic	2	2	<LOQ	1.42	2.42	0.02	2.44	<LOQ	<LOQ
12	Fig	Ultrasonic	2	2	<LOQ	0.73	2.57	0.02	2.52	<LOQ	<LOQ
13	Fig	Ultrasonic	2	2	0.04	1.10	2.27	0.01	2.42	<LOQ	0.01
16	Fig	Ultrasonic	3	2	0.05	1.54	3.03	0.03	4.68	0.02	0.01
17	Fig	Ultrasonic	3	2	0.04	1.37	3.47	0.04	6.12	0.02	0.01
18	Fig	Ultrasonic	3	2	0.04	1.79	3.37	0.05	5.84	0.01	0.01
20	Fig	Ultrasonic	3	2	0.04	2.82	3.03	0.02	3.56	0.01	0.01
21	Fig	Ultrasonic	3	2	<LOQ	0.68	2.76	0.01	1.95	<LOQ	<LOQ
22	Fig	Ultrasonic	3	2	<LOQ	30.61	2.72	0.01	2.68	<LOD	<LOQ
24	Fig	Ultrasonic	3	2	<LOQ	1.09	2.26	0.02	1.57	<LOQ	<LOQ
25	Fig	Ultrasonic	3	2	0.04	0.80	3.59	0.02	3.47	<LOQ	<LOQ
26	Fig	Ultrasonic	3	2	0.03	2.03	2.41	0.02	1.06	<LOQ	0.01
28	Fig	Conventional	1	2	0.00	299	456	13.3	2030	1.91	0.433
29	Fig	Conventional	2	2	0.00	19.8	50.3	0.538	1070	0.102	0.067
30	Fig	Conventional	3	2	0.00	26.5	57.9	2.19	873	0.183	0.088
32	Olive	Ultrasonic	1	1	0.717	13.9	24.7	0.20	10.038	0.164	0.086

33	Olive	Ultrasonic	1	1	0.403	9.71	20.9	0.19	9.626	0.131	0.064
34	Olive	Ultrasonic	1	1	0.320	6.20	20.4	0.16	8.025	0.105	0.040
37	Olive	Ultrasonic	1	2	0.496	7.52	22.6	0.21	4.453	0.164	0.104
38	Olive	Ultrasonic	1	2	0.465	3.97	21.9	0.19	3.567	0.155	0.046
39	Olive	Ultrasonic	1	2	0.389	6.93	22.5	0.14	4.414	0.132	0.036
42	Date	Ultrasonic	1	2	1.83	18.7	30.7	0.17	35.1	0.121	0.069
43	Date	Ultrasonic	1	2	0.799	44.9	22.4	0.15	7.9	0.116	0.077
44	Date	Ultrasonic	1	2	1.60	141	43.3	0.72	25.8	0.182	0.437
46	P_pear	Conventional	1	2	6.52	133	178	2.69	1990	3.18	0.644
47	P_pear	Conventional	2	2	1.99	29.4	48.1	0.628	720	0.491	0.158
48	P_pear	Conventional	3	2	2.06	16.9	67.4	0.825	25.8	0.773	0.17

Table E2: Summary table of the mean total amount of ^{59}Co, ^{133}Cs, ^{88}Sr, ^{232}Th and ^{238}U [µg], SD [µg], RSD [%], the minimum and maximum measurement [µg] and the number of measured aliquots. For the fruits measured by the conventional method, only the mean is given.

Fruit	Washing procedure	Wash number		^{59}Co	^{88}Sr	^{133}Cs	^{232}Th	^{238}U
Fig	Ultrasonic	1	Mean	0.06	2.60	0.02	0.01	0.02
			SD	0.03	0.09	0.00	0.00	0.01
			RSD	52%	4%	20%	13%	46%
			Min	0.04	2.52	0.02	0.01	0.01
			Max	0.10	2.70	0.02	0.01	0.03
			n	3	3	3	3	3
		2	Mean	0.05	2.79	0.02	0.01	0.01
			SD	0.01	0.009	0.004	0.004	0.001
			RSD	19%	0.3%	16%	27%	8%
			Min	0.04	2.27	0.01	0.01	0.01
			Max	0.06	3.28	0.04	0.02	0.01
			n	4	6	6	3	4
		3	Mean	0.04	2.96	0.03	0.01	0.01
			SD	0.008	0.46	0.01	0.005	0.001
			RSD	21%	16%	50%	39%	17%
			Min	0.03	2.26	0.01	0.01	0.01
			Max	0.05	3.59	0.05	0.02	0.01
			n	6	9	9	4	6
Fig	Conventional	1	Mean	5.82	456	13.3	1.91	0.433
		2	Mean	0.731	50.3	0.538	0.102	0.0672
		3	Mean	0.685	57.9	2.19	0.183	0.0879
Olive site 1	Ultrasonic	1	Mean	0.48	22	0.18	0.13	0.06
			SD	0.21	2	0.02	0.03	0.02
			RSD	44%	11%	12%	22%	37%
			Min	0.320	20.4	0.160	0.105	0.040
			Max	0.717	24.7	0.203	0.164	0.086
			n	3	3	3	3	3
Olive site 2	Ultrasonic	1	Mean	0.45	22.3	0.18	0.15	0.062
			SD	0.06	0.4	0.04	0.02	0.037
			RSD	12%	2%	19%	11%	59%
			Min	0.39	21.9	0.14	0.13	0.04
			Max	0.50	22.6	0.21	0.16	0.10
			n	3	3	3	3	3
Date	Ultrasonic	1	Mean	1.4	32.1	0.3	0.1	0.2
			SD	0.5	11	0.3	0.0	0.2
			RSD	38%	33%	94%	27%	108%
			Min	0.799	22	0.147	0.116	0.069
			Max	1.83	43	0.72	0.18	0.44
			n	3	3	3	3	3
Prickly pears	Conventional	1	Mean	6.52	178	2.69	3.18	0.644
		2	Mean	1.99	48.1	0.628	0.491	0.158

|		3	Mean	2.06	67.4	0.825	0.773	0.17

Table E3: *Results of certified reference material (CRM)1642f, NCS ZC 73036a and NIST 1570a analysed by ICP-MS for wash water samples from the pre-treatment of calcinated fruit. The samples were digested by HNO₃. Green = within certified range, red = outside certified range, orange = close to certified range.*

| Element	NIST 1643f	NCS DC 73324a	NCS ZC 73007
Caesium		🟩	🟩
Cobalt	🟩	🟩	
Strontium	🟩	🟧	🟧
Thorium		🟩	🟩
Uranium		🟩	🟧

F: XRF data

Table F 1: *Weight percentage concentration [%] of elements measured on the general assessment of fruits shells of dates, olives and prickly pears.*

|	O21	O11	D21	H21
K	83.92	79.15	65.53	28.34
Ca	8.14	12.84	10.09	52.40
Cl	3.12	2.86	12.14	1.66
Na	1.74	1.32	1.85	1.29
Fe	0.32	0.53	0.30	0.61
Al	0.52	0.68	0.34	2.74
Zn	0.35	0.27	0.21	0.20
Si	0.28	0.59	3.04	5.62
S	0.58	0.74	3.56	1.12
P	0.30	0.26	1.35	1.29
Cu	0.16	0.18	0.06	0.11
Mg	0.42	0.37	1.12	4.41
Mn	0.15	0.21	0.13	0.21
Rh	0	0	0	0
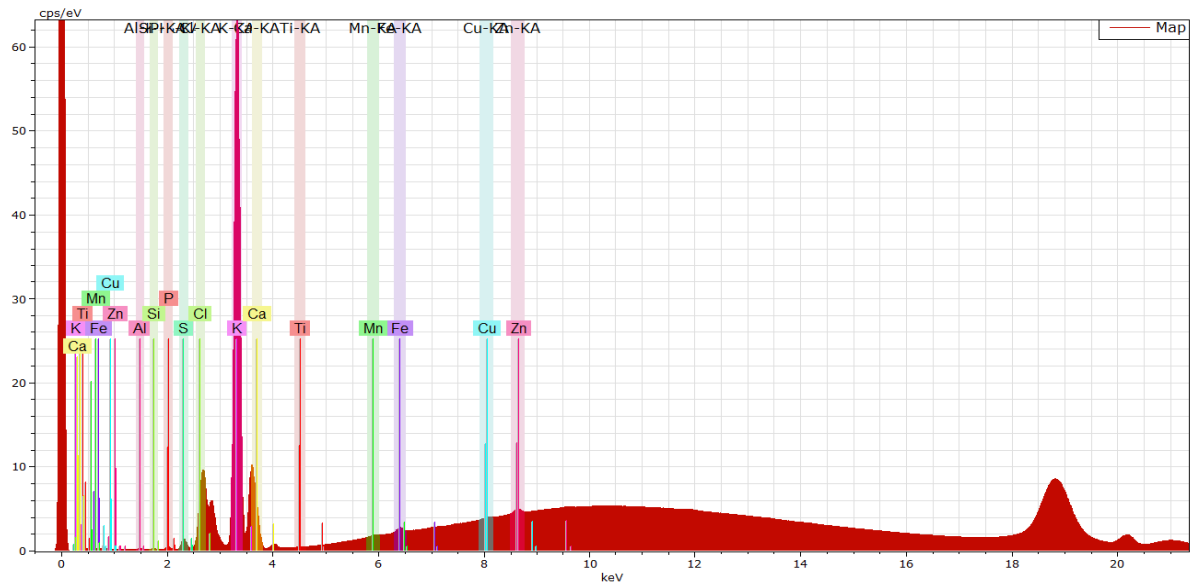
Figure F.2: *Spectra of the fruit skin sample measurement of olive measured at site 2 (O21). The counts per second (cps) is the response on the y-axis, with the energy [keV] on the x-axis.*
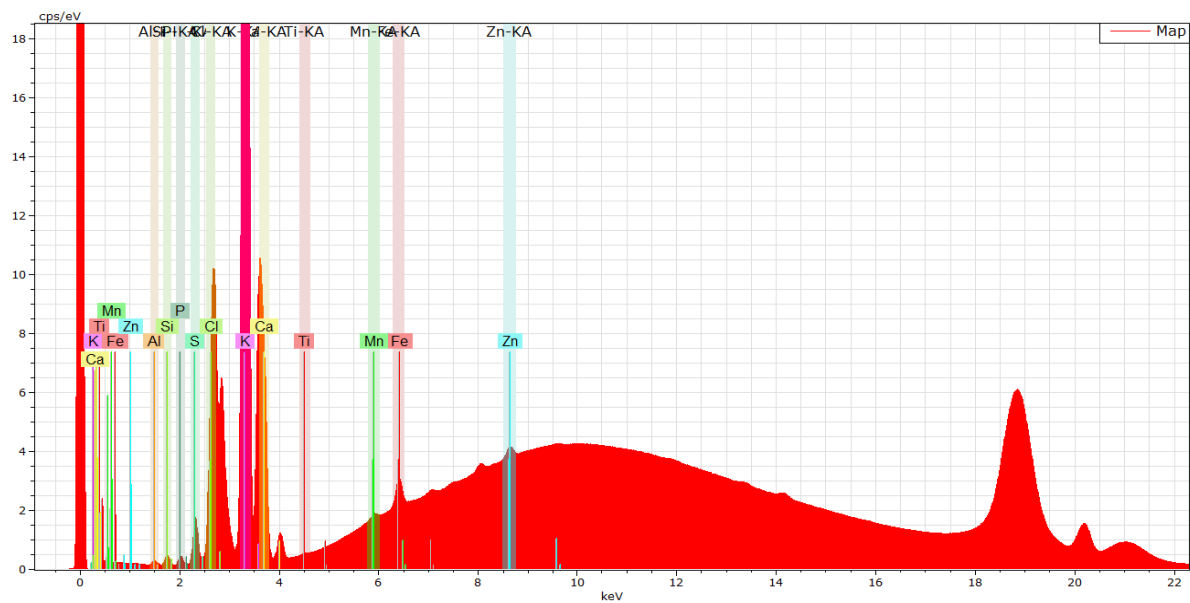
Figure F.3: *Spectra of the fruit skin sample measurement of olive measured at site 1 (O1).*

The counts per second (cps) is the response on the y-axis, with the energy [keV] on the x-axis.
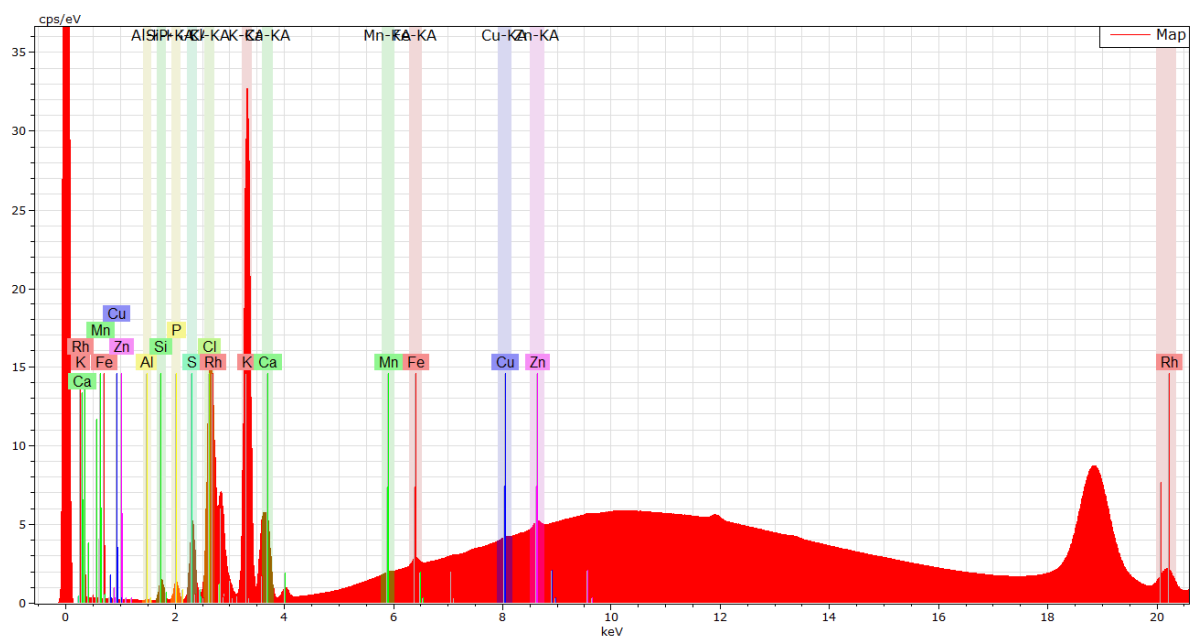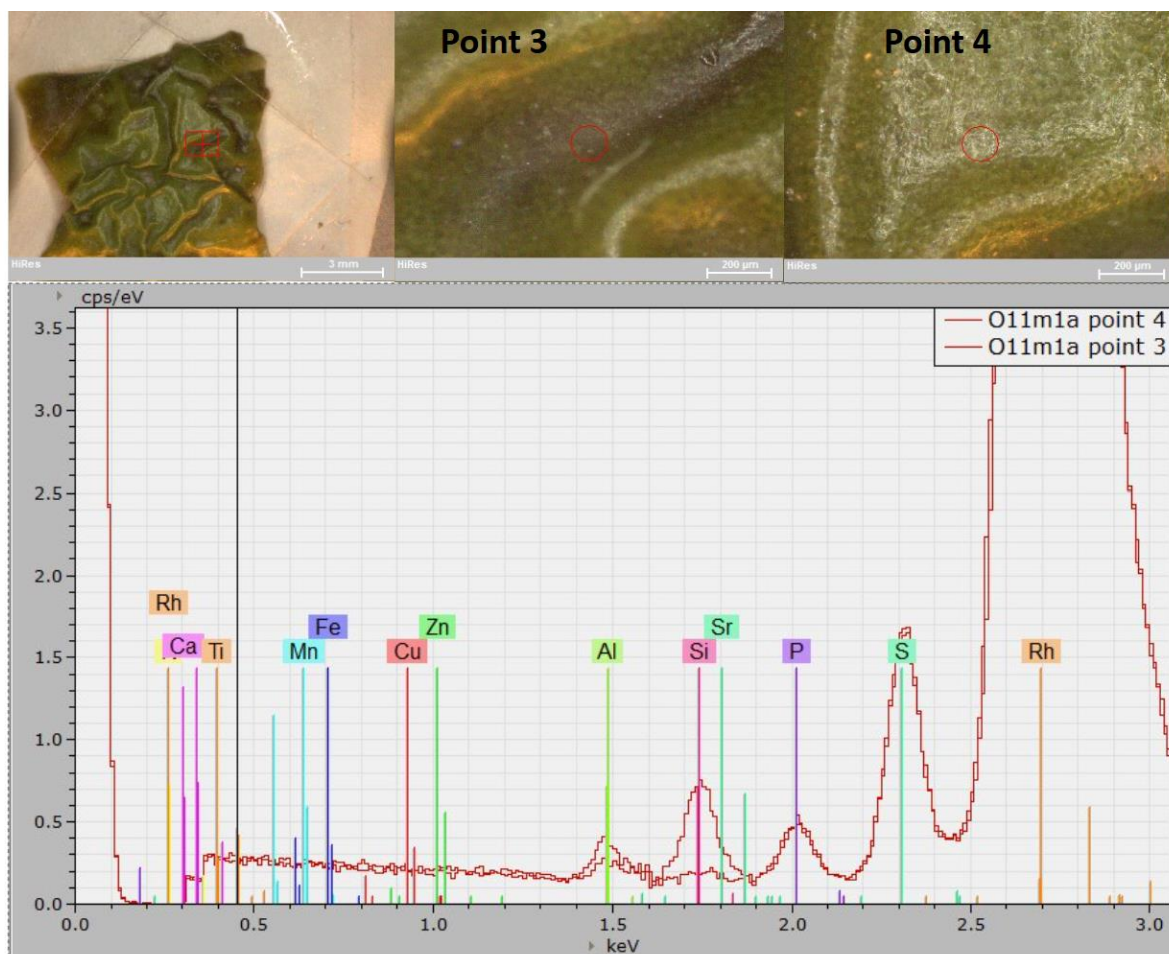

Figure F.4: *Spectra of the fruit skin sample measurement of date measured at site 2 (D21).*

The counts per second (cps) is the response on the y-axis, with the energy [keV] on the x-axis.
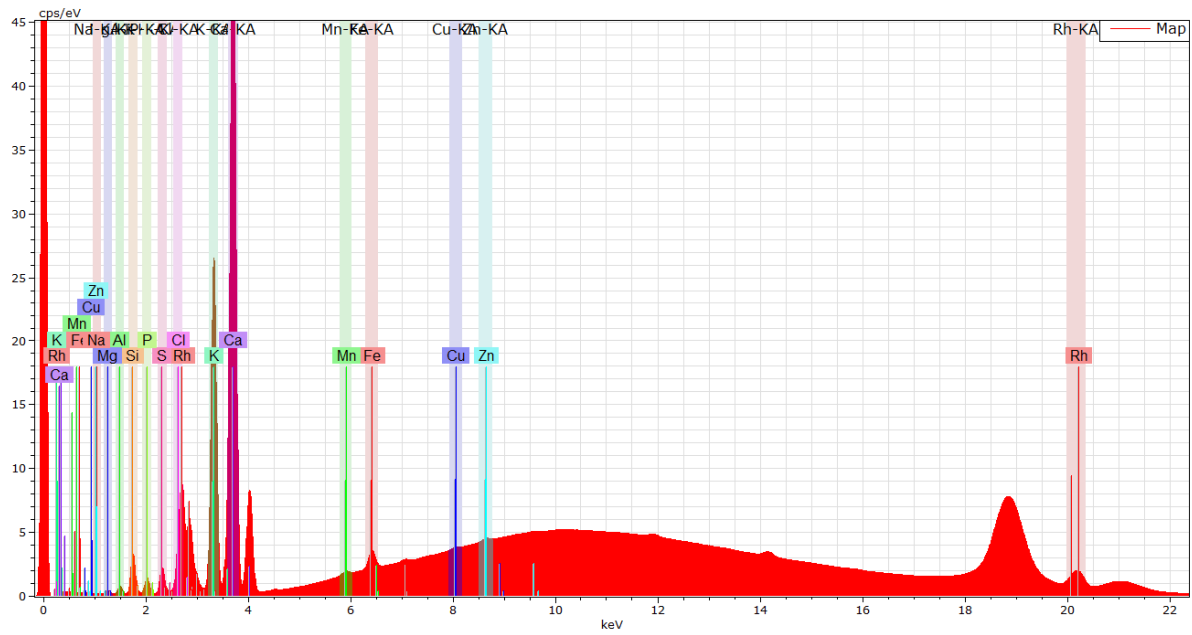
Figure F.5: *Spectra of the fruit skin sample measurement of fig measured at site 2 (H21). The counts per second (cps) is the response on the y-axis, with the energy [keV] on the x-axis.*

Figure F.6: Bottom: *Spectra of point 3 and 4 taken from the surface of sample O.1.1. with the energy [keV] on the x-axis and the counts per second [cps] on the y-axis. Point 3, taken at a hotspot in a crevasse on the surface had e.g the highest Si signal, while Point 4, taken just outside of the crevasse and hotspot had the lowest signal.* ***Top:*** *From the right, the area where the sample was taken, sample point 3 and sample point 4.*

Table F.7. *Weight percentage [%] of elements measured in point 3 and point 4 of sample O.1.1.*

	S	P	Si	Al	Ca	K	Fe	Mn	Cu	Sr	Zn
Point 3	0.49	0.22	0.77	0.84	14.18	82.58	0.31	0.16	0.15	0.05	0.23
Point 4	0.51	0.21	0.05	0.41	10.31	87.79	0.22	0.12	0.14	n.a	0.2

G: CRs and TFs
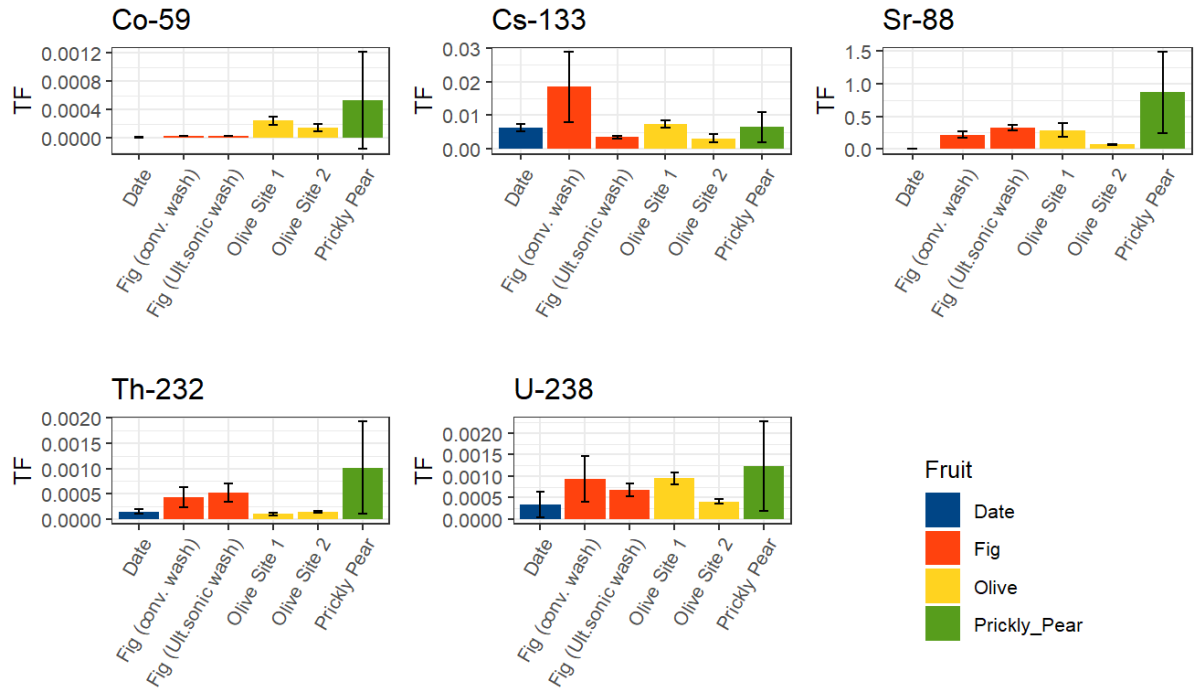
Figure G.1: *Transfer factors (TFs) of the five elements of interest, ^{59}Co, ^{133}Cs, ^{88}Sr, ^{232}Th and ^{238}U in the four measured fruits dates, figs, olives and prickly pears. The error bars are the SD for each group, with the fruit at different situations as the categorical variable and the TF as the response varable.*

Table G.2: *Calculated CR and standard deviation (SD) of ^{238}U, ^{232}Th, ^{133}Cs, ^{88}Sr and ^{59}Co in figs, olives dates and prickly pears at the two sites in Tabernas. The CR of figs are parted by if the ultrasonic or conventional method of pre-treatment were used.*

Fruit	Site	Method		^{238}U	^{232}Th	^{133}Cs	^{88}Sr	^{59}Co
Fig	2	Ultrasonic	CR	1.64E-04	1.28E-04	7.87E-04	7.48E-02	5.71E-04
			SD	2.3E-05	3.2E-05	4.5E-05	1.4E-02	3.0E-05
Fig	2	Coventional	CR	1.89E-04	8.44E-05	3.75E-03	4.31E-02	4.92E-04
			SD	1.4E-04	5.7E-05	2.3E-03	2.0E-02	2.1E-05
Olive	1	Ultrasonic	CR	4.56E-04	4.26E-05	3.09E-03	1.49E-01	1.55E-03
			SD	7.3E-05	9.2E-06	4.5E-04	5.6E-02	3.6E-04
Olive	2	Ultrasonic	CR	1.86E-04	5.98E-05	1.28E-03	3.43E-02	1.07E-03
			SD	1.5E-05	1.1E-05	4.0E-04	4.1E-03	3.4E-04
Date	2	Ultrasonic	CR	1.09E-04	4.23E-05	2.00E-03	1.44E-03	1.89E-04
			SD	8.6E-05	1.3E-05	3.5E-04	5.5E-04	6.9E-05
Prickly Pear	2	Coventional	CR	1.99E-04	1.70E-04	1.04E-03	1.40E-01	2.99E-03
			SD	1.8E-04	1.6E-04	8.4E-04	1.1E-01	2.5E-03

Table G.3: *Calculated TF and standard deviation (SD) of ^{238}U, ^{232}Th, ^{133}Cs, ^{88}Sr and ^{59}Co in figs, olives dates and prickly pears at the two sites in Tabernas. The TF of figs are parted by if the ultrasonic or conventional method of pre-treatment were used.*

Fruit	Site	Method		^{238}U	^{232}Th	^{133}Cs	^{88}Sr	^{59}Co
Fig	2	Ultrasonic	CR	6.81E-04	5.28E-04	3.56E-03	3.23E-01	2.54E-05
			SD	1.5E-04	1.8E-04	4.1E-04	4.3E-02	2.1E-06
Fig	2	Coventional	CR	9.33E-04	4.29E-04	1.84E-02	2.19E-01	2.66E-05
			SD	5.2E-04	2.0E-04	1.0E-02	5.2E-02	1.1E-06
Olive	1	Ultrasonic	CR	9.50E-04	9.80E-05	7.30E-03	2.90E-01	2.42E-04
			SD	1.4E-04	2.2E-05	1.1E-03	1.0E-01	6.1E-05
Olive	2	Ultrasonic	CR	4.04E-04	1.43E-04	3.13E-03	6.84E-02	1.46E-04
			SD	5.2E-05	1.6E-05	1.3E-03	8.3E-03	4.9E-05
Date	2	Ultrasonic	CR	3.42E-04	1.45E-04	6.26E-03	4.74E-03	5.63E-06
			SD	3.0E-04	4.8E-05	1.1E-03	1.9E-03	2.5E-06
Prickly Pear	2	Coventional	CR	1.22E-03	1.02E-03	6.46E-03	8.69E-01	5.32E-04
			SD	1.0E-03	9.1E-04	4.6E-03	6.2E-01	6.9E-04